

Transfer Learning Between U.S. Presidential Elections: How Should We Learn From A 2020 Ad Campaign To Inform 2024 Ad Campaigns?

Xinran Miao^{*1}, Jiwei Zhao^{1,2}, and Hyunseung Kang¹

¹Department of Statistics, University of Wisconsin-Madison

²Department of Biostatistics and Medical Informatics, University of Wisconsin-Madison

Abstract

For the 2024 U.S. presidential election, would negative, digital ads against Donald Trump impact voter turnout in Pennsylvania (PA), a key “tipping point” state? The gold standard to address this question, a randomized experiment where voters get randomized to different ads, yields unbiased estimates of the ad effect, but is very expensive. Instead, we propose a less-than-ideal, but significantly cheaper and likely faster framework based on transfer learning, where we transfer knowledge from a past ad experiment in 2020 to evaluate ads for 2024. A key component of our framework is a sensitivity analysis that quantifies the unobservable differences between past and future elections, which can be calibrated in a data-driven manner. We propose two estimators of the 2024 ad effect: a simple regression estimator with bootstrap, which we recommend for practitioners in this field, and an estimator based on the efficient influence function for broader applications. Using our framework, we estimate the effect of running a negative, digital ad campaign against Trump on voter turnout in PA for the 2024 election. Our findings indicate effect heterogeneity across counties of PA and among important subgroups stratified by gender, urbanicity, and education attainment.

Keywords: Causal inference; Exponential tilting; Generalizability; Sensitivity analysis; Transportability

^{*}The authors gratefully acknowledge Melody Huang, Ying Jin, Xiaobin Zhou, statistics student seminar participants at University of Wisconsin-Madison on April 29, 2024, and participants in the Online Causal Inference Seminar (OCIS) on April 30, 2024.

1 Introduction

1.1 Motivation: Learning From Past Ad Campaigns

During every election, campaigns run ads to influence the political narrative and voter turnout and in recent years, evaluated ad effectiveness through experiments. For example, in the most recent, 2020 U.S. presidential election, Aggarwal et al. (2023) conducted a large-scale, randomized experiment among 1,999,282 registered voters from Pennsylvania (PA), Wisconsin (WI), Michigan (MI), North Carolina (NC) and Arizona (AZ). They found that a negative, digital ad campaign against Donald Trump during the 2020 U.S. presidential election was ineffective in changing voter turnout. For other examples, see Gerber et al. (2011) and Kalla and Broockman (2018).

The main question we address in this paper is inspired by Aggarwal et al. (2023): similar to 2020, would negative digital ads against Trump be ineffective in changing voter turnout for the 2024 U.S. presidential election? In both 2020 and 2024 elections, Trump is the nominee for the Republican party and digital anti-Trump ads have been used throughout. But, as Aggarwal et al. (2023) cautioned, their null results may not generalize to elections that are less exceptional than 2020, notably when COVID-19 emerged. In 2024, voters face new issues including women’s rights, inflation, immigration, the Russo-Ukraine War and the Israel-Hamas War (Pew Research Center, 2024; Ipsos Core Political, 2024). Also, after the attack on the U.S. Capitol Building on January 6, 2021, a recent study (Loving and Smith, 2024) found that a significant number of Republican voters left their party and did not return. In short, there are unmeasurable and measurable changes between 2020 and 2024 in terms of electoral contexts and voter demographics.

The ideal approach to answer the paper’s question is to run a randomized experiment

in 2024, similar to the one in Aggarwal et al. (2023). However, ad campaigns are expensive; Aggarwal et al. (2023)’s experiment costed \$8.9 million U.S. dollars (USD). More recently, one super political action committee for the Democratic Party, which was characterized as “an ad-making laboratory...testing thousands of messages, social media posts and ads in the 2024 race, ranking them in order of effectiveness and approving only those that resonate with voters”, has already spent \$450 million USD for the 2024 election (Schleifer and Goldmacher, 2024).

Our approach to answer the question is less than ideal, but arguably significantly cheaper and likely quicker. Specifically, we use transfer learning with sensitivity analysis to “transfer” knowledge from the existing 2020 experiment by Aggarwal et al. (2023) while accounting for changes in context and voter demographics between 2020 and 2024. More formally, transfer learning uses the overlapping measurements about voters in 2020 and 2024 (e.g., gender, age group, party affiliation, voting history) to “adjust” for measurable differences between the two elections. We then use parameters from a sensitivity analysis to quantify any unmeasured differences between 2020 and 2024 (e.g., changes in electoral context) and propose an intuitive, data-driven procedure to calibrate/benchmark the magnitude of these parameters based on sample splitting and an idea from design sensitivity (Rosenbaum, 2004, 2020). For our data analysis, this calibration procedure assesses whether the unmeasured differences between 2020 and 2024 are larger compared to those between “blue-collar” states and non-blue-collar states in 2020; see Section 6.1 for details.

With our framework, we estimate the effect of negative, digital ads against Trump on voter turnout for the 2024 U.S. presidential election. We focus on roughly 4.9 million registered voters in Pennsylvania (PA) as our target population. PA is not only the largest swing state in terms of electoral votes, but also the “tipping point state” for the 2024

U.S. presidential election (e.g., FitzGerald (2024); FiveThirtyEight (2024)). We present a county-by-county analysis of the ad effect and a subgroup analysis among 20 politically important subgroups. We find that if 2020 and 2024 elections are similar with respect to some of the voters’ demographics (see Section 6.1), the negative digital ad campaign against Trump would decrease voter turnout in Fulton county for the 2024 election. Interestingly, Fulton county had the largest share of votes for Trump in 2020 among all 67 counties in PA (i.e., 85.41% votes for Trump). But, the ads are estimated to remain ineffective in all other counties of PA for the 2024 election. Also, if there are slight, unmeasured differences between 2020 and 2024, the ad campaign against Trump can change voter turnout in 55 out of 67 counties in PA; see Section 6 for details on interpreting sensitivity parameters. Comparing our results with the results of the 2020 election, our analysis suggests that the negative ads in 2024 impact mostly Trump-leaning counties in terms of depressing voter turnout. In the subgroup analysis, we find that anti-Trump ads can decrease voter turnout among female voters living in rural areas with low college education and increase voter turnout among non-female voters living in urban areas with high college education.

1.2 Related Work and Contributions

Our work builds upon several works on generalizing or transporting treatment effects from a source population (i.e., voters in the 2020 election) to a target population (i.e., voters in the 2024 election) under a sensitivity analysis framework (Nguyen et al., 2017; Nie et al., 2021; Colnet et al., 2021; Dahabreh et al., 2023; Zeng et al., 2023; Duong et al., 2023; Ek and Zachariah, 2023; Huang, 2024b). Specifically, we work under the exponential tilting sensitivity model (Robins et al., 2000), which has been used in works on generalizability and transportability (Franks et al., 2020; Dahabreh et al., 2020; Scharfstein et al., 2021;

Dahabreh et al., 2022), and make the following contributions.

- (a) We allow the source data (i.e., the 2020 data from Aggarwal et al. (2023)’s experiment)) to have more covariates than the target data (i.e., the 2024 PA voter registration data). Not only was this the case in our own data analysis, but this setting is also common when the source data is derived from a randomized experiment where detailed information about the study units is collected. Zeng et al. (2023) also considered this setup for a similar reason, but focused on efficient and minimax estimation. See also Supplement C.3 of Jin and Rothenhäusler (2024) who considered conditional inference under this setup.
- (b) We propose a simple regression estimator with nonparametric, percentile bootstrap to estimate the treatment effect in the target population. This is our recommended procedure for practitioners evaluating ads, or, more generally, evaluating treatments/policies for a target population where there are both measurable and unmeasurable differences between the source and target populations. We recommend this procedure because of its simplicity, theoretically attractive properties (e.g., consistency, asymptotic normality), and because the estimator based on the efficient influence function (EIF) lacks the “rate double robustness” property; see below. Also, while qualitatively suggested in several works in this area, we formally show one theoretically correct approach to conduct bootstrap-based inference for transfer learning; see Section 4.1.
- (c) We also propose an estimator based on the EIF. This result extends the novel results in Zeng et al. (2023) to the setting where sensitivity parameters are present. While this estimator is more widely applicable than that in (b), it is more complex, necessitates estimating four nuisance functions and is not doubly robust; see Section 4.2

(d) For either procedure (b) or (c), we propose a simple calibration procedure to generate a plausible, “reference” magnitude of the sensitivity parameter. Often in sensitivity analysis, practitioners are unsure whether a sensitive parameter is small or large as the parameter represents unobserved differences that cannot be adjusted by measured confounders. Unlike existing methods for calibration (e.g., Hsu and Small (2013); Cinelli and Hazlett (2020); Huang (2024b)) based on omitting a measured covariate, our calibration procedure uses the same covariates for calibration and sensitivity analysis and is inspired by a clever idea underlying design sensitivity (Rosenbaum, 2004, 2020) and sample splitting. Specifically, we create a data-driven “favorable” situation (Rosenbaum, 2020, Chapter 15) by splitting the source data in Aggarwal et al. (2023) and restricting the sensitivity parameters to values that are plausible in the partitioned data; see Section 5.

While the listed contributions are directly motivated from the statistical challenges in our data analysis, we believe they can be meaningful in other contexts, notably in generalizing the results of a randomized trial to a target population. More broadly, we hope our analysis pipeline centered on sensitivity analysis with transfer learning is useful to practitioners who want a simple, but theoretically valid approach for generalization or transportation tasks.

2 Transfer Learning Between Elections

2.1 Setup: Observed Data

Suppose we collect n_s i.i.d. samples from a source population and for each study unit $i \in \mathcal{I}_s = \{1, \dots, n_s\}$, we observe the following data:

$$\text{Source Data: } \{\mathbf{O}_i = (\mathbf{X}_i, A_i, Y_i, S_i = 1), i \in \mathcal{I}_s\}.$$

	Sample Indicator S_i	Observed Data			Counterfactuals		
		Covariates \mathbf{V}_i	$\mathbf{X}_i \setminus \mathbf{V}_i$	Treatment Assignment A_i	Outcome Y_i	$Y_i^{(1)}$	$Y_i^{(0)}$
Source (n_s) (2020 RCT data (Aggarwal et al., 2023))	1	✓	✓	1	✓	✓	
	1	✓	✓	0	✓		✓
Target (n_t) (2024 PA voter registration database)	0	✓					

Figure 2.1: A visualization of the data setup.

The variable $\mathbf{X}_i \in \mathcal{X}$ is the pre-treatment covariate (e.g., voter demographics), A_i is the binary treatment indicator (e.g., assigned to ad campaign against Trump or not), Y_i is the binary outcome (e.g., voted or not), and S_i indicates whether the study unit is from the source sample (i.e., $S_i = 1$) or not (i.e., $S_i = 0$). In our data analysis, the source data is from Aggarwal et al. (2023) where there were $n_s = 1,999,282$ registered voters from the five states: PA, WI, MI, NC, and AZ. We also collect n_t i.i.d. samples from the target population and for each study unit $i \in \mathcal{I}_t = \{n_s + 1, \dots, n_s + n_t = n\}$, we observe the following data¹:

$$\text{Target Data: } \{\mathbf{O}_i = (\mathbf{V}_i, S_i = 0), i \in \mathcal{I}_t\}.$$

The variable $\mathbf{V}_i \in \mathcal{V} \subseteq \mathcal{X}$ is a subset of the covariates in \mathcal{X} . In our data analysis, the target data is registered voters from PA’s voter registration database and \mathbf{V}_i is voter i ’s demographic information in the database (e.g., age group, gender, party affiliation, voting history). Because \mathbf{V}_i is present in both the source and the target data, we refer to it as a shared covariate. Figure 2.1 summarizes our data setup.

We make some remarks about the setup. First, if the covariates are discrete, some modeling assumptions about the outcome regression or the propensity score in Sections 4.1

¹For notational convenience, we overload the notation \mathbf{O}_i to represent the observed data from unit i . If the data is from the source, $\mathbf{O}_i = (\mathbf{X}_i, A_i, Y_i, S_i = 1)$ and if the data is from the target, $\mathbf{O}_i = (\mathbf{V}_i, S_i = 0)$.

and 4.2 are automatically satisfied. In our analysis, all covariates were discrete, including the voter’s age, which was measured by Aggarwal et al. (2023) as an age group. Second, we allow $\mathcal{V} \subseteq \mathcal{X}$ because, as far as we are aware of, there is no publicly available dataset of the 2024 voter population that measured the same attributes about voters as the source data from 2020. In general, we find that if the source population is from a randomized controlled trial, the covariates from it (i.e., \mathbf{X}_i) are richer than those from the target population (i.e., \mathbf{V}_i); see Zeng et al. (2023) who echoed a similar sentiment. Third, while we focus on binary outcomes Y_i due to our data analysis, our framework generalizes to a continuous outcome; see Section A of the Appendix. Fourth, similar to other works in transfer learning, we assume that the units in the source and the target data are independent and sampled from an infinite population in order to derive asymptotic properties of our estimators below. But, this may be a poor approximation in some settings; see Jin and Rothenhäusler (2024) for detailed discussions. Section 7 discusses this issue in the context of our data analysis.

2.2 Setup: Causal Estimands and Nuisance Parameters

We use the counterfactual framework to define causal effects. Let $Y_i^{(a)}$ be the counterfactual outcome of unit i when the treatment is, possibly contrary to fact, set to $a \in \{0, 1\}$. The causal estimand of interest, denoted as θ , is the average treatment effect in the target population (TATE):

$$\theta = \theta_1 - \theta_0, \text{ where } \theta_a = \mathbb{E}(Y_i^{(a)} \mid S_i = 0) \text{ and } a \in \{0, 1\}.$$

In our data analysis, θ is the average effect of a digital ad campaign against Trump on voter turnout among registered PA voters in 2024. We remark that for a binary outcome, other measures of treatment effects are possible, such as the risk ratio θ_1/θ_0 and the odds ratio $[\theta_1/(1 - \theta_1)][\theta_0/(1 - \theta_0)]^{-1}$. While we focus on mean differences (i.e. $\theta_1 - \theta_0$) like

Aggarwal et al. (2023), our results are derived for θ_a and thus, can be extended to cover the risk ratio and the odds ratio; see Ye et al. (2023) for an example.

We define the following functions, often referred to as nuisance parameters.

- The propensity score in the source population: $\pi(\mathbf{x}) = \mathbb{P}(A_i = 1 \mid \mathbf{X}_i = \mathbf{x}, S_i = 1)$, $\mathbf{x} \in \mathcal{X}$.
- The outcome models in the source population for each level of treatment $a \in \{0, 1\}$:
 - With all covariates \mathbf{X}_i : $\mu_a(\mathbf{x}) = \mathbb{E}(Y_i \mid \mathbf{X}_i = \mathbf{x}, A_i = a, S_i = 1)$, $\mathbf{x} \in \mathcal{X}$.
 - With the shared covariates \mathbf{V}_i : $\rho_a(\mathbf{v}) = \mathbb{E}(\mu_a(\mathbf{X}_i) \mid \mathbf{V}_i = \mathbf{v}, S_i = 1)$, $\mathbf{v} \in \mathcal{V}$.
- The ratio of probability densities of \mathbf{V}_i between the target and the source populations: $w(\mathbf{v}) = p_{\mathbf{V}_i|S=0}(\mathbf{v} \mid S_i = 0)/p_{\mathbf{V}_i|S=1}(\mathbf{v} \mid S_i = 1)$ where $p_{\mathbf{V}_i|S=s}(\cdot)$ denotes the conditional density of \mathbf{V}_i given $S_i = s$ and $\mathbf{v} \in \mathcal{V}$.

We conclude by defining the following notations for order and convergences. For two real sequences of numbers b_n and d_n , we denote $b_n = O(d_n)$ if $|b_n| \leq C|d_n|$ for a constant C and denote $b_n \asymp d_n$ if $b_n = O(d_n)$ and $d_n = O(b_n)$. We use \rightarrow_p to denote convergence in probability and \rightarrow_d to denote convergence in distribution. For a random variable Z_n and a real sequence of numbers b_n we denote $Z_n = o_p(b_n)$ if $Z_n/b_n \rightarrow_p 0$. For a measurable and integrable function $f(\cdot)$, we denote its L_2 norm with respect to \mathbb{P} by $\|f(\mathbf{O}_i)\| = \sqrt{\mathbb{E}\{f^2(\mathbf{O}_i)\}}$.

2.3 Causal Identification

To identify the TATE, it's common to make two sets of assumptions (Stuart et al., 2011; Tipton, 2013; Nguyen et al., 2017; Dahabreh et al., 2023; Zeng et al., 2023; Huang, 2024a,b).

The first set of assumptions ensures the identification of the average treatment effect (ATE) in the source population with the source data.

Assumption 2.1 (Identification of the ATE in the Source Population)

1. (Stable Unit Treatment Value Assumption, SUTVA, Rubin (1980)): $Y_i = Y_i^{(A_i)}$ if $S_i = 1$.
2. (Strong Ignorability, Rosenbaum and Rubin (1983)): $Y_i^{(1)}, Y_i^{(0)} \perp\!\!\!\perp A_i \mid \mathbf{X}_i, S_i = 1$ and $0 < \pi(\mathbf{x}) < 1$ for $\mathbf{x} \in \mathcal{X}$.

Assumption 2.1 is automatically satisfied if the source data is from a randomized controlled trial, such as our source data from Aggarwal et al. (2023). Also, to identify the TATE, SUTVA is not necessarily for the target population (i.e. $S_i = 0$). This is because the identification strategy under transfer learning is based on transferring information about the potential outcomes, not the observed outcomes.

The second set of assumptions ensures that we can generalize or transfer the identified ATE from the source population to the target population.

Assumption 2.2 (Positivity of S_i) $\mathbb{P}(S_i = 1 \mid \mathbf{V}_i = \mathbf{v}) > 0$ for $\mathbf{v} \in \mathcal{V}$; $\mathbb{P}(S_i = 0) > 0$.

Assumption 2.3 (Transportability) $Y_i^{(1)}, Y_i^{(0)} \perp\!\!\!\perp S_i \mid \mathbf{V}_i$.

The first part of Assumption 2.2 will be violated if there are some values of the shared covariates \mathbf{V}_i that are only observed in the target population, for instance if Aggarwal et al. (2023) focused only on young voters and the target population consists of voters from all ages. The second part of Assumption 2.2 will be violated if the target sample size is much smaller than the source sample size. Because both parts depend solely on observable quantities, Assumption 2.2 can be checked with data; see Figure 6.1 for an example.

Assumption 2.3, henceforth referred to as transportability, states that conditional on the shared covariates \mathbf{V}_i , the distributions of the potential outcomes are identically distributed between the source and the target populations. The assumption is violated if the distribution of the potential outcomes differ between the source and the target populations after adjusting for \mathbf{V}_i . For example, if \mathbf{V}_i only contains political party, Assumption 2.3 will be violated if within each political party, voter turnout under treatment or control is different between the 2020 and 2024 elections. Unfortunately, unlike Assumption 2.2, Assumption 2.3 depends on counterfactual quantities and cannot be checked with data. Furthermore, unlike strong ignorability in Assumption 2.1, we are not aware of a feasible experimental design to guarantee Assumption 2.3 in electoral contexts². This is the main motivation for us to embed sensitivity analysis within transfer learning so that our framework does not rely on Assumption 2.3; see Section 3.

Under Assumptions 2.1-2.3, the TATE can be identified (Zeng et al., 2023):

$$\theta = \mathbb{E}[\mathbb{E}\{\mu_1(\mathbf{X}_i) - \mu_0(\mathbf{X}_i) \mid \mathbf{V}_i, S_i = 1\} \mid S_i = 0]. \quad (2.1)$$

In words, θ is identified by first averaging the conditional average treatment effect in the source population (i.e., CATE or formally, $\mu_1(\mathbf{X}_i) - \mu_0(\mathbf{X}_i)$) over the shared covariates \mathbf{V}_i (i.e., the inner expectation in equation (2.1)) and second, averaging this quantity among units in the target population (i.e., the outer expectation in equation (2.1)). For estimation of θ under Assumptions 2.1-2.3, see Zeng et al. (2023).

²One experimental design to satisfy Assumption 2.3 is for the investigator to randomize the selection of study units into the source sample (Tipton, 2013; Cook, 2014; Tipton and Peck, 2017). In our data analysis, this design implies Aggarwal et al. (2023) randomized voters to be either in their 2020 study or to be a registered voter in PA for the 2024 election. We believe that this design is impractical and the “nonignorable selection bias” into the target or the source sample is unavoidable.

3 Sensitivity Analysis of Transportability

As discussed above, suppose transportability (i.e., Assumption 2.3) no longer holds and we measure the departure from it by the sensitivity parameter $\gamma_a \in \mathbb{R}$ for $a \in \{0, 1\}$. The parameter γ_a is the logarithm of the odds ratio of counterfactual outcomes between the target and source populations:

$$\gamma_a = \log \left(\frac{\text{ODD}_a(\mathbf{v}, 0)}{\text{ODD}_a(\mathbf{v}, 1)} \right), \quad \text{ODD}_a(\mathbf{v}, s) = \frac{\mathbb{P}(Y_i^{(a)} = 1 \mid \mathbf{V}_i = \mathbf{v}, S_i = s)}{\mathbb{P}(Y_i^{(a)} = 0 \mid \mathbf{V}_i = \mathbf{v}, S_i = s)}, \quad s \in \{0, 1\}, \mathbf{v} \in \mathcal{V}. \quad (3.1)$$

When $\gamma_a = 0$, i.e., the distribution of $Y_i^{(a)}$ is identical in the source and target populations conditioned on the shared covariates \mathbf{V}_i , Assumption 2.3 holds, and we recover the setting in Zeng et al. (2023). As γ_a moves away from 0, the degree of violation of transportability increases. For example, in our data analysis, $\gamma_1 = 0.05$ means that the counterfactual odd of voting in 2024 is $\exp(0.05) \approx 1.05$ times that in 2020 when a registered voter, possibly contrary to fact, gets negative ads against Trump. The sensitivity parameter γ_a is not identified and cannot be estimated. In this and the subsequent sections, we discuss the identification and estimation of the TATE with a given γ_a , and then in Section 5 we discuss a data-driven approach to calibrate this parameter.

Under the sensitivity model (3.1) and for a given $\gamma_a \in \mathbb{R}$, the expected counterfactual outcome under treatment level $a \in \{0, 1\}$ can be identified as follows.

Lemma 3.1 (Identification of TATE Under Sensitivity Model) *Suppose Assumptions 2.1, 2.2 and the sensitivity model in model (3.1) hold. For a given $\gamma_a \in \mathbb{R}$, the expected counterfactual outcome under treatment level $a \in \{0, 1\}$ is*

$$\begin{aligned} \mathbb{E}[Y_i^{(a)} \mid S_i = 0] &= \mathbb{E} \left[\frac{\exp(\gamma_a) \rho_a(\mathbf{V}_i)}{\exp(\gamma_a) \rho_a(\mathbf{V}_i) + 1 - \rho_a(\mathbf{V}_i)} \middle| S_i = 0 \right] \\ &= \theta_a(\gamma_a). \end{aligned} \quad (3.2)$$

To highlight the inclusion of the sensitivity analysis, we denote the mean counterfactual outcome under treatment level a by $\theta_a(\gamma_a)$ and the TATE by $\theta_1(\gamma_1) - \theta_0(\gamma_0)$. Despite the expanded notation, the interpretation of $\theta_a(\gamma_a)$ as an average of the counterfactual outcome $Y_i^{(a)}$ in the target population remains the same regardless of the value of γ_a . For example, in our data analysis, if $\gamma_1 = 0$, $\theta_1(0)$ is the proportion of registered PA voters who would vote in the 2024 election if all voters were assigned to anti-Trump digital ads and transportability held. If $\gamma_1 = 0.1$, $\theta_1(0.1)$ is the proportion of registered PA voters who would vote in the 2024 election if all voters were assigned to anti-Trump digital ads and transportability was violated by $\gamma_1 = 0.1$.

We conclude this section with a couple of remarks on the sensitivity model (3.1). First, this model was first proposed by Robins et al. (2000) as a non-parametric (just) identified model for describing selection bias in missing data. The model was later called an exponential tilting model (Rotnitzky et al., 2001; Birmingham et al., 2003), an extrapolation-factorization model (Linero and Daniels, 2018) and Tukey’s representation (Franks et al., 2020). The model was also used to conduct sensitivity analysis for unmeasured confounding in causal inference (Franks et al., 2020; Scharfstein et al., 2021) and for violation of the transportability assumption in generalizability (Dahabreh et al., 2022). In particular, when $\mathcal{V} = \mathcal{X}$, Lemma 3.1 recovers the identification of the TATE in Dahabreh et al. (2022). Second, we choose this model for sensitivity analysis as it (a) posits no testable implications on the data, (b) makes statistical inference tractable (e.g., asymptotic normality), and (c) has a simple, odds ratio interpretation. Third, the sensitivity model can be extended in various ways. For example, it can be extended to handle a continuous, counterfactual outcome where the extension would tilt the entire density of the counterfactual outcome; see Section A of the Appendix where we discuss identification, estimation, and interpretation

of the TATE under a sensitivity model for a continuous, counterfactual outcome. Also, extensions to model (3.1) can induce unmeasured differences as a function of the outcome $Y_i^{(a)}$ and covariates \mathbf{V}_i ; see Franks et al. (2020) and Scharfstein et al. (2021) for examples. In addition, model (3.1) can be reformulated under a selection model (see Section A of the Appendix) or under an R^2 -based model (Franks et al., 2020).

4 Estimation and Inference

4.1 Outcome Regression and Percentile Bootstrap

The analysis pipeline in this section is most appropriate when \mathcal{X} is discrete or, more generally, when the outcome regression model $\rho_a(\mathbf{v})$ can be consistently estimated at a parametric rate. This is the case in our data analysis where voter’s demographics are discrete variables. Even if \mathcal{X} is not discrete, we suggest investigators begin with the analysis in this section since it is not only simple, but also the alternative analysis based on the efficient influence function (EIF) does not have doubly robust rates; see Section 4.2.

From equation (3.2), a natural estimator of $\theta_a(\gamma_a)$ would be a plug-in estimator that takes a weighted average of an estimator of $\rho_a(\mathbf{v})$, denoted as $\hat{\rho}_a(\mathbf{v})$, among the target sample:

$$\hat{\theta}_{\text{OR},a}(\gamma_a) = \frac{1}{n_t} \sum_{i \in \mathcal{I}_t} \frac{\exp(\gamma_a) \hat{\rho}_a(\mathbf{V}_i)}{\exp(\gamma_a) \hat{\rho}_a(\mathbf{V}_i) + 1 - \hat{\rho}_a(\mathbf{V}_i)}. \quad (4.1)$$

Also, a simple estimator of $\hat{\rho}_a(\mathbf{v})$ is motivated by its definition where we regress $\hat{\mu}_a(\mathbf{x})$ on \mathbf{v} using least squares and $\hat{\mu}_a(\mathbf{x})$ is an estimate of $\mu_a(\mathbf{x})$. For example, if \mathcal{X} is discrete, both $\hat{\mu}_a(\mathbf{x})$ and $\hat{\rho}_a(\mathbf{v})$ can be expressed as

$$\hat{\mu}_a(\mathbf{x}) = \frac{\sum_{i \in \mathcal{I}_s} Y_i \mathbf{1}(A_i = a, \mathbf{X}_i = \mathbf{x})}{\sum_{i \in \mathcal{I}_s} \mathbf{1}(A_i = a, \mathbf{X}_i = \mathbf{x})}, \quad \hat{\rho}_a(\mathbf{v}) = \frac{\sum_{i \in \mathcal{I}_s} \hat{\mu}_a(\mathbf{X}_i) \mathbf{1}(\mathbf{V}_i = \mathbf{v})}{\sum_{i \in \mathcal{I}_s} \mathbf{1}(\mathbf{V}_i = \mathbf{v})}, \quad \mathbf{x} \in \mathcal{X}, \mathbf{v} \in \mathcal{V}, \quad (4.2)$$

where $\mathbf{1}(\cdot)$ is the indicator function. In the discrete case, the estimators in equation (4.2) are consistent. For inference, we recommend a nonparametric, percentile bootstrap (Efron, 1979) where the source and the target data are resampled separately and we take the $\alpha/2$ and $1 - \alpha/2$ quantiles of the bootstrapped estimates of $\hat{\theta}_{\text{OR},a}(\gamma_a)$, denoted $\hat{L}_a(\gamma_a; 1 - \alpha)$ and $\hat{U}_a(\gamma_a; 1 - \alpha)$ respectively. These quantiles are used to construct a $(1 - \alpha)$ confidence interval (CI), denoted as $\widehat{\text{CI}}_{\text{OR},a}(\gamma_a; 1 - \alpha) = \left[\hat{L}_a(\gamma_a; 1 - \alpha), \hat{U}_a(\gamma_a; 1 - \alpha) \right]$.

Formally, suppose $\rho_a(\mathbf{v})$ is indexed by a finite-dimensional parameter $\boldsymbol{\eta}_a$ and denote its estimate as $\rho_a(\mathbf{v}, \hat{\boldsymbol{\eta}}_a)$. Theorem 4.1 shows that under regularity conditions, the plug-in estimator $\hat{\theta}_{\text{OR},a}(\gamma_a)$ in (4.1) is consistent and the nonparametric, percentile bootstrap leads to a valid CI.

Theorem 4.1 (Theoretical Properties of the OR Estimator and Bootstrapped CI)

Suppose Assumptions 2.1 and 2.2 hold and $\theta_a(\gamma_a) \in \Theta$ where Θ is open and compact. Also suppose $\rho(\mathbf{v}; \boldsymbol{\eta}_a)$ is twice differentiable with respect to $\boldsymbol{\eta}_a$. If $\hat{\boldsymbol{\eta}}_a$ is an asymptotically linear estimate of $\boldsymbol{\eta}_a$ and $n_s \asymp n_t$, then $\hat{\theta}_{\text{OR},a}(\gamma_a) \rightarrow_p \theta_a(\gamma_a)$. Furthermore, if regularity conditions (B1)-(B4) in Section B of the Appendix hold, the bootstrap interval $\widehat{\text{CI}}_{\text{OR},a}(\gamma_a; 1 - \alpha)$ for $\alpha \in (0, 0.5)$ satisfies $\mathbb{P}(\theta_a(\gamma_a) \in \widehat{\text{CI}}_{\text{OR},a}(\gamma_a; 1 - \alpha)) \rightarrow 1 - \alpha$.

4.2 Efficient Influence Function

The analysis pipeline in this section is based on the efficient influence function (EIF) and is more general than that in Section 4.1, especially when \mathcal{V} is not discrete and the propensity score is unknown. However, it is more complex and requires estimating multiple nuisance functions. To motivate the estimator, we first derive the EIF of $\theta_a(\gamma_a)$ in Theorem 4.2.

Theorem 4.2 (Efficient Influence Function of $\theta_a(\gamma_a)$) *Under Assumptions 2.1 and 2.2,*

the EIF of $\theta_a(\gamma_a)$ is

$$\begin{aligned} \text{EIF}(\mathbf{O}_i, \theta_a(\gamma_a)) &= \frac{S_i w(\mathbf{V}_i)}{\mathbb{P}(S_i = 1)} \frac{\exp(\gamma_a)}{[\exp(\gamma_a) \rho_a(\mathbf{V}_i) + 1 - \rho_a(\mathbf{V}_i)]^2} \left[\left\{ \frac{A_i}{\pi(\mathbf{X}_i)} + \frac{1 - A_i}{1 - \pi(\mathbf{X}_i)} \right\} \{Y_i - \mu_a(\mathbf{X}_i)\} \right. \\ &\quad \left. + \mu_a(\mathbf{X}_i) - \rho_a(\mathbf{V}_i) \right] + \frac{1 - S_i}{\mathbb{P}(S_i = 0)} \left[\frac{\exp(\gamma_a) \rho_a(\mathbf{V}_i)}{\exp(\gamma_a) \rho_a(\mathbf{V}_i) + 1 - \rho_a(\mathbf{V}_i)} - \theta_a(\gamma_a) \right], \end{aligned}$$

Also, if the propensity score $\pi(\mathbf{X}_i)$ is known, the EIF of $\theta_a(\gamma_a)$ remains unchanged.

The EIF involves four nuisance quantities: the propensity score $\pi(\mathbf{X}_i)$, the ratio of densities of the covariates between the target and the source population $w(\mathbf{V}_i)$, and two outcome regression functions $\mu_a(\mathbf{X}_i)$ and $\rho_a(\mathbf{V}_i)$. When transportability holds, i.e., $\exp(\gamma_a) = 1$, Theorem 4.2 reduces to the EIF in Zeng et al. (2023).

We follow the modern trend in causal inference where we use cross-fitting (Chernozhukov et al., 2017; Kennedy, 2022) and the EIF to estimate $\theta_a(\gamma_a)$. Specifically, we randomly partition the source and target sample indices \mathcal{I}_s and \mathcal{I}_t into K disjoint sets, $\mathcal{I}_s^{(k)}$ and $\mathcal{I}_t^{(k)}$, respectively, for $k = 1, 2, \dots, K$, and let $\mathcal{I}^{(k)} = \mathcal{I}_s^{(k)} \cup \mathcal{I}_t^{(k)}$. For each k , the nuisance functions are estimated with data in $\mathcal{I} \setminus \mathcal{I}^{(k)}$ and they are denoted as $\hat{\pi}^{(k)}(\mathbf{x})$, $\hat{\mu}_a^{(k)}(\mathbf{x})$, $\hat{w}^{(k)}(\mathbf{v})$ and $\hat{\rho}_a^{(k)}(\mathbf{v})$. We then plug them into the ‘‘uncentered’’ EIF and evaluate it with the data in $\mathcal{I}^{(k)}$, i.e.,

$$\begin{aligned} \hat{\theta}_{\text{EIF},a}^{(k)}(\gamma_a) &= \frac{1}{|\mathcal{I}_s^{(k)}|} \sum_{i \in \mathcal{I}_s^{(k)}} \frac{\exp(\gamma_a) \hat{w}^{(k)}(\mathbf{V}_i)}{[\exp(\gamma_a) \hat{\rho}_a^{(k)}(\mathbf{V}_i) + 1 - \hat{\rho}_a^{(k)}(\mathbf{V}_i)]^2} \left[\left\{ \frac{A_i}{\hat{\pi}^{(k)}(\mathbf{X}_i)} + \frac{1 - A_i}{1 - \hat{\pi}^{(k)}(\mathbf{X}_i)} \right\} \{Y_i - \hat{\mu}_a^{(k)}(\mathbf{X}_i)\} \right. \\ &\quad \left. + \hat{\mu}_a^{(k)}(\mathbf{X}_i) - \hat{\rho}_a^{(k)}(\mathbf{V}_i) \right] + \frac{1}{|\mathcal{I}_t^{(k)}|} \sum_{i \in \mathcal{I}_t^{(k)}} \frac{\exp(\gamma_a) \hat{\rho}_a^{(k)}(\mathbf{V}_i)}{\exp(\gamma_a) \hat{\rho}_a^{(k)}(\mathbf{V}_i) + 1 - \hat{\rho}_a^{(k)}(\mathbf{V}_i)}. \end{aligned}$$

Finally, we take an average of $\hat{\theta}_{\text{EIF},a}^{(k)}(\gamma_a)$ to arrive at the EIF-based cross-fitting estimator of $\theta_a(\gamma_a)$, which we denote as $\hat{\theta}_{\text{EIF},a}(\gamma_a) = K^{-1} \sum_{k=1}^K \hat{\theta}_{\text{EIF},a}^{(k)}(\gamma_a)$. Theorem 4.3 shows that $\hat{\theta}_{\text{EIF},a}(\gamma_a)$ is consistent, asymptotically normal, and semiparametrically efficient.

Theorem 4.3 (Theoretical Properties of the EIF-Based Estimator) *Suppose Assumptions 2.1 and 2.2 hold and there exist $c, C > 0$ such that $c < \hat{\pi}^{(k)}(\mathbf{x})$, $\hat{w}^{(k)}(\mathbf{v}) < C$ and*

$\widehat{\rho}_a^{(k)}(\mathbf{v}) \in [0, 1]$ for $\mathbf{v} \in \mathcal{V}$ and $\mathbf{x} \in \mathcal{X}$. Then, the following holds:

(i) [Conditional Double Robustness]. Suppose $\widehat{\rho}_a^{(k)}$ is a consistent estimator of $\rho_a^{(k)}$ (i.e., $\|\widehat{\rho}_a^{(k)}(\mathbf{V}_i) - \rho_a^{(k)}(\mathbf{V}_i)\| = o_p(1)$). Then, $\widehat{\theta}_{\text{EIF},a}(\gamma_a) \rightarrow_p \theta_a(\gamma_a)$ if

$$\|\widehat{\pi}^{(k)}(\mathbf{X}_i) - \pi^{(k)}(\mathbf{X}_i)\| \cdot \|\widehat{\mu}_a^{(k)}(\mathbf{X}_i) - \mu_a^{(k)}(\mathbf{X}_i)\| = o_p(1), \quad (4.3)$$

(ii) [Asymptotic normality and Semiparametric Efficiency] Suppose $\widehat{\rho}_a^{(k)}$, $\widehat{\mu}_a^{(k)}$, $\widehat{w}^{(k)}$, and $\widehat{\pi}^{(k)}$ are consistent estimators with the following rates:

$$\|\widehat{\pi}^{(k)}(\mathbf{X}_i) - \pi^{(k)}(\mathbf{X}_i)\| \cdot \|\widehat{\mu}_a^{(k)}(\mathbf{X}_i) - \mu_a^{(k)}(\mathbf{X}_i)\| = o_p(n^{-1/2}), \quad (4.4a)$$

$$\|\widehat{w}^{(k)}(\mathbf{V}_i) - w^{(k)}(\mathbf{V}_i)\| \cdot \|\widehat{\rho}_a^{(k)}(\mathbf{V}_i) - \rho_a^{(k)}(\mathbf{V}_i)\| = o_p(n^{-1/2}), \quad \text{and} \quad (4.4b)$$

$$\|\widehat{\rho}_a^{(k)}(\mathbf{V}_i) - \rho_a^{(k)}(\mathbf{V}_i)\|^2 = o_p(n^{-1/2}). \quad (4.4c)$$

Then, $\sqrt{n} \left\{ \widehat{\theta}_{\text{EIF},a}(\gamma_a) - \theta_a(\gamma_a) \right\} \rightarrow_d N(0, \sigma_{\text{EIF},a}^2(\gamma_a))$ where $\sigma_{\text{EIF},a}^2(\gamma_a) = \mathbb{E}[\{\text{EIF}(\mathbf{O}_i, \theta_a(\gamma_a))\}^2]$.

(iii) [Consistent Estimator of Standard Error] Suppose the same assumptions in (ii) hold.

Then, $\widehat{\sigma}_{\text{EIF},a}^2(\gamma_a) \rightarrow_p \sigma_{\text{EIF},a}^2(\gamma_a)$, where $\widehat{\sigma}_{\text{EIF},a}^2(\gamma_a) = K^{-1} \sum_{k=1}^K \frac{1}{|\mathcal{I}^{(k)}|} \sum_{i \in \mathcal{I}^{(k)}} \left\{ \widehat{\text{EIF}}^{(k)}(\mathbf{O}_i, \widehat{\theta}_{\text{EIF},a}(\gamma_a)) \right\}^2$ and $\widehat{\text{EIF}}^{(k)}(\mathbf{O}_i, \widehat{\theta}_{\text{EIF},a}(\gamma_a))$ is the empirical counterpart of $\text{EIF}^{(k)}(\mathbf{O}_i, \widehat{\theta}_{\text{EIF},a}(\gamma_a))$ with plug-in estimates of the nuisance parameters $\widehat{\pi}^{(k)}$, $\widehat{\rho}_a^{(k)}$, $\widehat{w}^{(k)}$, and $\widehat{\mu}_a^{(k)}$.

Part (i) of Theorem 4.3 states that $\widehat{\theta}_{\text{EIF},a}(\gamma_a)$ is *conditionally doubly robust* in that if $\widehat{\rho}_a^{(k)}(\mathbf{v})$ is consistent, $\widehat{\theta}_{\text{EIF},a}(\gamma_a)$ is consistent when either $\widehat{\pi}^{(k)}(\mathbf{x})$ or $\widehat{\mu}_a^{(k)}(\mathbf{x})$, but not necessarily both, is consistent. Part (ii) states that if all the nuisance parameters are estimated consistently at the rates in equations (4.4a)-(4.4c), $\widehat{\theta}_{\text{EIF},a}(\gamma_a)$ is asymptotically normal and semiparametrically efficient. We remark that when transportability holds, our result recovers Theorem 5 of Zeng et al. (2023), which does not require equation (4.4c). In other words, equation (4.4c) can be viewed as the cost of violating transportability. Finally, for inference, parts (ii) and (iii) of Theorem 4.3 imply an asymptotically valid, $1 - \alpha$ CI of $\theta_a(\gamma_a)$ is

$\hat{\theta}_{\text{EIF},a}(\gamma_a) \pm z_{1-\alpha/2} \sqrt{\hat{\sigma}_{\text{EIF},a}^2(\gamma_a)}$ where $z_{1-\alpha/2}$ is the $1 - \alpha/2$ quantile of the standard normal distribution.

Equation (4.4c) requires that we not only consistently estimate the outcome regression $\rho_a(\mathbf{v})$, but also estimate it at a sufficiently fast rate. If $\rho_a(\mathbf{v})$ is a finite-dimensional, parametric function as in Theorem 4.1, equation (4.4c) is satisfied with a parametric estimator. However, if $\rho_a(\mathbf{v})$ is a non-parametric function, for instance a Lipschitz function with smoothness m , we effectively need $m \geq d/2$ where d is the dimension of \mathbf{V}_i to satisfy (4.4c); see Kennedy (2023). In particular, we cannot estimate $\rho_a(\mathbf{v})$ at a slow rate in hopes that another estimator of the nuisance function can “compensate” for the slow rate; this is referred to as the mixed bias property or rate double robustness (e.g., Rotnitzky et al. (2020), Kennedy (2022)). In contrast, a common approach to satisfy equation (4.4a) is to obtain data from an RCT where the propensity score is known a priori and to estimate the outcome regression using a flexible, machine learning method, which may converge slowly.

5 Calibrating the Sensitivity Parameters

5.1 A Three-Step Calibration Procedure

Suppose that an investigator estimates the TATE for a range of (γ_0, γ_1) using the methods in Sections 4.1 or 4.2 and finds that some estimates are statistically significant at the $\alpha = 0.05$ level while others are not. Perhaps, the investigator went a step further and found the “smallest” (γ_0, γ_1) where the estimate becomes insignificant (or significant). In both cases, a natural question to ask is what values of the sensitivity parameters indicate plausible deviations between the source and target populations. More generally, finding a plausible, “reference” set of sensitivity parameters has been a long-standing question in

sensitivity analysis and this task is often referred to as calibration or benchmarking (Cinelli and Hazlett, 2020; Huang, 2024b). In this section, we present a calibration procedure that generates “reference” values of the sensitivity parameters using an idea underlying design sensitivity (Rosenbaum, 2004, 2020); see Section 5.2 for more discussion. The calibration procedure is roughly divided into three steps, and a visualization of this procedure for Philadelphia county is in Figure D.1 of the Appendix.

The first step partitions the source data from Aggarwal et al. (2023) into “blue collar” states (PA, MI, WI), denoted as \mathcal{I}_{s_1} , and non-blue collar states (AZ, NC), denoted as \mathcal{I}_{s_2} . In general, the two partitions \mathcal{I}_{s_1} and \mathcal{I}_{s_2} of the source data are chosen to have unmeasurable differences between them. For example, with the blue collar and non-blue collar states, there may be differences in socioeconomic status, labor markets, and region-specific politics (i.e., Midwestern states versus non-Midwestern states) not captured by \mathbf{V}_i .

The second step temporarily treats the voters in non-blue collar states as the “proxy” target population and constructs two $1 - \alpha$ CIs of the TATE in this proxy target population:

- (Our Transfer Learning Approach): We treat the blue collar states as the “proxy” source population and use the methods in Sections 4.1 or 4.2 to infer the proxy target population. We denote the resulting confidence interval as $\widehat{\text{CI}}_{s_1 \rightarrow s_2}(\gamma_0, \gamma_1; 1 - \alpha)$.
- (Standard Approach): Using the proxy target data only (i.e., data from non-blue collar states), we compute a valid $(1 - \alpha)$ CI of the TATE, say the Wald confidence interval based on the difference-in-means estimator, and denote it as $\widehat{\text{CI}}_{s_2}(1 - \alpha)$.

A key insight is that if Assumption 2.1 holds, the CI from the standard approach (i.e., $\widehat{\text{CI}}_{s_2}(1 - \alpha)$) will cover the ATE in the proxy target population. In our example where the source data is generated from a randomized experiment, Assumption 2.1 holds by design

and $\widehat{\text{CI}}_{s_2}(1-\alpha)$ has valid coverage of the ATE among the non-blue collar states. In contrast, the CI from transfer learning $\widehat{\text{CI}}_{s_1 \rightarrow s_2}(\gamma_0, \gamma_1; 1-\alpha)$ may not cover the true ATE in the proxy target population unless (γ_0, γ_1) are chosen correctly to measure the true difference between the proxy source and the proxy target population.

Recognizing that $\widehat{\text{CI}}_{s_2}(1-\alpha)$ is a valid CI with only Assumption 2.1, we “calibrate” the transported $\widehat{\text{CI}}_{s_1 \rightarrow s_2}(\gamma_0, \gamma_1; 1-\alpha)$ by keeping the values of (γ_0, γ_1) where both CIs overlap, or formally $\mathcal{C}_1 = \{(\gamma_0, \gamma_1) \mid \widehat{\text{CI}}_{s_1 \rightarrow s_2}(\gamma_0, \gamma_1; 1-\alpha) \cap \widehat{\text{CI}}_{s_2}(1-\alpha) \neq \emptyset\}$. In other words, \mathcal{C}_1 represent plausible sensitivity parameters that capture the true unmeasured differences between the two populations. Also, conducting the original sensitivity analysis of the TATE with the sensitivity parameters in \mathcal{C}_1 restricts the original analysis to unobservable differences that the investigator designed by creating meaningful/explainable partitions of the source population.

We conclude the section with some brief remarks on implementing the calibration procedure. First, we recommend repeating the three steps above, but with the roles of the proxy target and the source populations reversed, yielding another set \mathcal{C}_2 of sensitivity parameters. The intersection $\mathcal{C} = \mathcal{C}_1 \cap \mathcal{C}_2$ consists of what we call the *plausible values* of the sensitivity parameters. Also, if any value in \mathcal{C} leads to statistically significant effects, we say that the treatment effect is *sensitive* for the effect. In contrast, if none of the values in \mathcal{C} lead to statistically significant effects, we say that the treatment effect is *insensitive* for the effect. Second, to better account for sampling variability between the original target and source populations, we recommend re-scaling the standard errors in the calibration procedure to match the ratio of the size of the original source population and the original target population; see Section D of the Appendix for details.

5.2 Comparison to Existing Methods

The inspiration for the calibration procedure comes from Rosenbaum’s extensive works on design sensitivity, specifically the notion of a “favorable situation” in Chapter 15 of Rosenbaum (2020) to benchmark designs of observational studies in terms of robustness against unmeasured confounding. Specifically, the proxy target population in our calibration procedure is similar to Rosenbaum’s favorable situation in that the investigator chooses a situation where the ATE is known and is free from hidden bias. In our setup, the proxy target’s ATE is not unknown, but can be unbiasedly estimated under Assumption 2.1 only; we do not need transportability, i.e., the assumption that we are conducting sensitivity analysis for, to identify the proxy target’s ATE. Also, roughly speaking, the set \mathcal{C}_1 contains sensitivity parameters that will “reject” towards the favorable situation. However, unlike design sensitivity, which, in our setting, would be roughly equivalent to taking the “limit” of the set \mathcal{C}_1 when sample size increases and using this limit to benchmark designs of observational studies, we directly use \mathcal{C}_1 to calibrate/benchmark our sensitivity parameters.

Another common way of calibrating sensitivity parameters is to omit an observed covariate (e.g., (Hsu and Small, 2013; Cinelli and Hazlett, 2020; Ek and Zachariah, 2023; Huang, 2024b)). But, as discussed in Section 6.2 of Cinelli and Hazlett (2020), this can lead to a misleading understanding of the magnitude of unmeasured confounding. Our calibration procedure avoids this issue by using the same covariates for sensitivity analysis and calibration.

Finally, similar to other calibration procedures, our calibration procedure cannot “...rule out the existence of killer confounders” (Huang, 2024b) and, if used incorrectly, can give misleading conclusions about the magnitude of the violation of transportability. For ex-

ample, we believe that an ineffective use of our procedure is to create a partition where there are no unmeasurable differences between the two proxy populations. Nevertheless, compared to omitting a confounder, we believe creating dissimilar partitions of the study sample can be a promising way to calibrate unobservable differences between the source and the target populations.

6 Ad Effects in Pennsylvania for the 2024 Election

6.1 Setup

We apply our approach to study the effect of running a negative, digital ad campaign against Trump among registered voters in PA for the 2024 U.S. presidential election. The target data is from the PA’s voter registration database as of April 15, 2024, which initially contained 8,716,343 registered voters. To harmonize with the source data by Aggarwal et al. (2023), we took a subset of voters in the PA database who are between 18 and 55 years old. We also recoded age, political party registration, and voting history in the PA database to match the definitions in the source data. In the end, we had $n_t = 4,880,729$ registered voters in the target data and the shared covariates \mathbf{V}_i included gender, age groups, party, and a subset of the voting history. The source covariates \mathbf{X}_i included \mathbf{V}_i , race, and a richer set of voting history. Figure 6.1 shows all of the covariates. For more details on the data description and data cleaning, see Section E of the Appendix.

For all 67 counties in PA, we estimate the ad effect in Section 6.2. We also conduct a subgroup analysis by gender, urbanicity, and education in Section 6.3. Due to page constraints and since all covariates are discrete, we present the results from the OR estimator and discuss the results from the EIF estimator in Section E of the Appendix; except for

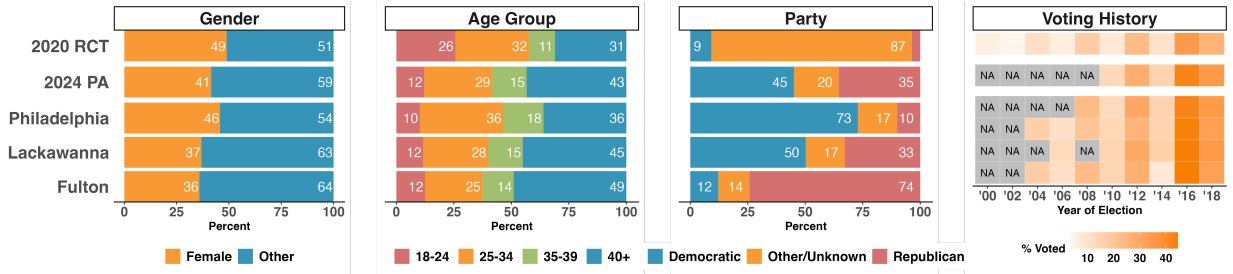


Figure 6.1: Covariate distributions from the 2020 RCT by Aggarwal et al. (2023) (i.e., the source data), 2024 PA voters (i.e., the target data), and selected counties in PA during 2024. “NA” means the corresponding variable is missing.

some discrepancies noted in Section 7, the two estimators reach the same conclusion. The regression function $\rho_a(\mathbf{v})$ is estimated by regressing $\hat{\mu}_a(\mathbf{x})$ on \mathbf{v} . Following Aggarwal et al. (2023), $\mu_a(\mathbf{x})$ is estimated by weighted least squares where the weights are the inverse propensity scores. We consider γ_a 's between -0.05 and 0.05 and as discussed above, obtain calibrated sensitivity parameters by partitioning the source data into blue-collar states (i.e., PA, WI, MI) and non blue-collar states (i.e., AZ, NC). Following Aggarwal et al. (2023), \widehat{CI}_{s_1} and \widehat{CI}_{s_2} in the calibration procedure are based on weighted least squares that regresses the outcome on the treatment and pre-treatment covariates and the weights are the inverse of the propensity scores. Throughout the analysis, we set the significance level at $\alpha = 0.05$.

6.2 Ad Effect by Counties: Key Takeaways

When transportability holds, the digital ads against Trump decreases turnout in Fulton county.

When $\gamma_0 = \gamma_1 = 0$ (i.e., transportability holds), the ad effect is negative and barely significant in Fulton county (95% CI: $[-1.64\%, -0.04\%]$, p-value: 0.04), and insignificant

in all other 66 counties; see Section E of the Appendix for the exact numbers. In other words, if the difference in voter turnout between PA voters in 2024 and the voters in 2020 can be adjusted with \mathbf{V}_i , then the ads will be ineffective in almost all counties for the 2024 election, except for Fulton county, which is slightly significant. Interestingly, Fulton county had the largest share of votes for Trump in the 2020 U.S. presidential election, with 85.41% of votes in Fulton county for Trump.

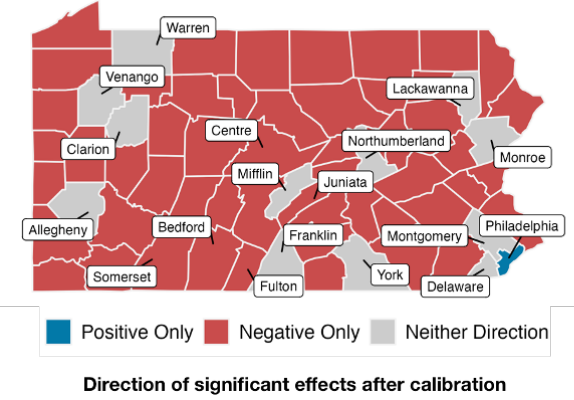
After calibration, (a) Philadelphia county is sensitive for a positive ad effect (i.e., increase turnout), (b) 54 counties are sensitive for a negative ad effect (i.e., decreased turnout), and (c) 12 counties are insensitive for an ad effect.

When $\gamma_0\gamma_1 \neq 0$ (i.e., transportability is violated), the digital ads against Trump can have statistically significant effects among the calibrated values of the sensitivity parameters; see the left panel of Figure 6.2. Philadelphia county is sensitive for a positive effect and 54 counties are sensitive for a negative effect. In words, under a range of unmeasured differences defined by the unmeasured differences between blue-collar and non blue-collar states in the source data, receiving ads against Trump can increase voter turnout in Philadelphia county and decrease voter turnout in 54 counties.

Finally, 12 counties are insensitive for a significant ad effect. In other words, even if the unmeasured differences between the 2020 and 2024 populations exist, but the magnitude of the differences is in the calibration/reference set \mathcal{C} generated from the source data, running ads against Trump will not change voter turnout in 12 counties. We remark that this does not mean that the ads are actually ineffective in the 12 counties; rather, the ads are ineffective if we only consider magnitudes of the unmeasured differences between blue-collar and non blue-collar states in the source data.

In general, we see that the direction of the ad effect after calibration roughly corre-

Sensitivity of Ad Effect for the 2024 U.S. Presidential Election



Trump's Share (%) of Votes in the 2020 U.S. Presidential Election

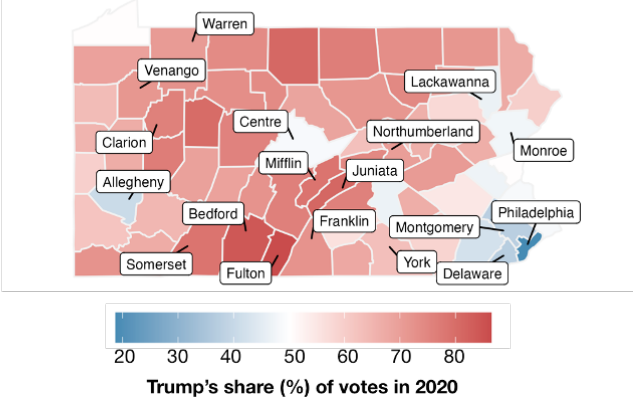


Figure 6.2: Sensitivity analysis of the ad effect for each county in PA. Left: Counties that are sensitive for a positive effect (i.e., increased turnout; in blue) or a negative effect (i.e., decreased turnout; in red). Counties that are insensitive for an effect are in gray. Right: Trump's share of votes in the 2020 U.S. presidential election.

sponds to Trump's share of votes in the 2020 U.S. presidential elections; see Figure 6.2. Philadelphia county, which was estimated to have a positive effect, has a history of voting for Democratic presidential candidates by large margins. Also, Bedford, Juniata, and Somerset counties, which were estimated to be sensitive for a negative effect, voted for Trump in 2020 by large numbers; Trump received 83%, 80%, and 77% of the votes from Bedford, Juniata, and Somerset counties, respectively. Combined with the result from Fulton county above, counties that strongly supported Trump in 2020 are likely to have negative effects during the 2024 election.

6.3 Subgroup Analysis

After overturning of *Roe v. Wade* in 2022, many argued that voter turnout will vary substantially by gender and urbanicity, especially compared to past elections (e.g., Shea and Jacobs (2023); Fair Vote (2024)). To study whether the effect of the ad will also vary

by voter demographics, we estimate the effect of running a negative, digital ad campaign against Trump among 20 subgroups of voters. The 20 subgroups are defined by a three-way interaction between gender (female versus not female), urbanicity (rural versus urban), and education attainment (five levels). Specifically, we use the U.S. Census to obtain information about whether (a) a PA voter lives in a rural or an urban census tract and (b) a PA voter lives in a zipcode with a certain level of educational attainment. Education attainment is categorized by the percentage of people with a Bachelor’s degree or higher and is in increments of 20% (i.e., $(0, 20\%]$, $(20, 40\%]$, $(40, 60\%]$, $(60, 80\%]$, $(80, 100\%]$). Section E of the Appendix contains further details about the subgroups.

Figure 6.3 summarizes the results. Under transportability, we find some variations in the ad effect among different subgroups of voters, but none of the effects are statistically significant. Voters in urban areas have non-negative ad effects regardless of gender and educational attainment and the magnitude of the effect roughly increases with educational attainment. Among voters in rural areas, the ad effect is positive among females living in areas with high educational attainment and the magnitude of this effect is comparable to voters who live in urban areas. The ad effect is most negative among female voters living in rural areas with low educational attainment. In other words, in the 2024 election, running against Trump can suppress turnout among female voters living in rural areas with low educational attainment.

When transportability is violated and after calibration, the ad effect is sensitive in a negative direction among female voters living in rural areas with moderate to low educational attainment. The ad effect is sensitive in a positive direction among non-female voters living in urban areas with high educational attainment. The ad effect is sensitive in both directions among non-female voters living in a rural area with high educational

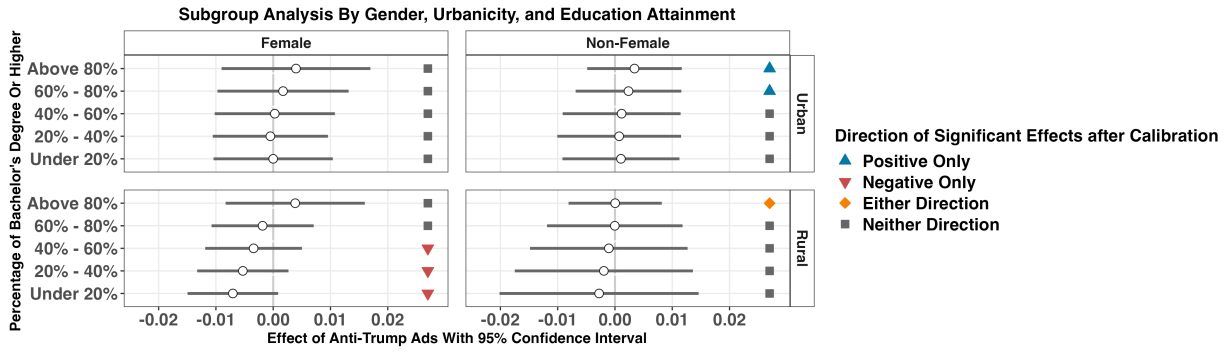


Figure 6.3: Subgroup analysis by gender, urbanicity, and levels of education attainment in a voter’s zipcode. The bar represents the 95% CI of the ad effect under transportability. On the right, statistically significant effects after calibration are colored in blue, red, and orange for positive, negative, and bidirectional effects. Insignificant results are colored gray. attainment. In other words, if the unmeasured differences considered in the calibration set \mathcal{C} are plausible, the digital ads against Trump will have a statistically significant effect among six subgroups of PA voters in 2024.

7 Discussion

This paper proposes to use transfer learning with sensitivity analysis to address whether running a digital ad campaign against Trump is effective in changing voter turnout in PA for the 2024 U.S. presidential elections. While not ideal compared to running a randomized trial during the 2024 election, the proposed approach is considerably cheaper as it leverages existing, large-scale experimental data from Aggarwal et al. (2023) and uses sensitivity analysis to account for shifts in context and voter demographics between elections. We present two estimation procedures for the TATE, one based on outcome regression (OR) modeling with bootstrapped CIs (i.e., the recommended procedure) and another based on the EIF. For each procedure, we show that it leads to consistent estimates of the TATE and

asymptotically valid $1 - \alpha$ CIs; see Section G of the Appendix for a simulation study that corroborates the theoretical conclusions empirically. Finally, inspired by ideas from design sensitivity, we present a calibration procedure based on partitioning the source population and use it to generate a set of reference magnitudes of the sensitivity parameters.

The analyses based on the OR estimator and the EIF estimator were similar, but not identical. Specifically, the subgroup analysis based on the EIF estimator was identical to that in Section 6.3 except the effect is insensitive in the negative direction for non-female voters living in rural areas with more than 80% having Bachelor’s degree or higher. The county-by-county analysis based on the EIF estimator yielded no significant results under transportability. After calibration, the analysis based on the EIF estimator produced three more counties sensitive for a positive effect and 34 fewer counties sensitive for a negative effect than those in Section 6. However, the sensitive counties follow the same trend with respect to percentage of votes for Trump in 2020; see Section E of the Appendix. We remark that the widths of the CIs from the EIF estimator and those from the OR estimator did not uniformly dominate each other.

One major reason for the difference between the EIF estimator and the OR estimator is due to the numerical instability from estimating the density ratio $w(\mathbf{v})$, one of the four nuisance functions in the EIF estimator. The density ratio is difficult to estimate when the positivity condition (i.e., Assumption 2.2) is nearly violated in finite sample and this was the case for less-populated counties in PA. Importantly, an unstable estimate of the density ratio leads to less robust “extrapolation” of the source population into the target population. Given these concerns in our data and the discreteness of \mathcal{X} , we decided to present our findings based on the OR estimator.

Our framework assumed that the target and source samples are independent and there

are no overlapping voters between the two samples. But in our analysis, it's plausible that a registered voter in PA for the 2020 election remained a registered voter in PA for the 2024 election. Unfortunately, the source data from Aggarwal et al. (2023) does not identify the voter's residence exactly. Nevertheless, to allay concerns on potentially overlapping voters, we repeated our analysis with a restricted source data consisting of $n_s = 662,225$ voters from NC and AZ only. The results from this analysis follow the same trends as above, but with less statistically significant results due to a much smaller sample size. Specifically, the county-by-county analysis results in no counties that are significant under transportability. Even after calibration, no counties are sensitive for positive effects and three fewer counties are sensitive for negative effects than those in Section 6.2. Also, the subgroup analysis did not yield any significant effects after calibration. For more details, including various robustness checks related to decisions we made during the data pre-processing step, see Sections E and F of the Appendix.

While restricting the source data to NC and AZ removes concerns on overlapping voters, it increases the implausibility of the transportability since the target population is less similar to the restricted source data (i.e., voters in 2020 in NC and AZ) than the original source data (i.e., voters in 2020 from the five states including PA). We generally believe that the source and the target population should be as similar as possible to minimize bias and thus, we decide to report the analysis where the source data contains voters from five states including PA.

Our framework implicitly assumes that the units in the target and the source data are sampled from an infinite population of voters. But, it may be more appropriate to treat the PA voter registration database as a finite population or a large sample from a finite population. These questions about sampling from a finite population and overlapping units

between finite populations raised several interesting, theoretical questions about semiparametric efficiency. Due to space constraints and this paper’s emphasis on application, we address them in an upcoming paper.

Finally, as we were finalizing the manuscript for submission during the summer of 2024, the incumbent President Joe Biden has dropped out of the 2024 U.S. presidential election in late July of 2024; our original analysis plan assumed that President Biden is the Democratic Party’s nominee for the presidency. While we believe the interpretations from our analysis about ads will still be plausible since Trump is the nominee for the Republican party and the digital ad campaign consists of negative ads against Trump, we caution readers from over-interpreting the results. Notably, our calibration procedure based on blue-collar and non blue-collar states could under-estimate the dramatic shift in electoral context after Biden dropped out of the race and the consequences of this unprecedented event in American politics.

References

- Aggarwal, M., Allen, J., Coppock, A., Frankowski, D., Messing, S., Zhang, K., Barnes, J., Beasley, A., Hantman, H., and Zheng, S. (2023). A 2 million-person, campaign-wide field experiment shows how digital advertising affects voter turnout. *Nature Human Behaviour*, 7(3):332–341.
- Birmingham, J., Rotnitzky, A., and Fitzmaurice, G. M. (2003). Pattern–mixture and selection models for analysing longitudinal data with monotone missing patterns. *Journal of the Royal Statistical Society Series B: Statistical Methodology*, 65(1):275–297.
- Carroll, R. J., Fan, J., Gijbels, I., and Wand, M. P. (1997). Generalized partially linear

- single-index models. *Journal of the American Statistical Association*, 92(438):477–489.
- Cheng, G. and Huang, J. Z. (2010). Bootstrap consistency for general semiparametric M-estimation. *The Annals of Statistics*, 38(5):2884 – 2915.
- Chernozhukov, V., Chetverikov, D., Demirer, M., Duflo, E., Hansen, C., and Newey, W. (2017). Double/debiased/neyman machine learning of treatment effects. *American Economic Review*, 107(5):261–265.
- Cinelli, C. and Hazlett, C. (2020). Making sense of sensitivity: Extending omitted variable bias. *Journal of the Royal Statistical Society Series B: Statistical Methodology*, 82(1):39–67.
- Colnet, B., Josse, J., Scornet, E., and Varoquaux, G. (2021). Generalizing a causal effect: sensitivity analysis and missing covariates. *arXiv preprint arXiv:2105.06435*.
- Cook, T. D. (2014). Generalizing causal knowledge in the policy sciences: External validity as a task of both multi-attribute representation and multi-attribute extrapolation. *Journal of Policy Analysis and Management*, pages 527–536.
- Dahabreh, I. J., Robertson, S. E., Steingrimsson, J. A., Stuart, E. A., and Hernán, M. A. (2020). Extending inferences from a randomized trial to a new target population. *Statistics in Medicine*, 39(14):1999–2014.
- Dahabreh, I. J., Robins, J. M., Haneuse, S. J., Robertson, S. E., Steingrimsson, J. A., and Hernán, M. A. (2022). Global sensitivity analysis for studies extending inferences from a randomized trial to a target population. *arXiv preprint arXiv:2207.09982*.
- Dahabreh, I. J., Robins, J. M., Haneuse, S. J.-P., Saeed, I., Robertson, S. E., Stuart, E. A., and Hernán, M. A. (2023). Sensitivity analysis using bias functions for studies extend-

- ing inferences from a randomized trial to a target population. *Statistics in Medicine*, 42(13):2029–2043.
- Duong, N. Q., Pitts, A. J., Kim, S., and Miles, C. H. (2023). Sensitivity analysis for transportability in multi-study, multi-outcome settings. *arXiv preprint arXiv:2301.02904*.
- Efron, B. (1979). Bootstrap Methods: Another Look at the Jackknife. *The Annals of Statistics*, 7(1):1 – 26.
- Ek, S. and Zachariah, D. (2023). Externally valid policy evaluation combining trial and observational data. *arXiv preprint arXiv:2310.14763*.
- Fair Vote (2024). Voter turnout. <https://fairvote.org/resources/voter-turnout/>. Accessed: 2024-09-03.
- FitzGerald, J. (2024). Seven swing states set to decide the 2024 US election. <https://www.bbc.com/news/articles/c511pyn3xw3o>. Accessed: 2024-08-24.
- FiveThirtyEight (2024). Who is favored to win the 2024 presidential election? <https://projects.fivethirtyeight.com/2024-election-forecast/>. Accessed: 2024-08-25.
- Franks, A. M., D’Amour, A., and Feller, A. (2020). Flexible sensitivity analysis for observational studies without observable implications. *Journal of the American Statistical Association*, 115(532):1730–1746.
- Gerber, A. S., Gimpel, J. G., Green, D. P., and Shaw, D. R. (2011). How large and long-lasting are the persuasive effects of televised campaign ads? results from a randomized field experiment. *American Political Science Review*, 105(1):135–150.
- Hsu, J. Y. and Small, D. S. (2013). Calibrating sensitivity analyses to observed covariates in observational studies. *Biometrics*, 69(4):803–811.

- Huang, M. (2024a). Overlap violations in external validity. *arXiv preprint arXiv:2403.19504*.
- Huang, M. Y. (2024b). Sensitivity analysis for the generalization of experimental results. *Journal of the Royal Statistical Society Series A: Statistics in Society*.
- Ipsos Core Political (2024). March 2024 reuters/ipsos core political. <https://www.ipsos.com/en-us/march-2024-reutersipsos-core-political/>. Accessed: 2024-04-23.
- Jin, Y. and Rothenhäusler, D. (2024). Tailored inference for finite populations: conditional validity and transfer across distributions. *Biometrika*, 111(1):215–233.
- Kalla, J. L. and Broockman, D. E. (2018). The minimal persuasive effects of campaign contact in general elections: Evidence from 49 field experiments. *American Political Science Review*, 112(1):148–166.
- Kallus, N. and Mao, X. (2024). On the role of surrogates in the efficient estimation of treatment effects with limited outcome data. *Journal of the Royal Statistical Society Series B: Statistical Methodology*, page qkae099.
- Kennedy, E. H. (2022). Semiparametric doubly robust targeted double machine learning: a review. *arXiv preprint arXiv:2203.06469*.
- Kennedy, E. H. (2023). Towards optimal doubly robust estimation of heterogeneous causal effects. *Electronic Journal of Statistics*, 17(2):3008–3049.
- Linero, A. R. and Daniels, M. J. (2018). Bayesian approaches for missing not at random outcome data: the role of identifying restrictions. *Statistical Science*, 33(2):198 – 213.
- Loving, S. and Smith, D. A. (2024). Riot in the party? Voter registrations in the aftermath of the January 6, 2021 capitol insurrection. *Party Politics*, 30(2):209–222.

- Newey, W. K. and McFadden, D. (1994). Large sample estimation and hypothesis testing. *Handbook of Econometrics*, 4:2111–2245.
- Nguyen, T. Q., Ebnesajjad, C., Cole, S. R., and Stuart, E. A. (2017). Sensitivity analysis for an unobserved moderator in rct-to-target-population generalization of treatment effects. *The Annals of Applied Statistics*, 11(1):225–247.
- Nie, X., Imbens, G., and Wager, S. (2021). Covariate balancing sensitivity analysis for extrapolating randomized trials across locations. *arXiv preprint arXiv:2112.04723*.
- Pew Research Center (2024). Americans’ top policy priority for 2024: Strengthening the economy. <https://www.pewresearch.org/politics/2024/02/29/americans-top-policy-priority-for-2024-strengthening-the-economy/>. Accessed: 2023-04-23.
- Præstgaard, J. and Wellner, J. A. (1993). Exchangeably weighted bootstraps of the general empirical process. *The Annals of Probability*, pages 2053–2086.
- Robins, J. M., Rotnitzky, A., and Scharfstein, D. O. (2000). Sensitivity analysis for selection bias and unmeasured confounding in missing data and causal inference models. In *Statistical Models in Epidemiology, the Environment, and Clinical Trials*, pages 1–94. Springer.
- Rosenbaum, P. R. (2004). Design sensitivity in observational studies. *Biometrika*, 91(1):153–164.
- Rosenbaum, P. R. (2020). *Design of Observational Studies*. Springer, 2nd edition.
- Rosenbaum, P. R. and Rubin, D. B. (1983). The central role of the propensity score in observational studies for causal effects. *Biometrika*, 70(1):41–55.

- Rotnitzky, A., Scharfstein, D., Su, T.-L., and Robins, J. (2001). Methods for conducting sensitivity analysis of trials with potentially nonignorable competing causes of censoring. *Biometrics*, 57(1):103–113.
- Rotnitzky, A., Smucler, E., and Robins, J. M. (2020). Characterization of parameters with a mixed bias property. *Biometrika*, 108(1):231–238.
- Rubin, D. B. (1980). Randomization analysis of experimental data: The fisher randomization test comment. *Journal of the American Statistical Association*, 75(371):591–593.
- Scharfstein, D. O., Nabi, R., Kennedy, E. H., Huang, M.-Y., Bonvini, M., and Smid, M. (2021). Semiparametric sensitivity analysis: Unmeasured confounding in observational studies. *arXiv preprint arXiv:2104.08300*.
- Schleifer, T. and Goldmacher, S. (2024). Inside the secretive \$700 million ad-testing factory for Kamala Harris. <https://www.nytimes.com/2024/10/17/us/elections/future-forward-kamala-harris-ads.html>. Accessed: 2024-10-19.
- Shao, J. and Tu, D. (1995). *The Jackknife and Bootstrap*. Springer Series in Statistics. Springer, New York, NY, 1 edition.
- Shea, D. and Jacobs, N. F. (2023). *The Rural Voter: The Politics of Place and the Disuniting of America*. Columbia University Press.
- Stuart, E. A., Cole, S. R., Bradshaw, C. P., and Leaf, P. J. (2011). The use of propensity scores to assess the generalizability of results from randomized trials. *Journal of the Royal Statistical Society: Series A (Statistics in Society)*, 174(2):369–386.
- Tipton, E. (2013). Improving generalizations from experiments using propensity score

- subclassification: Assumptions, properties, and contexts. *Journal of Educational and Behavioral Statistics*, 38(3):239–266.
- Tipton, E. and Peck, L. R. (2017). A design-based approach to improve external validity in welfare policy evaluations. *Evaluation Review*, 41(4):326–356.
- Vaart, A. v. d. and Wellner, J. A. (1996). *Weak Convergence and Empirical Processes: With Applications to Statistics*. Springer Series in Statistics. Springer Science & Business Media, illustrated, reprint edition.
- van der Vaart, A. W. (1998). *Asymptotic Statistics*. Cambridge University Press.
- Wellner, J. A. (2005). Empirical processes: Theory and applications. *Notes for a course given at Delft University of Technology*, 17.
- Wellner, J. A. and Zhan, Y. (1996). Bootstrapping z-estimators. *University of Washington Department of Statistics Technical Report*, 308(5).
- Ye, T., Bannick, M., Yi, Y., and Shao, J. (2023). Robust variance estimation for covariate-adjusted unconditional treatment effect in randomized clinical trials with binary outcomes. *Statistical Theory and Related Fields*, 7(2):159–163.
- Zeng, Z., Kennedy, E. H., Bodnar, L. M., and Naimi, A. I. (2023). Efficient generalization and transportation. *arXiv preprint arXiv:2302.00092*.
- Zhang, Y., Chakraborty, A., and Bradic, J. (2023). Double robust semi-supervised inference for the mean: selection bias under MAR labeling with decaying overlap. *Information and Inference: A Journal of the IMA*, 12(3):2066–2159.

Appendix

This Appendix provides supplementary materials for the manuscript titled “Transfer Learning Between U.S. Presidential Elections: How should we learn from a 2020 ad campaign to inform 2024 campaigns?”. Section A details the alternative formulations and extensions of the sensitivity model (3.1). Sections B and C provide additional details and proofs for inference procedures based on the OR estimator and the EIF-based estimator introduced in Sections 4.1 and 4.2 of the main text, respectively. Section D provides details of the calibration procedure of sensitivity parameters. Section E provides additional results for analyzing the ad effect in PA in 2024. Section F repeats the analysis on PA when excluding voters in PA, WI, MI from the source data (i.e., restricting the source data to voters from NC and AZ). Section G presents a simulation study where the simulation data were generated to mimic the data from Aggarwal et al. (2023).

A Extensions and Interpretations of the Sensitivity Model

A.1 Exponential Tilting for Continuous Outcomes

The proposed sensitivity model (3.1) is not limited to binary outcomes. It can be equivalently expressed for a general, possibly continuous outcome with support \mathcal{Y} . Suppose the conditional density of the potential outcome on the target population is shifted from that of the source by an exponential tilting shift,

$$p_{Y^{(a)}|\mathbf{V},S=0}(y_a | \mathbf{v}, S_i = 0) \propto \exp(\gamma_a y_a) \cdot p_{Y^{(a)}|\mathbf{V},S=1}(y_a | \mathbf{v}, S_i = 1), \quad \forall \mathbf{v} \in \mathcal{V}, \quad (\text{A.1})$$

where \propto represents “proportional to” and $p_{Y^{(a)}|\mathbf{V},S=s}$ represents the conditional probability density function of $Y_i^{(a)} \mid \mathbf{V}_i, S_i = s$ for $s = 0, 1$. When $\gamma_a = 0$, (A.1) reduces to $p_{Y^{(a)}|\mathbf{V},S=0}(y_a \mid \mathbf{v}, S_i = 0) = p_{Y^{(a)}|\mathbf{V},S=0}(y_a \mid \mathbf{V}_i = \mathbf{v}, S_i = 1)$ and thereby transportability (Assumption 2.3) holds. When $\gamma_a \neq 0$, γ_a measures the violation to the transportability assumption by the degree in shifts of the conditional densities.

Under (A.1) and for a given γ_a , the expected potential outcome under treatment level a can be identified as follows.

Lemma A.1 (Identification of TATE for A General Outcome Under Sensitivity Model)

Suppose Assumptions 2.1, 2.2 and the sensitivity model in equation (A.1) hold. For a given $\gamma_a \in \mathbb{R}$, the expected potential outcome under treatment level $a \in \{0, 1\}$ is

$$\begin{aligned} \mathbb{E}[Y_i^{(a)} \mid S_i = 0] &= \mathbb{E} \left(\frac{\mathbb{E}[\mathbb{E}\{\exp(\gamma_a Y_i) Y_i \mid \mathbf{X}_i, A_i = a, S_i = 1\} \mid \mathbf{V}_i, S_i = 1]}{\mathbb{E}[\mathbb{E}\{\exp(\gamma_a Y_i) \mid \mathbf{X}_i, A_i = a, S_i = 1\} \mid \mathbf{V}_i, S_i = 1]} \mid S_i = 0 \right), \\ &= \theta_a(\gamma_a). \end{aligned} \tag{A.2}$$

For a binary outcome, Lemma A.1 reduces to Lemma 3.1. When $\mathcal{X} = \mathcal{V}$, Lemma A.1 recovers the identification result in Dahabreh et al. (2022). When $\gamma_a = 0$, i.e., transportability holds, Lemma A.1 recovers the identification result in Zeng et al. (2023).

From (A.1), the difference between the two conditional densities at $y_a \in \mathcal{Y}$ is quantified by $\exp(\gamma_a y_a)$ up to some normalizing constant. An extension is to replace $\exp(\gamma_a y_a)$ with $\exp\{\gamma_a \delta(y_a, \mathbf{v})\}$ where $\delta(y_a, \mathbf{v})^3$ is a statistic including y_a and \mathbf{v} . One may also further generalize γ_a to a vector or generalize the exponential function to other forms based on experts’ knowledge. We note that the choice should ensure the density $p_{Y^{(a)}|\mathbf{V},S=0}$ is well-defined and we refer readers to Franks et al. (2020); Scharfstein et al. (2021) for practical choices.

³If $\delta(y_a, \mathbf{v}, \gamma_a)$ can be factorized to $\delta_1(y_a, \gamma_a)\delta_2(\mathbf{v}, \gamma_a)$ then it can be replaced with $\delta_1(y_a, \gamma_a)$.

A.2 Selection Model

An alternative view to the sensitivity model is via the selection to the source, in particular, via the probability of $S_i = 1$. From this perspective, sensitivity model (A.1) implies a partially linear logistic regression model (Carroll et al., 1997) on the selection of S_i :

$$\mathbb{P}(S_i = 1 \mid Y_i^{(a)} = y_a, \mathbf{V}_i = \mathbf{v}) = \text{expit}(-\gamma_a y_a - \eta(\mathbf{v}, \gamma_a)), \quad \forall y_a \in \mathcal{Y}, \mathbf{v} \in \mathcal{V}, \quad (\text{A.3})$$

$$\eta(\mathbf{v}, \gamma_a) = \log \left(\frac{\mathbb{P}(S_i = 0)}{\mathbb{P}(S_i = 1)} \frac{w(\mathbf{v})}{\mathbb{E} \left\{ \exp(\gamma_a Y_i^{(a)}) \mid \mathbf{V}_i = \mathbf{v}, S_i = 1 \right\}} \right),$$

where $\text{expit}(t) = 1/\{1 + \exp(-t)\}$ for any $t \in \mathbb{R}$ is known as the logistic function. The selection model (A.3) indicates that the participation S_i is determined by both the potential outcome and the covariate \mathbf{V}_i . After the logistic transformation, the selection probability is associated with $Y_i^{(a)}$ linearly with coefficient γ_a . If $\gamma_a = 0$, then the selection will depend on \mathbf{V}_i only, which reduces to the case where the difference between the target and the source is fully characterized by \mathbf{V}_i , i.e., when the transportability holds.

A.3 Estimation for a Continuous Outcome

The identification condition (A.2) directs an OR estimator through

$$\hat{\theta}_{\text{OR},a}^{\text{cont}}(\gamma_a) = \frac{1}{n_t} \sum_{i \in \mathcal{I}_t} \frac{\hat{\mathbb{E}} \left\{ \exp(\gamma_a Y_i^{(a)}) Y_i^{(a)} \mid \mathbf{V}_i, S_i = 1 \right\}}{\hat{\mathbb{E}} \left\{ \exp(\gamma_a Y_i^{(a)}) \mid \mathbf{V}_i, S_i = 1 \right\}}.$$

To motivate an EIF-based estimator, we present the EIF in Theorem A.2, which is a generalization of Theorem 4.2 to continuous outcomes.

Theorem A.2 *Under Assumptions 2.1 and 2.2 and sensitivity model (A.1), the EIF for $\theta_a(\gamma_a)$ is*

$$\begin{aligned} & \text{EIF}^{\text{cont}}(\mathbf{O}_i, \theta_a(\gamma_a)) \\ &= \frac{S_i w(\mathbf{V}_i)}{\mathbb{P}(S_i = 1)} \left\{ \frac{A_i}{\pi(\mathbf{X}_i)} + \frac{1 - A_i}{1 - \pi(\mathbf{X}_i)} \right\} \left[\frac{\exp(\gamma_a Y_i) Y_i}{\mathbb{E} \left\{ \exp(\gamma_a Y_i^{(a)}) \mid \mathbf{V}_i, S_i = 1 \right\}} - \frac{\mathbb{E} \left\{ \exp(\gamma_a Y_i) Y_i \mid \mathbf{X}_i, A = A_i, S_i = 1 \right\}}{\mathbb{E} \left\{ \exp(\gamma_a Y_i^{(a)}) \mid \mathbf{V}_i, S_i = 1 \right\}} \right] \end{aligned}$$

$$\begin{aligned}
& \left[\frac{\exp(\gamma_a Y_i) \mathbb{E}\{\exp(\gamma_a Y_i^{(a)}) Y_i^{(a)} \mid \mathbf{V}_i, S_i = 1\}}{[\mathbb{E}\{\exp(\gamma_a Y_i^{(a)}) \mid \mathbf{V}_i, S_i = 1\}]^2} + \frac{\mathbb{E}\{\exp(\gamma_a Y_i) \mid \mathbf{X}_i, A = A_i, S_i = 1\} \mathbb{E}\{\exp(\gamma_a Y_i^{(a)}) Y_i^{(a)} \mid \mathbf{V}_i, S_i = 1\}}{[\mathbb{E}\{\exp(\gamma_a Y_i^{(a)}) \mid \mathbf{V}_i, S_i = 1\}]^2} \right] \\
& + \frac{S_i w(\mathbf{V}_i)}{\mathbb{P}(S_i = 1)} \left(\frac{\mathbb{E}\{e^{\gamma_a Y_i} Y_i \mid \mathbf{X}_i, A = A_i, S_i = 1\}}{\mathbb{E}\{\exp(\gamma_a Y_i^{(a)}) \mid \mathbf{V}_i, S_i = 1\}} - \frac{\mathbb{E}\{e^{\gamma_a Y_i} Y_i^{(a)} \mid \mathbf{V}_i, S_i = 1\} \mathbb{E}\{e^{\gamma_a Y_i} \mid \mathbf{X}_i, A = A_i, S_i = 1\}}{[\mathbb{E}\{\exp(\gamma_a Y_i^{(a)}) \mid \mathbf{V}_i, S_i = 1\}]^2} \right) \\
& + \frac{1 - S_i}{\mathbb{P}(S_i = 0)} \left[\frac{\mathbb{E}\{\exp(\gamma_a Y_i^{(a)}) Y_i^{(a)} \mid \mathbf{V}_i, S_i = 1\}}{\mathbb{E}\{\exp(\gamma_a Y_i^{(a)}) \mid \mathbf{V}_i, S_i = 1\}} - \theta_a(\gamma_a) \right].
\end{aligned}$$

EIF^{cont}($\mathbf{O}_i, \theta_a(\gamma_a)$) reduces to EIF($\mathbf{O}_i, \theta_a(\gamma_a)$) in Theorem 4.2 for a binary outcome. It motivates the following EIF-based cross-fitting estimator:

$$\hat{\theta}_{\text{EIF,a}}^{\text{cont}}(\gamma_a) = \frac{1}{K} \sum_{k=1}^K \hat{\theta}_{\text{EIF,a}}^{\text{cont},(k)}(\gamma_a),$$

where $\hat{\theta}_{\text{EIF,a}}^{\text{cont},(k)}(\gamma_a)$ is the estimate at k -th partition of the cross-fitting procedure as described in Section 4.2,

$$\begin{aligned}
& \hat{\theta}_{\text{EIF,a}}^{\text{cont},(k)}(\gamma_a) \\
& = \frac{1}{|\mathcal{I}_s^{(k)}|} \sum_{i \in \mathcal{I}_s^{(k)}} \hat{w}^{(k)}(\mathbf{V}_i) \left(\left\{ \frac{A_i}{\hat{\pi}^{(k)}(\mathbf{X}_i)} + \frac{1 - A_i}{1 - \hat{\pi}^{(k)}(\mathbf{X}_i)} \right\} \left[\frac{\exp(\gamma_a Y_i) Y_i}{\hat{\mathbb{E}}^{(k)}\{e^{\gamma_a Y_i^{(a)}} \mid \mathbf{V}_i, S_i = 1\}} - \frac{\hat{\mathbb{E}}^{(k)}\{e^{\gamma_a Y_i} Y_i \mid \mathbf{X}_i, A_i, S_i = 1\}}{\hat{\mathbb{E}}^{(k)}\{e^{\gamma_a Y_i^{(a)}} \mid \mathbf{V}_i, S_i = 1\}} \right. \right. \\
& \quad \left. \left. - \frac{e^{\gamma_a Y_i} \hat{\mathbb{E}}^{(k)}\{e^{\gamma_a Y_i^{(a)}} Y_i^{(a)} \mid \mathbf{V}_i, S_i = 1\}}{[\hat{\mathbb{E}}^{(k)}\{e^{\gamma_a Y_i^{(a)}} \mid \mathbf{V}_i, S_i = 1\}]^2} + \frac{\hat{\mathbb{E}}^{(k)}\{e^{\gamma_a Y_i} \mid \mathbf{X}_i, A_i, S_i = 1\} \hat{\mathbb{E}}^{(k)}\{e^{\gamma_a Y_i^{(a)}} Y_i^{(a)} \mid \mathbf{V}_i, S_i = 1\}}{[\hat{\mathbb{E}}\{e^{\gamma_a Y_i^{(a)}} \mid \mathbf{V}_i, S_i = 1\}]^2} \right] \right. \\
& \quad \left. + \frac{\hat{\mathbb{E}}^{(k)}\{e^{\gamma_a Y_i} Y_i \mid \mathbf{X}_i, A_i, S_i = 1\} \hat{\mathbb{E}}^{(k)}\{e^{\gamma_a Y_i^{(a)}} \mid \mathbf{V}_i, S_i = 1\} - \hat{\mathbb{E}}^{(k)}\{e^{\gamma_a Y_i^{(a)}} Y_i^{(a)} \mid \mathbf{V}_i, S_i = 1\} \hat{\mathbb{E}}^{(k)}\{e^{\gamma_a Y_i} \mid \mathbf{X}_i, A_i, S_i = 1\}}{[\hat{\mathbb{E}}^{(k)}\{\exp(\gamma_a Y_i^{(a)}) \mid \mathbf{V}_i, S_i = 1\}]^2} \right) \\
& \quad + \frac{1}{|\mathcal{I}_t^{(k)}|} \sum_{i \in \mathcal{I}_t^{(k)}} \frac{\hat{\mathbb{E}}^{(k)}\{\exp(\gamma_a Y_i^{(a)}) Y_i^{(a)} \mid \mathbf{V}_i, S_i = 1\}}{\hat{\mathbb{E}}^{(k)}\{\exp(\gamma_a Y_i^{(a)}) \mid \mathbf{V}_i, S_i = 1\}}.
\end{aligned}$$

B Details and Proofs for the Outcome Regression Based Estimation

This section provides details and proofs for the inference procedure with the OR estimator proposed in Section 4.1. We detail the bootstrap procedure in Section B.1, state regularity conditions for the bootstrap consistency in Section B.2, and prove Theorem 4.1 in Section B.3.

B.1 Details for the Bootstrap

We detail the nonparametric, percentile bootstrap for the inference with the OR estimator. In each bootstrap iteration, we resample with replacement the source and target samples, respectively, to have sizes n_s and n_t , and construct an OR estimator with the resampled data. After repeating the bootstrap iterations for a large number of times, say B times, we calculate the $\alpha/2$ and $1 - \alpha/2$ quantiles of the resulting bootstrap estimates, denoted as $\hat{L}_a(\gamma_a; 1 - \alpha)$ and $\hat{U}_a(\gamma_a; 1 - \alpha)$. By Theorem 4.1, the interval $\widehat{\text{CI}}_{\text{OR},a}(\gamma_a) = [\hat{L}_a(\gamma_a; 1 - \alpha), \hat{U}_a(\gamma_a; 1 - \alpha)]$ is a consistent confidence interval for $\theta_a(\gamma_a)$. A step-by-step procedure is provided in Algorithm 1.

We note that underlying true quantiles of the bootstrap estimates are estimated by their empirical counterparts ($\hat{L}_a(\gamma_a; 1 - \alpha)$ and $\hat{U}_a(\gamma_a; 1 - \alpha)$). This estimation step introduces an additional random error. Since this error can be made arbitrarily small by resampling the data for sufficiently many times, our proof supposes that $\hat{L}_a(\gamma_a; 1 - \alpha)$ and $\hat{U}_a(\gamma_a; 1 - \alpha)$ are the exact quantiles of bootstrap estimates. This argument follows the approach in Chapter 23 of van der Vaart (1998). For numerical results throughout the paper, the bootstrap iterations are repeated for $B = 1000$ times.

B.2 Regularity Conditions for the Bootstrap

Recall that we suppose the $\rho_a(\mathbf{v})$ is indexed by a finite-dimensional parameter $\boldsymbol{\eta}_a$. Specifically, suppose the parameter $\boldsymbol{\eta}_a$ is estimated through an estimating equation,

$$\frac{1}{n_s} \sum_{i \in \mathcal{I}_s} \mathbf{S}(\mathbf{O}_i, \hat{\boldsymbol{\eta}}_a) = \mathbf{0}$$

with a known $\mathbf{S}(\mathbf{O}_i, \boldsymbol{\eta}_a)$. Let $\boldsymbol{\beta}_a(\gamma_a) = [\boldsymbol{\eta}_a^\top, \theta_a(\gamma_a)]^\top$ and

$$\boldsymbol{\phi}_a(\mathbf{O}_i, \boldsymbol{\beta}_a(\gamma_a)) = \left[\frac{S_i}{\mathbb{P}(S_i = 1)} \mathbf{S}(\mathbf{O}_i, \boldsymbol{\eta}_a)^\top, \frac{1 - S_i}{\mathbb{P}(S_i = 0)} \phi_a(\mathbf{V}_i, \theta_a(\gamma_a), \boldsymbol{\eta}_a) \right]^\top, \text{ where}$$

Algorithm 1 Outcome regression estimator with nonparametric, percentile bootstrap

Require: Sensitivity parameters γ_a , confidence level $1 - \alpha$, bootstrap iteration B .

- 1: **Step 1:** Estimate $\hat{\rho}_a(\mathbf{v})$ using the source data.
- 2: **Step 2:** Estimate $\hat{\theta}_{\text{OR},a}(\gamma_a)$ as in (4.1).
- 3: **Step 3:** Nonparametric, percentile bootstrap
- 4: **for** b in $1, \dots, B$ **do**
- 5: Resample source and target data with replacement at sizes n_s and n_t , respectively.
- 6: With the resampled data, obtain $\hat{\theta}_{\text{OR},a}^{*,b}(\gamma_a)$.
- 7: **end for**
- 8: Calculate the $\alpha/2$ and $1 - \alpha/2$ quantiles of $\left\{ \hat{\theta}_{\text{OR},a}^{*,b}(\gamma_a) \right\}_{b=1}^B$, denoted as $\hat{L}_a(\gamma_a; 1 - \alpha)$ and $\hat{U}_a(\gamma_a; 1 - \alpha)$ where

$$\begin{aligned} \hat{L}_a(\gamma_a; 1 - \alpha) &= \hat{Q}^*(\alpha/2), \quad \hat{U}_a(\gamma_a; 1 - \alpha) = \hat{Q}^*(1 - \alpha/2), \\ \hat{Q}^*(\tau) &= \inf_t \left\{ \frac{1}{B} \sum_{b=1}^B \mathbf{1}(\hat{\theta}_{\text{OR}}^{*,b}(\gamma_a) \leq t) \geq \tau \right\}, \forall \tau \in (0, 1). \end{aligned}$$

Ensure: The OR estimator $\hat{\theta}_{\text{OR}}(\gamma_a)$ with a $(1 - \alpha)$ confidence interval $\widehat{\text{CI}}_{\text{OR},a}(\gamma_a; 1 - \alpha) = [\hat{L}_a(\gamma_a; 1 - \alpha), \hat{U}_a(\gamma_a; 1 - \alpha)]$.

$$\phi_a(\mathbf{V}_i, \theta_a(\gamma_a), \boldsymbol{\eta}_a) = \frac{\exp(\gamma_a) \rho_a(\mathbf{V}_i, \boldsymbol{\eta}_a)}{\exp(\gamma_a) \rho_a(\mathbf{V}_i, \boldsymbol{\eta}_a) + 1 - \rho_a(\mathbf{V}_i, \boldsymbol{\eta}_a)} - \theta_a(\gamma_a).$$

Then $\hat{\boldsymbol{\beta}}_a(\gamma_a) = [\hat{\boldsymbol{\eta}}_a^T, \hat{\theta}_a(\gamma_a)]^T$ can be alternatively expressed as the solution to the estimating equation

$$\frac{1}{n} \sum_{i=1}^n \phi_a(\mathbf{O}_i, \hat{\boldsymbol{\beta}}_a(\gamma_a)) = \mathbf{0}.$$

We define the bootstrap estimator $\hat{\boldsymbol{\beta}}_a^*(\gamma_a)$ as the solution to

$$\frac{1}{n} \sum_{i=1}^n W_{n,i} \phi(\mathbf{O}_i, \hat{\boldsymbol{\beta}}_a^*(\gamma_a)) = \mathbf{0},$$

where $(W_{n,1}, \dots, W_{n,n_s}) \sim \text{Multinomial}(n_s; 1/n_s, \dots, 1/n_s)$ and $(W_{n,n_s+1}, \dots, W_{n,n}) \sim \text{Multinomial}(n_t; 1/n_t, \dots, 1/n_t)$.

We assume the following regularity conditions.

- (B1) $\mathbb{E}\{\phi(\mathbf{O}_i, \boldsymbol{\beta}_a(\gamma_a))\} = \mathbf{0}$ with a unique solution $\boldsymbol{\beta}_a(\gamma_a)$.
- (B2) Parameter $\boldsymbol{\beta}_a(\gamma_a)$ is contained in a compact parameter space Ξ and $\mathbb{E} \sup_{\boldsymbol{\beta}_a(\gamma_a) \in \Xi} \|\phi\|_1 < \infty$.
- (B3) $\mathbb{E} (\sup_{\boldsymbol{\beta}_a(\gamma_a) \in \Xi} \|\partial \phi_a^2 / \partial \boldsymbol{\beta}_a(\gamma_a)^2\|) < \infty$.
- (B4) The function class $\{\phi_a(\mathbf{O}_i, \boldsymbol{\beta}_a(\gamma_a)), \boldsymbol{\beta}_a(\gamma_a) \in \Xi\}$ is \mathbb{P} -Donsker and $\mathbb{E} \|\phi_a(\mathbf{O}_i, \tilde{\boldsymbol{\beta}}_a(\gamma_a)) - \phi_a(\mathbf{O}_i, \boldsymbol{\beta}_a(\gamma_a))\|^2 \rightarrow 0$ as long as $\|\tilde{\boldsymbol{\beta}}_a(\gamma_a) - \boldsymbol{\beta}_a(\gamma_a)\| \rightarrow 0$.

Condition (B1) is essentially assuming $\mathbb{E}\{\mathbf{S}(\mathbf{O}, \boldsymbol{\eta}_a)\} = \mathbf{0}$ with the unique solution being the true parameter $\boldsymbol{\eta}_a$. Condition (B2) guarantees that ϕ_a is \mathbb{P} -Glivenko-Cantelli by Wellner (2005, Lemma 6.1). Condition (B3) and (B4) are standard regularity conditions for the complexity of the function class and the smoothness of the estimating equation.

B.3 Proof of Theorem 4.1

Before proving Theorem 4.1, we state the asymptotic Normality of the OR estimator in Theorem B.1. Next in Theorem B.2, we show that the bootstrap estimator is also asymptotically Normal with the same asymptotic variance. Finally we prove the bootstrap CI consistency in Theorem 4.1.

Theorem B.1 (OR estimator) *Suppose Assumptions 2.1 and 2.2 hold and $n_s \asymp n_t$. Also suppose $\rho_a(\mathbf{v}, \boldsymbol{\eta}_a)$ is twice differentiable with respect to $\boldsymbol{\eta}_a$ and $\hat{\boldsymbol{\eta}}_a$ is an asymptotically linear estimate of $\boldsymbol{\eta}_a$ with some influence function $\mathbf{g}_a(\mathbf{O}, \boldsymbol{\eta}_a)$; i.e., $\sqrt{n}(\hat{\boldsymbol{\eta}}_a - \boldsymbol{\eta}_a) =$*

$\frac{1}{\sqrt{n}} \sum_{i=1}^n \mathbf{g}(\mathbf{O}_i, \boldsymbol{\eta}_a) + o_p(1)$. If $\theta_a(\gamma_a) \in \Theta$ where Θ is open and compact, then $\hat{\theta}_{\text{OR},a}(\gamma_a) \rightarrow_p \theta_a(\gamma_a)$ and $\hat{\theta}_{\text{OR},a}(\gamma_a)$ is asymptotically linear with influence function

$$\psi_a(\mathbf{O}_i, \theta_a(\gamma_a), \boldsymbol{\eta}_a) = \frac{1 - S_i}{\mathbb{P}(S_i = 0)} \phi_a(\mathbf{V}_i, \theta_a(\gamma_a), \boldsymbol{\eta}_a) + \mathbb{E}(\partial \phi_a / \partial \boldsymbol{\eta}_a^T | S_i = 0) \mathbf{g}_a(\mathbf{O}_i, \boldsymbol{\eta}_a).$$

Consequently,

$$\sqrt{n}(\hat{\theta}_{\text{OR},a} - \theta_a) = \frac{1}{\sqrt{n}} \sum_{i=1}^n \psi_a(\mathbf{O}_i, \theta_a(\gamma_a), \boldsymbol{\eta}_a) + o_p(1) \rightarrow_d N(0, \sigma_{\text{OR},a}^2(\gamma_a)), \text{ where}$$

$$\sigma_{\text{OR},a}^2(\gamma_a) = \mathbb{E}\{\psi_a^2(\mathbf{O}_i, \theta_a(\gamma_a), \boldsymbol{\eta}_a)\}.$$

Proof of Theorem B.1. Without loss of generality, we prove the results for $\theta_1(\gamma_1)$. We suppress the dependence of θ_1 on γ_1 for notation simplicity.

Since Θ is compact and $\rho_1(\mathbf{v})$ is between zero and one, by Newey and McFadden (1994, Lemma 2.4), we have that

$$\sup_{\theta_1 \in \Theta} \left\| \frac{1}{n_t} \sum_{i \in \mathcal{I}_t} \frac{\exp(\gamma_1) \rho_1(\mathbf{V}_i)}{\exp(\gamma_1) \rho_1(\mathbf{V}_i) + 1 - \rho_1(\mathbf{V}_i)} - \theta_1 \right\| = o_p(1).$$

In addition, we note that by the asymptotic linearity of $\hat{\boldsymbol{\eta}}$,

$$\|\hat{\rho}_1(\mathbf{V}_i) - \rho_1(\mathbf{V}_i)\| = \partial \rho_1 / \partial \boldsymbol{\eta}_1^T (\boldsymbol{\eta}_1 - \hat{\boldsymbol{\eta}}_1) + o_p(1) = o_p(1). \quad (\text{B.1})$$

Now we establish consistency by (van der Vaart, 1998, Theorem 5.9). Note that

$$\begin{aligned} & \sup_{\theta_1 \in \Theta} \left\| \frac{1}{n_t} \sum_{i \in \mathcal{I}_t} \frac{\exp(\gamma_1) \hat{\rho}_1(\mathbf{V}_i)}{\exp(\gamma_1) \hat{\rho}_1(\mathbf{V}_i) + 1 - \hat{\rho}_1(\mathbf{V}_i)} - \theta_1 \right\| \\ & \leq \left\| \frac{1}{n_t} \sum_{i \in \mathcal{I}_t} \frac{\exp(\gamma_1) \hat{\rho}_1(\mathbf{V}_i)}{\exp(\gamma_1) \hat{\rho}_1(\mathbf{V}_i) + 1 - \hat{\rho}_1(\mathbf{V}_i)} - \frac{1}{n_t} \sum_{i \in \mathcal{I}_t} \frac{\exp(\gamma_1) \rho_1(\mathbf{V}_i)}{\exp(\gamma_1) \rho_1(\mathbf{V}_i) + 1 - \rho_1(\mathbf{V}_i)} \right\| \\ & \quad + \sup_{\theta_1 \in \Theta} \left\| \frac{1}{n_t} \sum_{i \in \mathcal{I}_t} \frac{\exp(\gamma_1) \rho_1(\mathbf{V}_i)}{\exp(\gamma_1) \rho_1(\mathbf{V}_i) + 1 - \rho_1(\mathbf{V}_i)} - \theta_1 \right\| \\ & \leq \frac{\exp(\gamma_1)}{\min\{1, \exp(\gamma_1)\}} \left\| \frac{1}{n_t} \sum_{i \in \mathcal{I}_t} \hat{\rho}_1(\mathbf{V}_i) - \frac{1}{n_t} \sum_{i \in \mathcal{I}_t} \rho_1(\mathbf{V}_i) \right\| + o_p(1), \\ & = o_p(1), \end{aligned}$$

where the first inequality follows from triangle inequality, the second inequality follows from the boundedness of $\rho_1(\mathbf{v})$ and the compactness of the parameter space, and the last inequality follows from (B.1). By van der Vaart (1998, Theorem 5.9), $\hat{\theta}_1$ is consistent for θ_1 .

Finally we prove the asymptotic Normality. With Taylor expansion, we have

$$\begin{aligned} 0 &= \frac{1}{n_t} \sum_{i \in \mathcal{I}_t} \phi_1(\mathbf{V}_i, \hat{\theta}_1, \hat{\boldsymbol{\eta}}_1) \\ &= \frac{1}{n_t} \sum_{i \in \mathcal{I}_t} \phi_1(\mathbf{V}_i, \theta_1, \boldsymbol{\eta}_1) + \frac{1}{n_t} \sum_{i \in \mathcal{I}_t} \frac{\partial \phi_1}{\partial \theta_1}(\hat{\theta}_1 - \theta_1) \\ &\quad + \frac{1}{n_t} \sum_{i \in \mathcal{I}_t} \frac{\partial \phi_1}{\partial \boldsymbol{\eta}_1^T}(\hat{\boldsymbol{\eta}}_1 - \boldsymbol{\eta}_1) + \frac{1}{n_t} \sum_{i \in \mathcal{I}_t} (\tilde{\boldsymbol{\eta}}_1 - \boldsymbol{\eta}_1)^T \frac{\partial^2 \phi_1}{\partial \boldsymbol{\eta}_1 \partial \boldsymbol{\eta}_1^T}(\tilde{\boldsymbol{\eta}}_1 - \boldsymbol{\eta}_1)/2, \end{aligned}$$

where $\tilde{\boldsymbol{\eta}}_1$ is between $\boldsymbol{\eta}_1$ and $\hat{\boldsymbol{\eta}}_1$. Multiplying both sides with \sqrt{n} and rearranging terms, we have

$$\sqrt{n}(\hat{\theta}_1 - \theta_1) = \sqrt{n} \frac{1 - S_i}{\hat{\mathbb{P}}(S_i = 0)} \phi_1(\mathbf{V}_i, \theta_1, \boldsymbol{\eta}_1) + \frac{1}{\sqrt{n}} \sum_{i=1}^n \frac{\mathbb{P}(S_i = 0)}{\hat{\mathbb{P}}(S_i = 0)} \mathbb{E}(\partial \phi_1 / \partial \boldsymbol{\eta}_1^T \mid S_i = 0) \mathbf{g}_1(\mathbf{O}_i, \boldsymbol{\eta}_1) + o_p(1).$$

Since $\hat{\mathbb{P}}(S_i = 0) = n_t/n$ converges to $\mathbb{P}(S_i = 0)$ almost surely, we have

$$\sqrt{n}(\hat{\theta}_1 - \theta_1) = \sqrt{n} \frac{S_i}{\mathbb{P}(S_i = 1)} \phi_1(\mathbf{V}_i, \theta_1, \boldsymbol{\eta}_1) + \frac{1}{\sqrt{n}} \sum_{i=1}^n \mathbb{E}(\partial \phi_1 / \partial \boldsymbol{\eta}_1^T \mid S_i = 0) \mathbf{g}_1(\mathbf{O}_i, \boldsymbol{\eta}_1) + o_p(1).$$

The proof is completed. \square

Next we consider the asymptotic properties for the bootstrap estimator. The resampling procedure during each bootstrap iteration can be viewed as using a weighted sample, where the weights are determined by Multinomial distributions. Therefore, for a bootstrap quantity, for example $\hat{\theta}_{\text{OR},a}^*(\gamma_a)$, there are two sources of randomness: the randomness from the observed data and the randomness from the bootstrap weights. To distinguish between them, until the end of this subsection we denote by $\mathbb{P}_{\mathbf{O}}$ the probability measure for the observed data and \mathbb{P}_W the probability measure for bootstrap weights, and $\mathbb{P}_{\mathbf{O}W}$ the probability measure on the product space (recall that the bootstrap weights are independent of

data). Similar rules apply to the notation of expectations: $\mathbb{E}_{\mathbf{O}}$, \mathbb{E}_W and $\mathbb{E}_{\mathbf{O}W}$, respectively. A formal treatment of these notations can be found from Cheng and Huang (2010).

Theorem B.2 (Bootstrap Consistency) *Suppose conditions in Theorem B.1 as well as conditions (B1) and (B2) hold, then $\hat{\theta}_a^*(\gamma_a) \rightarrow \theta_a(\gamma_a)$ in $\mathbb{P}_{\mathbf{O}W}$ -probability. Suppose additionally conditions (B3) and (B4), then conditional on observations, the bootstrap estimate $\hat{\theta}_{\text{OR},a}^*(\gamma_a)$ satisfies*

$$\sqrt{n}(\hat{\theta}_{\text{OR},a}^*(\gamma_a) - \hat{\theta}_{\text{OR},a}(\gamma_a)) \mid \{\mathbf{O}_i\}_{i=1}^n \rightarrow_d N(0, \mathbb{E}\{\psi_a^2(\mathbf{O}_i, \theta_a(\gamma_a), \boldsymbol{\eta}_a)\}) \text{ in } \mathbb{P}_{\mathbf{O}}\text{-probability.}$$

Proof of Theorem B.2. We start by proving the consistency, i.e., $\hat{\theta}_a^*(\gamma_a) \rightarrow \theta_a(\gamma_a)$ in $\mathbb{P}_{\mathbf{O}W}$ -probability. By Lemma 6.1 of Wellner (2005), condition (B2) guarantees that ϕ_a is \mathbb{P} -Gilvenko-Cantelli. Together with condition (B1), by the multiplier Gilvenko-Cantelli theorem (Vaart and Wellner, 1996, 3.6.16),

$$\sup_{\boldsymbol{\beta}_a(\gamma_a) \in \Xi} \left| \frac{1}{n} \sum_{i=1}^n W_{n,i} \phi_a(\theta_a(\gamma_a), \boldsymbol{\eta}_a) - \mathbb{P}_{\mathbf{O}} \phi_a(\theta_a(\gamma_a), \boldsymbol{\eta}_a) \right| \rightarrow 0 \text{ in } \mathbb{E}_{\mathbf{O}W} \text{ probability.}$$

Then the consistency for $\hat{\theta}_{\text{OR},a}^*(\gamma_a)$ follows from Corollary 3.2.3 of Vaart and Wellner (1996).

Next, to prove the asymptotic Normality, it's sufficient to show

$$\sqrt{n}(\hat{\boldsymbol{\beta}}_a^*(\gamma_a) - \hat{\boldsymbol{\beta}}_a(\gamma_a)) \mid \{\mathbf{O}_i\}_{i=1}^n \rightarrow_d N(0, \boldsymbol{\Sigma}_a(\gamma_a)),$$

in $\mathbb{P}_{\mathbf{O}}$ -probability, where

$$\boldsymbol{\Sigma}_a(\gamma_a) = \mathbb{E}_{\mathbf{O}} \left\{ \frac{\partial \phi_a(\mathbf{O}, \boldsymbol{\beta}_a(\gamma_a))}{\partial \boldsymbol{\beta}_a(\gamma_a)} \right\}^{-1} \mathbb{E}_{\mathbf{O}} \{ \phi_a(\mathbf{O}, \boldsymbol{\beta}_a(\gamma_a)) \phi_a(\mathbf{O}, \boldsymbol{\beta}_a(\gamma_a))^{\text{T}} \} \left[\mathbb{E}_{\mathbf{O}} \left\{ \frac{\partial \phi_a(\mathbf{O}, \boldsymbol{\beta}_a(\gamma_a))}{\partial \boldsymbol{\beta}_a(\gamma_a)} \right\}^{-1} \right]^{\text{T}}.$$

From there, the asymptotic Normality of $\hat{\theta}_{\text{OR},a}^*(\gamma_a)$ follows from Delta Method.

To show (B.2), we follow Wellner and Zhan (1996) or Cheng and Huang (2010). In particular, the asymptotic Normality in (B.2) holds under regularity conditions (B1) to (B4) and additional conditions (W1) to (W3) on the bootstrap weights:

(W1) $\int_0^\infty \{\mathbb{P}_W(|W_{ni}| > t)\}^{1/2} dt \leq C < \infty$ for some constant C .

(W2) $\lim_{\lambda \rightarrow \infty} \limsup_{n \rightarrow \infty} \sup_{t \geq \lambda} t^2 \mathbb{P}_W(W_{ni} \geq t) = 0$.

(W3) $\sum_{i=1}^n (W_{ni} - 1)^2/n \rightarrow c$ for some constant c .

We are left to verify (W1)-(W3), which can be implied from conditions (W1')-(W3') by Lemma 3.1 of Præstgaard and Wellner (1993).

(W1') $\limsup_{n \rightarrow \infty} \mathbb{E}_W(W_{n,i}^4) < \infty$.

(W2') There exists a constant c such that $\mathbb{E}_W(W_{ni}^2) \rightarrow 1 + c^2$.

(W3') $\text{Cov}_W(W_{n,i}^2, W_{n,j}^2) \leq 0, i \neq j$.

Finally we verify (W1')-(W3'). Let $n^{(k)} = n(n-1) \cdots (n-k+1)$ for integer k . Without loss of generality suppose $i, j \in \mathcal{I}_s$.

$$\mathbb{E}_W(W_{n,i}^2) = 2 - 1/n_s \rightarrow 2,$$

$$\mathbb{E}_W(W_{n,i}^4) = 1 + 7n_s^{(2)}/n_s^2 + 6n_s^{(3)}/n_s^3 + n_s^{(4)}/n_s^4 \leq 15,$$

$$\begin{aligned} \text{Cov}_W(W_{ni}^2, W_{nj}^2) &= \frac{1}{n_s^4} \left[\left\{ n_s^{(4)} - (n_s^{(2)})^2 \right\} + 2n_s \{ n_s^{(3)} - n_s \cdot n_s^{(2)} \} + n_s^2 \{ n_s^{(2)} - n_s^2 \} \right] \\ &\leq 0. \end{aligned}$$

Hence, (W1')-(W3') are satisfied. \square

Now we are ready to prove the confidence interval consistency result in Theorem 4.1. This proof resembles the classic proofs for bootstrap CI consistency (Shao and Tu, 1995; van der Vaart, 1998).

Proof of Theorem 4.1. The consistency of $\hat{\theta}_{\text{OR},a}(\gamma_a)$ has been proven in Theorem B.1. Here we prove the bootstrap confidence interval consistency.

Let Ψ_a be the cumulative distribution function (c.d.f.) of $N(0, \sigma_{\text{OR},a}^2(\gamma_a))$. Let $\hat{\Psi}_a$ and $\hat{\Psi}_a^*$ be the empirical distribution functions of $\sqrt{n}(\hat{\theta}_{\text{OR},a}(\gamma_a) - \theta_a(\gamma_a))$ and $\sqrt{n}(\hat{\theta}_{\text{OR},a}^*(\gamma_a) -$

$\hat{\theta}_{\text{OR},a}(\gamma_a)$), respectively. Then $\hat{\Psi}_a \rightarrow_d \Psi_a$ by Theorem B.1 and $\hat{\Psi}_a^* \mid \{\mathbf{O}_i\}_{i=1}^n \rightarrow_d \Psi_a$ in $\mathbb{P}_{\mathbf{O}}$ -probability by Theorem B.2. For the latter, there exists a subsequence that converges almost surely. For simplicity we assume the whole sequence converges almost surely; similar arguments have been made in Lemma 23.3 of van der Vaart (1998) and Cheng and Huang (2010). Applying the quantile convergence theorem (van der Vaart, 1998, Lemma 21.2) onto the random distribution functions $\hat{\Psi}_a^*$, we have $(\hat{\Psi}_a^*)^{-1}(\tau)$ converges to $\Psi_a^{-1}(\tau)$ almost surely for any $\tau \in (0, 1)$. By Slutsky's theorem,

$$\sqrt{n}(\hat{\theta}_{\text{OR},a}(\gamma_a) - \theta_a(\gamma_a)) - (\hat{\Psi}_a^*)^{-1}(\alpha/2) \rightarrow_d N(0, \sigma_{\text{OR},a}^2(\gamma_a)) - \Psi_a^{-1}(\alpha/2).$$

Further noting $\sqrt{n}(\hat{L}_a(\gamma_a) - \hat{\theta}_a(\gamma_a)) = (\hat{\Psi}_a^*)^{-1}(\alpha/2)$, we have

$$\mathbb{P}(\hat{L}_a(\gamma_a) \leq \theta_a(\gamma_a)) = \mathbb{P}(\sqrt{n}\{\hat{L}_a(\gamma_a) - \hat{\theta}_{\text{OR},a}(\gamma_a)\} \leq \sqrt{n}(\theta_a(\gamma_a) - \hat{\theta}_{\text{OR},a}(\gamma_a))) \quad (\text{B.2})$$

$$= \mathbb{P}((\hat{\Psi}_a^*)^{-1}(\alpha/2) \leq \sqrt{n}\{\theta_a(\gamma_a) - \hat{\theta}_{\text{OR},a}(\gamma_a)\}) \quad (\text{B.3})$$

$$= \mathbb{P}(\sqrt{n}\{\theta_a - \hat{\theta}_{\text{OR},a}(\gamma_a)\} \leq -(\hat{\Psi}_a^*)^{-1}(\alpha/2)) \quad (\text{B.4})$$

$$\rightarrow 1 - \alpha/2 \text{ as } n \rightarrow \infty. \quad (\text{B.5})$$

The proof of $\mathbb{P}(\hat{U}_a(\gamma_a) \geq \theta_a(\gamma_a)) \rightarrow 1 - \alpha/2$ follows similarly and is therefore omitted. The confidence interval consistency follows. \square

C Details and Proofs for the EIF-Based Estimation

C.1 Estimating the Density Ratio

By Bayes rule, $w(\mathbf{v})$ can be expressed in terms of the selection probability $\mathbb{P}(S_i = 1 \mid \mathbf{V}_i = \mathbf{v})$ for $\mathbf{v} \in \mathcal{V}$,

$$w(\mathbf{v}) = \frac{\mathbb{P}(S_i = 1) \mathbb{P}(S_i = 0 \mid \mathbf{V}_i = \mathbf{v})}{\mathbb{P}(S_i = 0) \mathbb{P}(S_i = 1 \mid \mathbf{V}_i = \mathbf{v})}.$$

Therefore, one can obtain $\hat{w}(\mathbf{v})$ with $n_s \hat{\mathbb{P}}(S_i = 0 \mid \mathbf{V}_i = \mathbf{v}) / \{n_t \hat{\mathbb{P}}(S_i = 1 \mid \mathbf{V}_i = \mathbf{v})\}$, where $\hat{\mathbb{P}}(S_i = 1 \mid \mathbf{V}_i = \mathbf{v})$ can be obtained from a binary regression model or classification model. For example, when \mathcal{V} is discrete, one may estimate this probability for any $\mathbf{v} \in \mathcal{V}$ by calculating the proportion of source samples among all samples with the same covariate:

$$\hat{\mathbb{P}}(S_i = 1 \mid \mathbf{V}_i = \mathbf{v}) = \frac{\sum_{i=1}^n \mathbb{I}(S_i = 1, \mathbf{V}_i = \mathbf{v})}{\sum_{i=1}^n \mathbb{I}(\mathbf{V}_i = \mathbf{v})}, \quad \hat{w}(\mathbf{v}) = \frac{n_s \hat{\mathbb{P}}(S_i = 0 \mid \mathbf{V}_i = \mathbf{v})}{n_t \hat{\mathbb{P}}(S_i = 1 \mid \mathbf{V}_i = \mathbf{v})}. \quad (\text{C.1})$$

To account for the possible imbalance between the source and target samples (i.e., n_s and n_t may differ a lot), we employ the offset logistic regression proposed by Zhang et al. (2023) and extended by Kallus and Mao (2024). A direction calculation from the Bayes rule suggests:

$$\log(\mathbb{P}(S_i = 1 \mid \mathbf{V}_i = \mathbf{v}) / \mathbb{P}(S_i = 0 \mid \mathbf{V}_i = \mathbf{v})) = -\log(w(\mathbf{v})) + \log(\mathbb{P}(S_i = 1) / \mathbb{P}(S_i = 0)),$$

which motivates positing a logistic regression model on $\mathbb{P}(S_i = 1 \mid \mathbf{V}_i = \mathbf{v})$ with regression parameter $\boldsymbol{\beta}$ and offset term $\log(n_s/n_t)$:

$$\log(\mathbb{P}(S_i = 1 \mid \mathbf{V}_i = \mathbf{v}) / \mathbb{P}(S_i = 0 \mid \mathbf{V}_i = \mathbf{v})) = \boldsymbol{\beta}^T \mathbf{V}_i + \log(n_s/n_t), \quad \hat{w}(\mathbf{v}) = \exp\left(-\hat{\boldsymbol{\beta}}^T \mathbf{v}\right). \quad (\text{C.2})$$

The convergence rate for the regression coefficient has been established in Zhang et al. (2023) which can be translated to the convergence rate of $w(\mathbf{v})$ (Kallus and Mao, 2024). The estimation can be easily implemented using the `glm` package in R with the argument `offset`.

C.2 Proof of Theorem 4.2 and Theorem A.2

We prove Theorem A.2, the EIF for a general outcome under sensitivity model (A.1). It includes Theorem 4.2 as a special case for a binary outcome. To simplify notation, we suppress the dependence of the TATE on γ_a and enote the expected potential outcome on

the target population at treatment level a as θ_a for $a = 0, 1$. We also drop the subscript i and denote by \mathbf{O} a generic random variable, which consists of $(\mathbf{X}, Y, S = 1)$ for the source and $(\mathbf{V}, S = 0)$ for the target. Denote by $p_{\mathbf{V}|S=1}$, $p_{\mathbf{X}|\mathbf{V},S=1}$, $p_{Y|\mathbf{X},A,S=1}$ the density functions of the conditional distributions of $\mathbf{V} | S$, $\mathbf{X} | \mathbf{V}, S = 1$ and $Y | \mathbf{X}, A, S = 1$, respectively.

We start with the case where $\pi(\mathbf{X})$ is unknown and therefore considered as a nuisance parameter. For clarity we denote its true value as $\pi_0(\mathbf{X})$. For a generic observation \mathbf{O} , the log-likelihood can be written as

$$\begin{aligned} l(\mathbf{O}) = & (1 - S)\log(p_{\mathbf{V}|S=0}(\mathbf{V} | S = 0)) + S\log(p_{\mathbf{V}|S=1}(\mathbf{V} | S = 1)) \\ & + S\log(p_{\mathbf{X}|\mathbf{V},S=1}(\mathbf{X} | \mathbf{V}, S = 1)) + AS\log(\pi(\mathbf{X})) + S(1 - A)\log(1 - \pi(\mathbf{X})) \\ & + SA\log(p_{Y|\mathbf{X},A=1,S=1}(Y | \mathbf{X}, A = 1, S = 1)) + S(1 - A)\log(p_{Y|\mathbf{X},A=0,S=1}(Y | \mathbf{X}, A = 0, S = 1)). \end{aligned}$$

Consider the Hilbert space Λ that contains all one-dimensional zero-mean measurable functions of the observed data with finite variance. Consider $p_{Y|\mathbf{X},A=0,S=1}$, $p_{Y|\mathbf{X},A=1,S=1}$, $\pi(\mathbf{X})$, $p_{\mathbf{X}|\mathbf{V},S=1}$, $p_{\mathbf{V}|S=0}$ and $p_{\mathbf{V}|S=1}$ as nuisance functions and denote their nuisance tangent spaces as $\Lambda_{Y|\mathbf{X},A=1,S=1}$, $\Lambda_{Y|\mathbf{X},A=0,S=1}$, Λ_π , $\Lambda_{\mathbf{X}|S=1}$, $\Lambda_{\mathbf{V}|S=1}$ and $\Lambda_{\mathbf{V}|S=0}$, respectively. Then

$$\Lambda = \Lambda_{Y|\mathbf{X},A=1,S=1} \oplus \Lambda_{Y|\mathbf{X},A=0,S=1} \oplus \Lambda_\pi \oplus \Lambda_{\mathbf{X}|S=1} \oplus \Lambda_{\mathbf{V}|S=1} \oplus \Lambda_{\mathbf{V}|S=0},$$

where \oplus is the direct sum between orthogonal spaces, and

$$\Lambda_{Y|\mathbf{X},A=1,S=1} = \{SAb_1(Y, \mathbf{X}) : \mathbb{E}[\mathbf{b}_1(Y, \mathbf{X}) | \mathbf{X}, A = 1, S = 1] = \mathbf{0}\},$$

$$\Lambda_{Y|\mathbf{X},A=0,S=1} = \{S(1 - A)\mathbf{b}_2(Y, \mathbf{X}) : \mathbb{E}[\mathbf{b}_2(Y, \mathbf{X}) | \mathbf{X}, A = 0, S = 1] = \mathbf{0}\},$$

$$\Lambda_\pi = \{S[A - \pi_0(\mathbf{x})]\mathbf{b}_3(\mathbf{X}) : 0 < \pi_0(\mathbf{X}) < 1\},$$

$$\Lambda_{\mathbf{X}|S=1} = \{S\mathbf{b}_4(\mathbf{X}) : \mathbb{E}[\mathbf{b}_4(\mathbf{X}) | \mathbf{V}, S = 1] = \mathbf{0}\},$$

$$\Lambda_{\mathbf{V}|S=1} = \{S\mathbf{b}_5(\mathbf{V}) : \mathbb{E}[\mathbf{b}_5(\mathbf{V}) | S = 1] = \mathbf{0}\},$$

$$\Lambda_{\mathbf{V}|S=0} = \{(1 - S)\mathbf{b}_6(\mathbf{V}) : \mathbb{E}[\mathbf{b}_6(\mathbf{V}) | S = 0] = \mathbf{0}\}.$$

Without loss of generality, we derive the EIF for θ_1 . The EIF for θ_0 is analogous and thus omitted for brevity. Consider parametric submodels indexed by parameter $\boldsymbol{\alpha}$ where $\boldsymbol{\alpha} = \mathbf{0}$ represents the true data generating process. We re-express the log-likelihood under the parametric submodel,

$$\begin{aligned}
l(\mathbf{O}, \boldsymbol{\alpha}) &= (1 - S)\log p_{\mathbf{V}|S=0}(\mathbf{V} | S = 0; \boldsymbol{\alpha}) + S\log p_{\mathbf{V}|S=1}(\mathbf{V} | S = 1; \boldsymbol{\alpha}) \\
&\quad + S\log p_{\mathbf{X}|\mathbf{V},S=1}(\mathbf{X} | \mathbf{V}, S = 1; \boldsymbol{\alpha}) + AS\log\pi(\mathbf{x}; \boldsymbol{\alpha}) + S(1 - A)\log(1 - \pi(\mathbf{X}; \boldsymbol{\alpha})) \\
&\quad + SA\log p_{Y|\mathbf{X},A=1,S=1}(Y | \mathbf{X}, A = 1, S = 1; \boldsymbol{\alpha}) \\
&\quad + S(1 - A)\log p_{Y|\mathbf{X},A=0,S=1}(Y | \mathbf{X}, A = 0, S = 1; \boldsymbol{\alpha}).
\end{aligned}$$

Define the score function

$$\begin{aligned}
\mathbf{S}(\mathbf{O}) &= \left. \frac{\partial l(\mathbf{O}, \boldsymbol{\alpha})}{\partial \boldsymbol{\alpha}} \right|_{\boldsymbol{\alpha}=\mathbf{0}} \\
&= SAS_1(Y, \mathbf{X}) + S(1 - A)\mathbf{S}_2(Y, \mathbf{X}) + S \left. \frac{\partial [\{A\log(\pi(\mathbf{X}; \boldsymbol{\alpha})) + (1 - A)\log(1 - \pi(\mathbf{X}; \boldsymbol{\alpha}))\}]}{\partial \boldsymbol{\alpha}} \right|_{\boldsymbol{\alpha}=\mathbf{0}} \\
&\quad + SS_4(\mathbf{X}) + SS_5(\mathbf{V}) + (1 - S)\mathbf{S}_6(\mathbf{V}), \text{ where} \\
\mathbf{S}_1(Y, \mathbf{X}) &= \left. \frac{\partial \log p_{Y|\mathbf{X},A=1,S=1}(Y | \mathbf{X}, A = 1, S = 1; \boldsymbol{\alpha})}{\partial \boldsymbol{\alpha}} \right|_{\boldsymbol{\alpha}=\mathbf{0}}, \\
\mathbf{S}_2(Y, \mathbf{X}) &= \left. \frac{\partial \log p_{Y|\mathbf{X},A=0,S=1}(Y | \mathbf{X}, A = 0, S = 1; \boldsymbol{\alpha})}{\partial \boldsymbol{\alpha}} \right|_{\boldsymbol{\alpha}=\mathbf{0}}, \\
\mathbf{S}_4(\mathbf{X}) &= \left. \frac{\partial \log p_{\mathbf{X}|\mathbf{V},S=1}(\mathbf{X} | \mathbf{V}, S = 1; \boldsymbol{\alpha})}{\partial \boldsymbol{\alpha}} \right|_{\boldsymbol{\alpha}=\mathbf{0}}, \\
\mathbf{S}_5(\mathbf{V}) &= \left. \frac{\partial \log p_{\mathbf{V}|S=1}(\mathbf{V} | S = 1; \boldsymbol{\alpha})}{\partial \boldsymbol{\alpha}} \right|_{\boldsymbol{\alpha}=\mathbf{0}}, \\
\mathbf{S}_6(\mathbf{V}) &= \left. \frac{\partial \log p_{\mathbf{V}|S=0}(\mathbf{V} | S = 0; \boldsymbol{\alpha})}{\partial \boldsymbol{\alpha}} \right|_{\boldsymbol{\alpha}=\mathbf{0}},
\end{aligned}$$

and $SAS_1(Y, \mathbf{X}) \in \Lambda_{Y|\mathbf{X},A=1,S=1}$, $S(1 - A)\mathbf{S}_2(Y, \mathbf{X}) \in \Lambda_{Y|\mathbf{X},A=0,S=1}$, $SS_4(\mathbf{X}) \in \Lambda_{\mathbf{X}|S=1}$, $SS_5(\mathbf{V}) \in \Lambda_{\mathbf{V}|S=1}$, $(1 - S)\mathbf{S}_6(\mathbf{V}) \in \Lambda_{\mathbf{V}|S=0}$.

Next, we show that

$$\mathbb{E} [\phi_1^{\text{cont}}(\mathbf{O}, \theta_1) \mathbf{S}(\mathbf{O})] = \frac{\partial \theta_1}{\partial \boldsymbol{\alpha}} \Big|_{\boldsymbol{\alpha}=\mathbf{0}}, \quad (\text{C.3})$$

where

$$\begin{aligned} & \phi_1^{\text{cont}}(\mathbf{O}, \theta_1(\gamma_1)) \\ &= \frac{Sw(\mathbf{V})}{\mathbb{P}(S=1)\pi(\mathbf{X})} \left[\frac{\exp(\gamma_1 Y) Y}{\mathbb{E}\{\exp(\gamma_1 Y^{(1)}) \mid \mathbf{V}, S=1\}} - \frac{\mathbb{E}\{\exp(\gamma_1 Y) Y \mid \mathbf{X}, A=1, S=1\}}{\mathbb{E}\{\exp(\gamma_1 Y^{(1)}) \mid \mathbf{V}, S=1\}} \right. \\ & \quad \left. - \frac{\exp(\gamma_1 Y) \mathbb{E}\{\exp(\gamma_1 Y^{(1)}) Y^{(1)} \mid \mathbf{V}, S=1\}}{[\mathbb{E}\{\exp(\gamma_1 Y^{(1)}) \mid \mathbf{V}, S=1\}]^2} + \frac{\mathbb{E}\{\exp(\gamma_1 Y) \mid \mathbf{X}, A=1, S=1\} \mathbb{E}\{\exp(\gamma_1 Y^{(1)}) Y^{(1)} \mid \mathbf{V}, S=1\}}{[\mathbb{E}\{\exp(\gamma_1 Y^{(1)}) \mid \mathbf{V}, S=1\}]^2} \right] \\ & + \frac{Sw(\mathbf{V})}{\mathbb{P}(S=1)} \frac{\mathbb{E}\{e^{\gamma_1 Y} Y \mid \mathbf{X}, A=1, S=1\} \mathbb{E}\{e^{\gamma_1 Y^{(1)}} \mid \mathbf{V}, S=1\} - \mathbb{E}\{e^{\gamma_1 Y^{(1)}} Y^{(1)} \mid \mathbf{V}, S=1\} \mathbb{E}\{e^{\gamma_1 Y} \mid \mathbf{X}, A=1, S=1\}}{[\mathbb{E}\{\exp(\gamma_1 Y^{(1)}) \mid \mathbf{V}, S=1\}]^2} \\ & + \frac{1-S}{\mathbb{P}(S=0)} \left[\frac{\mathbb{E}\{\exp(\gamma_1 Y^{(1)}) Y^{(1)} \mid \mathbf{V}, S=1\}}{\mathbb{E}\{\exp(\gamma_1 Y^{(1)}) \mid \mathbf{V}, S=1\}} - \theta_1 \right]. \end{aligned}$$

To show (C.3), we calculate its right-hand side:

$$\frac{\partial \theta_1}{\partial \boldsymbol{\alpha}} \Big|_{\boldsymbol{\alpha}=\mathbf{0}} = \mathbb{E} (w(\mathbf{V}) \mathbb{E} [\mathbb{E}\{B_1(Y^{(1)}, \mathbf{X}) \mathbf{S}_1(Y, \mathbf{X}) \mid \mathbf{X}, A=1, S=1\} \mid \mathbf{V}, S=1] \mid S=1) \quad (\text{C.4})$$

$$+ \mathbb{E} [\mathbb{E}\{w(\mathbf{V}) B_4(\mathbf{X}) \mathbf{S}_4(\mathbf{X}) \mid \mathbf{V}, S=1\} \mid S=1] \quad (\text{C.5})$$

$$+ \mathbb{E}\{\mathbb{E}(Y^{(1)} \mathbf{S}_6(\mathbf{V}) \mid S=0)\}, \quad (\text{C.6})$$

where

$$\begin{aligned} B_1(Y^{(1)}, \mathbf{X}) &= \frac{e^{\gamma_1 Y^{(1)}} Y^{(1)}}{\mathbb{E}\{e^{\gamma_1 Y^{(1)}} \mid \mathbf{V}, S=1\}} - \frac{e^{\gamma_1 Y^{(1)}} \mathbb{E}\{e^{\gamma_1 Y^{(1)}} Y^{(1)} \mid \mathbf{V}, S=1\}}{[\mathbb{E}\{e^{\gamma_1 Y^{(1)}} \mid \mathbf{V}, S=1\}]^2}, \\ B_4(\mathbf{X}) &= \frac{\mathbb{E}\{e^{\gamma_1 Y} Y \mid \mathbf{X}, A=1, S=1\} \mathbb{E}\{e^{\gamma_1 Y^{(1)}} \mid \mathbf{V}, S=1\}}{[\mathbb{E}\{e^{\gamma_1 Y^{(1)}} \mid \mathbf{V}, S=1\}]^2} \\ & \quad - \frac{\mathbb{E}\{e^{\gamma_1 Y^{(1)}} Y^{(1)} \mid \mathbf{V}, S=1\} \mathbb{E}\{e^{\gamma_1 Y} \mid \mathbf{X}, A=1, S=1\}}{[\mathbb{E}\{e^{\gamma_1 Y^{(1)}} \mid \mathbf{V}, S=1\}]^2}. \end{aligned}$$

Further, note that

$$\begin{aligned} (\text{C.4}) &= \mathbb{E} (w(\mathbf{V}) \mathbb{E} [\mathbb{E}\{B_1(Y^{(1)}, \mathbf{X}) \mathbf{S}_1(Y, \mathbf{X}) \mid \mathbf{X}, A=1, S=1\} \mid \mathbf{V}, S=1] \mid S=1) \\ &= \mathbb{E} \left(\frac{SAw(\mathbf{V})}{\mathbb{P}(S=1)\pi(\mathbf{X})} [B_1(Y^{(1)}, \mathbf{X}) - \mathbb{E}\{B_1(Y^{(1)}, \mathbf{X}) \mid \mathbf{X}, A=1, S=1\}] \mathbf{S}(\mathbf{O}) \right), \end{aligned}$$

$$(C.5) = \mathbb{E} \left(\frac{S}{\mathbb{P}(S=1)} \{B_4(\mathbf{X}) - \mathbb{E}[B_4(\mathbf{X}) \mid \mathbf{V}, S=1]\} \mathbf{S}(\mathbf{O}) \right),$$

$$(C.6) = \mathbb{E} \left\{ \frac{1-S}{\mathbb{P}(S=0)} [\mathbb{E}(Y^{(1)} \mid \mathbf{V}, S=0) - \theta_1] \mathbf{S}(\mathbf{O}) \right\} \\ = \mathbb{E} \left\{ \frac{1-S}{\mathbb{P}(S=0)} \left[\frac{\mathbb{E} \{ \exp(\gamma_1 Y^{(1)}) Y^{(1)} \mid \mathbf{V}, S=1 \}}{\mathbb{E} \{ \exp(\gamma_1 Y^{(1)}) \mid \mathbf{V}, S=1 \}} - \theta_1 \right] \mathbf{S}(\mathbf{O}) \right\},$$

we have

$$\left. \frac{\partial \theta_1}{\partial \boldsymbol{\alpha}} \right|_{\boldsymbol{\alpha}=\mathbf{0}} = (C.4) + (C.5) + (C.6) = \mathbb{E} [\phi_1^{\text{cont}}(\mathbf{O}, \theta_1) \mathbf{S}(\mathbf{O})].$$

Finally, we verify that $\phi_1^{\text{cont}}(\mathbf{O}, \theta_1) \in \Lambda$ since

$$\frac{SAw(\mathbf{V})}{\mathbb{P}(S=1)\pi(\mathbf{X})} [B_1(y^{(1)}, \mathbf{x}) - \mathbb{E}\{B_1(Y^{(1)}, \mathbf{X}) \mid \mathbf{x}, A=1, S=1\}] \in \Lambda_{Y|\mathbf{X}, A=1, S=1}, \\ \frac{S}{\mathbb{P}(S=1)} \{B_4(\mathbf{X}) - \mathbb{E}[B_4(\mathbf{X}) \mid \mathbf{v}, S=1]\} \in \Lambda_{\mathbf{X}|S=1}, \text{ and} \\ \frac{1-S}{\mathbb{P}(S=0)} \left[\frac{\mathbb{E} \{ \exp(\gamma_1 Y^{(1)}) Y^{(1)} \mid \mathbf{V}, S=1 \}}{\mathbb{E} \{ \exp(\gamma_1 Y^{(1)}) \mid \mathbf{V}, S=1 \}} - \theta_1 \right] \in \Lambda_{\mathbf{V}|S=0}.$$

Therefore, $\phi_1^{\text{cont}}(\mathbf{O}, \theta_1)$ is the EIF in Theorem A.2, i.e., $\text{EIF}_1^{\text{cont}}(\mathbf{O}, \theta_1)$. Moreover, if the outcome is binary, we can re-express the followings:

$$\mathbb{E}\{\exp(\gamma_1 Y) Y \mid \mathbf{X}, A=1, S=1\} = \exp(\gamma_1) \mu_1(\mathbf{X}), \\ \mathbb{E}\{\exp(\gamma_1 Y) \mid \mathbf{X}, A=1, S=1\} = \exp(\gamma_1) \mu_1(\mathbf{X}) + 1 - \mu_1(\mathbf{X}), \\ \mathbb{E}\{\exp(\gamma_1 Y^{(1)}) Y^{(1)} \mid \mathbf{V}, S=1\} = \exp(\gamma_1) \rho_1(\mathbf{V}), \\ \mathbb{E}\{\exp(\gamma_1 Y^{(1)}) \mid \mathbf{V}, S=1\} = \exp(\gamma_1) \rho_1(\mathbf{V}) + 1 - \rho_1(\mathbf{V}).$$

Plugging in them to $\text{EIF}^{\text{cont}}(\mathbf{O}, \theta_1)$ yields $\text{EIF}(\mathbf{O}, \theta_1)$ as the expression of the EIF for a binary outcome in Theorem 4.2.

Next, we suppose $\pi(\mathbf{X})$ is known as its true value $\pi_0(\mathbf{X})$. Then $\pi(\mathbf{X})$ is no longer considered as a nuisance function and the Hilbert space Λ can now be decomposed as

$$\Lambda = \Lambda_{Y|\mathbf{X}, A=1, S=1} \oplus \Lambda_{Y|\mathbf{X}, A=0, S=1} \oplus \Lambda_{\mathbf{X}|S=0} \oplus \Lambda_{\mathbf{V}|S=1} \oplus \Lambda_{\mathbf{V}|S=0}.$$

Under the parametric submodel, the log-likelihood becomes

$$\begin{aligned}
l(\mathbf{O}, \boldsymbol{\alpha}) &= (1 - S) \log p_{\mathbf{V}|S=0}(\mathbf{V} | S = 0; \boldsymbol{\alpha}) + S \log p_{\mathbf{V}|S=1}(\mathbf{V} | S = 1; \boldsymbol{\alpha}) \\
&\quad + S \log p_{\mathbf{X}|\mathbf{V},S=1}(\mathbf{X} | \mathbf{V}, S = 1; \boldsymbol{\alpha}) + AS \log \pi_0(\mathbf{X}) + S(1 - A) \log(1 - \pi_0(\mathbf{X})) \\
&\quad + SA \log p_{Y|\mathbf{X},A=1,S=1}(Y | \mathbf{X}, A = 1, S = 1; \boldsymbol{\alpha}) \\
&\quad + S(1 - A) \log p_{Y|\mathbf{X},A=0,S=1}(Y | \mathbf{X}, A = 0, S = 1; \boldsymbol{\alpha}).
\end{aligned}$$

Then the score function becomes

$$\begin{aligned}
\mathbf{S}(\mathbf{O}) &= \left. \frac{\partial l(\mathbf{O}, \boldsymbol{\alpha})}{\partial \boldsymbol{\alpha}} \right|_{\boldsymbol{\alpha}=\mathbf{0}} \\
&= SAS_1(Y, \mathbf{X}) + S(1 - A)\mathbf{S}_2(Y, \mathbf{X}) + S\mathbf{S}_4(\mathbf{X}) + S\mathbf{S}_5(\mathbf{V}) + (1 - S)\mathbf{S}_6(\mathbf{V}),
\end{aligned}$$

where we still have $SAS_1(Y, \mathbf{X}) \in \Lambda_{Y|\mathbf{X},A=1,S=1}$, $S(1 - A)\mathbf{S}_2(Y, \mathbf{X}) \in \Lambda_{Y|\mathbf{X},A=0,S=1}$, $S\mathbf{S}_4(\mathbf{X}) \in \Lambda_{\mathbf{X}|S=1}$, $S\mathbf{S}_5(\mathbf{V}) \in \Lambda_{\mathbf{V}|S=1}$, $(1 - S)\mathbf{S}_6(\mathbf{V}) \in \Lambda_{\mathbf{V}|S=0}$. Therefore, $\mathbb{E}[\phi_1^{\text{cont}}(\mathbf{O}, \theta_1)\mathbf{S}(\mathbf{O})] = \left. \frac{\partial \theta_1}{\partial \boldsymbol{\alpha}} \right|_{\boldsymbol{\alpha}=\mathbf{0}}$ holds following the same argument as we've shown.

C.3 Lemma C.1

In this section we characterize the plug-in bias for the EIF-based estimator $\hat{\theta}_{\text{EIF},a}(\gamma_a)$. For the generality of the conclusion and to avoid overloading the notation, we assume the nuisance functions are estimated from an independent sample. We introduce the general notation for the uncentered EIF,

$$\begin{aligned}
&\varphi_a(\mathbf{O}_i) \\
&= \frac{S_i w(\mathbf{V}_i)}{\mathbb{P}(S_i = 1)} \frac{\exp(\gamma_a)}{[\exp(\gamma_a)\rho_a(\mathbf{V}_i) + 1 - \rho_a(\mathbf{V}_i)]^2} \left[\left\{ \frac{A_i}{\pi(\mathbf{X}_i)} + \frac{1 - A_i}{1 - \pi(\mathbf{X}_i)} \right\} \{Y_i - \mu_a(\mathbf{X}_i)\} + \mu_a(\mathbf{X}_i) - \rho_a(\mathbf{V}_i) \right] \\
&\quad + \frac{1 - S_i}{\mathbb{P}(S_i = 0)} \frac{\exp(\gamma_a)\rho_a(\mathbf{V}_i)}{\exp(\gamma_a)\rho_a(\mathbf{V}_i) + 1 - \rho_a(\mathbf{V}_i)},
\end{aligned}$$

and its estimate

$$\hat{\varphi}_a(\mathbf{O}_i)$$

$$\begin{aligned}
&= \frac{S_i \hat{w}(\mathbf{V}_i)}{\hat{\mathbb{P}}(S_i = 1)} \frac{\exp(\gamma_a)}{[\exp(\gamma_a) \hat{\rho}_a(\mathbf{V}_i) + 1 - \hat{\rho}_a(\mathbf{V}_i)]^2} \left[\left\{ \frac{A_i}{\hat{\pi}(\mathbf{X}_i)} + \frac{1 - A_i}{1 - \hat{\pi}(\mathbf{X}_i)} \right\} \{Y_i - \hat{\mu}_a(\mathbf{X}_i)\} + \hat{\mu}_a(\mathbf{X}_i) - \hat{\rho}_a(\mathbf{V}_i) \right] \\
&\quad + \frac{1 - S_i}{\hat{\mathbb{P}}(S_i = 0)} \frac{\exp(\gamma_a) \hat{\rho}_a(\mathbf{V}_i)}{\exp(\gamma_a) \hat{\rho}_a(\mathbf{V}_i) + 1 - \hat{\rho}_a(\mathbf{V}_i)},
\end{aligned}$$

where $\hat{\mathbb{P}}(S_i = 1) = n_s/n$, $\hat{\mu}_a(\mathbf{X}_i)$, $\hat{\rho}_a(\mathbf{V}_i)$, $\hat{\pi}(\mathbf{X}_i)$ and $\hat{w}(\mathbf{V}_i)$ are estimated from an independent sample.

Lemma C.1 *There exists a constant C such that*

$$\begin{aligned}
|\mathbb{E}\{\hat{\varphi}_a(\mathbf{O}_i) - \varphi_a(\mathbf{O}_i)\}| &\leq C (\|\hat{\mu}_a(\mathbf{X}_i) - \mu_a(\mathbf{X}_i)\| \cdot \|\hat{\pi}(\mathbf{X}_i) - \pi(\mathbf{X}_i)\| + \|\hat{\rho}_a(\mathbf{V}_i) - \rho_a(\mathbf{V}_i)\| \cdot \|\hat{w}(\mathbf{V}_i) - w(\mathbf{V}_i)\| \\
&\quad + \|\hat{\rho}_a(\mathbf{V}_i) - \rho_a(\mathbf{V}_i)\|^2).
\end{aligned}$$

In particular, if $\gamma_1 = \gamma_0 = 0$, there exists a constant C such that

$$|\mathbb{E}\{\hat{\varphi}_a(\mathbf{O}_i) - \varphi_a(\mathbf{O}_i)\}| \leq C (\|\hat{\mu}_a(\mathbf{X}_i) - \mu_a(\mathbf{X}_i)\| \cdot \|\hat{\pi}(\mathbf{X}_i) - \pi(\mathbf{X}_i)\| + \|\hat{\rho}_a(\mathbf{V}_i) - \rho_a(\mathbf{V}_i)\| \cdot \|\hat{w}(\mathbf{V}_i) - w(\mathbf{V}_i)\|)$$

Proof of Lemma C.1: Without loss of generality, we prove the case for $a = 1$.

$$\begin{aligned}
&\mathbb{E}\{\hat{\varphi}_1(\mathbf{O}_i) - \varphi_1(\mathbf{O}_i)\} \\
&= \mathbb{E}\{\hat{\varphi}_1(\mathbf{O}_i)\} - \theta_1 \\
&= \mathbb{E}\{\hat{\varphi}_1(\mathbf{O}_i)\} - \mathbb{E} \left[\frac{1 - S_i}{\mathbb{P}(S_i = 0)} \frac{\exp(\gamma_1) \rho_1(\mathbf{V}_i)}{\exp(\gamma_1) \rho_1(\mathbf{V}_i) + 1 - \rho_1(\mathbf{V}_i)} \right] \\
&= \mathbb{E} \left[\frac{S_i \hat{w}(\mathbf{V}_i)}{\hat{\mathbb{P}}(S_i = 1)} \frac{\exp(\gamma_1)}{[\exp(\gamma_1) \hat{\rho}_1(\mathbf{V}_i) + 1 - \hat{\rho}_1(\mathbf{V}_i)]^2} \frac{A}{\hat{\pi}(\mathbf{X}_i)} \{\mu_1(\mathbf{X}_i) - \hat{\mu}_1(\mathbf{X}_i)\} \right] \\
&\quad + \mathbb{E} \left[\frac{S_i \hat{w}(\mathbf{V}_i)}{\hat{\mathbb{P}}(S_i = 1)} \frac{\exp(\gamma_1)}{[\exp(\gamma_1) \hat{\rho}_1(\mathbf{V}_i) + 1 - \hat{\rho}_1(\mathbf{V}_i)]^2} \{\hat{\mu}_1(\mathbf{X}_i) - \mu_1(\mathbf{X}_i)\} \right] \\
&\quad - \mathbb{E} \left[\frac{S_i \hat{w}(\mathbf{V}_i)}{\hat{\mathbb{P}}(S_i = 1)} \frac{\exp(\gamma_1)}{[\exp(\gamma_1) \hat{\rho}_1(\mathbf{V}_i) + 1 - \hat{\rho}_1(\mathbf{V}_i)]^2} \{\hat{\rho}_1(\mathbf{V}_i) - \rho_1(\mathbf{V}_i)\} \right] \\
&\quad + \mathbb{E} \left[\frac{1 - S_i}{\hat{\mathbb{P}}(S_i = 0)} \frac{\exp(\gamma_1) \hat{\rho}_1(\mathbf{V}_i)}{\exp(\gamma_1) \hat{\rho}_1(\mathbf{V}_i) + 1 - \hat{\rho}_1(\mathbf{V}_i)} - \frac{1 - S_i}{\mathbb{P}(S_i = 0)} \frac{\exp(\gamma_1) \rho_1(\mathbf{V}_i)}{\exp(\gamma_1) \rho_1(\mathbf{V}_i) + 1 - \rho_1(\mathbf{V}_i)} \right] \\
&= \mathbb{E} \left[\frac{S_i \hat{w}(\mathbf{V}_i)}{\hat{\mathbb{P}}(S_i = 1) \hat{\pi}(\mathbf{X}_i)} \frac{\exp(\gamma_1)}{[\exp(\gamma_1) \hat{\rho}_1(\mathbf{V}_i) + 1 - \hat{\rho}_1(\mathbf{V}_i)]^2} \{\hat{\pi}(\mathbf{X}_i) - \pi(\mathbf{X}_i)\} \{\hat{\mu}_1(\mathbf{X}_i) - \mu_1(\mathbf{X}_i)\} \right]
\end{aligned}$$

$$\begin{aligned}
& - \mathbb{E} \left[\left\{ \frac{\mathbb{P}(S_i = 1) - \widehat{\mathbb{P}}(S_i = 1)}{\widehat{\mathbb{P}}(S_i = 1)\mathbb{P}(S_i = 1)} + \frac{1}{\mathbb{P}(S_i = 1)} \right\} S_i \widehat{w}(\mathbf{V}_i) \frac{\exp(\gamma_1)}{[\exp(\gamma_1)\widehat{\rho}_1(\mathbf{V}_i) + 1 - \widehat{\rho}_1(\mathbf{V}_i)]^2} \{\widehat{\rho}_1(\mathbf{V}_i) - \rho_1(\mathbf{V}_i)\} \right] \\
& + \mathbb{E} \left(\frac{(1 - S_i) \exp(\gamma_1) [\widehat{\rho}_1(\mathbf{V}_i) \{\exp(\gamma_1)\rho_1(\mathbf{V}_i) + 1 - \rho_1(\mathbf{V}_i)\} - \rho_1(\mathbf{V}_i) \{\exp(\gamma_1)\widehat{\rho}_1(\mathbf{V}_i) + 1 - \widehat{\rho}_1(\mathbf{V}_i)\}]}{\mathbb{P}(S_i = 0)\widehat{\mathbb{P}}(S_i = 0) \{\exp(\gamma_1)\widehat{\rho}_1(\mathbf{V}_i) + 1 - \widehat{\rho}_1(\mathbf{V}_i)\} \{\exp(\gamma_1)\rho_1(\mathbf{V}_i) + 1 - \rho_1(\mathbf{V}_i)\}} \right) \\
& \leq O(1) \cdot \mathbb{E} [\{\widehat{\pi}(\mathbf{X}_i) - \pi(\mathbf{X}_i)\} \{\widehat{\mu}_1(\mathbf{X}_i) - \mu_1(\mathbf{X}_i)\}] \\
& - \mathbb{E} \left[\frac{S_i \widehat{w}(\mathbf{V}_i)}{\mathbb{P}(S_i = 1)} \frac{\exp(\gamma_1)}{[\exp(\gamma_1)\widehat{\rho}_1(\mathbf{V}_i) + 1 - \widehat{\rho}_1(\mathbf{V}_i)]^2} \{\widehat{\rho}_1(\mathbf{V}_i) - \rho_1(\mathbf{V}_i)\} \right] \\
& + \mathbb{E} \left[\frac{(1 - S_i)}{\mathbb{P}(S_i = 0)} \frac{\exp(\gamma_1)}{\{\exp(\gamma_1)\widehat{\rho}_1(\mathbf{V}_i) + 1 - \widehat{\rho}_1(\mathbf{V}_i)\} \{\exp(\gamma_1)\rho_1(\mathbf{V}_i) + 1 - \rho_1(\mathbf{V}_i)\}} \{\widehat{\rho}_1(\mathbf{V}_i) - \rho_1(\mathbf{V}_i)\} \right] \\
& \leq O(1) \cdot \mathbb{E} [\{\widehat{\pi}(\mathbf{X}_i) - \pi(\mathbf{X}_i)\} \{\widehat{\mu}_1(\mathbf{X}_i) - \mu_1(\mathbf{X}_i)\}] \\
& + \mathbb{E} \left[\frac{S_i}{\mathbb{P}(S_i = 1)} \frac{\exp(\gamma_1) \{1 - \exp(\gamma_1)\} \{\widehat{\rho}_1(\mathbf{V}_i) - \rho_1(\mathbf{V}_i)\} \{\widehat{w}(\mathbf{V}_i) - w(\mathbf{V}_i)\}}{\{\exp(\gamma_1)\widehat{\rho}_1(\mathbf{V}_i) + 1 - \widehat{\rho}_1(\mathbf{V}_i)\}^2 \{\exp(\gamma_1)\rho_1(\mathbf{V}_i) + 1 - \rho_1(\mathbf{V}_i)\}} \right] \\
& + \mathbb{E} \left[\frac{S w(\mathbf{V}_i)}{\mathbb{P}(S_i = 1)} \frac{\exp(\gamma_1) \{1 - \exp(\gamma_1)\} \{\widehat{\rho}_1(\mathbf{V}_i) - \rho_1(\mathbf{V}_i)\}^2}{\{\exp(\gamma_1)\widehat{\rho}_1(\mathbf{V}_i) + 1 - \widehat{\rho}_1(\mathbf{V}_i)\}^2 \{\exp(\gamma_1)\rho_1(\mathbf{V}_i) + 1 - \rho_1(\mathbf{V}_i)\}} \right] \\
& \leq O(1) \cdot \mathbb{E} [\{\widehat{\pi}(\mathbf{X}_i) - \pi(\mathbf{X}_i)\} \{\widehat{\mu}_1(\mathbf{X}_i) - \mu_1(\mathbf{X}_i)\}] + O(1) \cdot \mathbb{E} [\{\widehat{w}(\mathbf{V}_i) - w(\mathbf{V}_i)\} \{\widehat{\rho}_1(\mathbf{V}_i) - \rho_1(\mathbf{V}_i)\}] \\
& + O(1) \cdot \mathbb{E} [\{\widehat{\rho}_1(\mathbf{V}_i) - \rho_1(\mathbf{V}_i)\}^2] \\
& \leq O(1) \{ \|\widehat{\mu}_a(\mathbf{X}_i) - \mu_a(\mathbf{X}_i)\| \cdot \|\widehat{\pi}(\mathbf{X}_i) - \pi(\mathbf{X}_i)\| + \|\widehat{\rho}_a(\mathbf{V}_i) - \rho_a(\mathbf{V}_i)\| \cdot \|\widehat{w}(\mathbf{V}_i) - w(\mathbf{V}_i)\| \\
& + \|\widehat{\rho}_a(\mathbf{V}_i) - \rho_a(\mathbf{V}_i)\|^2 \}
\end{aligned}$$

When $\gamma_1 = 0$, following the same procedure and using the fact that $\exp(\gamma_1) = 1$, we have

$$\begin{aligned}
& \mathbb{E} \{\widehat{\varphi}_1(\mathbf{O}_i) - \varphi_1(\mathbf{O}_i)\} \\
& \leq O(1) \{ \|\widehat{\mu}_a(\mathbf{X}_i) - \mu_a(\mathbf{X}_i)\| \cdot \|\widehat{\pi}(\mathbf{X}_i) - \pi(\mathbf{X}_i)\| + \|\widehat{\rho}_a(\mathbf{V}_i) - \rho_a(\mathbf{V}_i)\| \cdot \|\widehat{w}(\mathbf{V}_i) - w(\mathbf{V}_i)\| \}.
\end{aligned}$$

C.4 Proof of Theorem 4.3

The EIF-based estimator is $\widehat{\theta}_{\text{EIF}}(\gamma_a) = \widehat{\theta}_{\text{EIF},1} - \widehat{\theta}_{\text{EIF},0}$ with $\widehat{\theta}_{\text{EIF},a}(\gamma_a) = \frac{1}{K} \sum_{k=1}^K \frac{1}{|\mathcal{I}^{(k)}|} \sum_{i \in \mathcal{I}^{(k)}} \widehat{\varphi}(\mathbf{O}_i)$.

Without loss of generality, we consider the proof for $\widehat{\theta}_{\text{EIF},a}(\gamma_a)$ and drop γ_a in notation for

simplicity. We have

$$\widehat{\theta}_{\text{EIF},a} - \theta_a = \left\{ \frac{1}{K} \sum_{k=1}^K \frac{1}{|\mathcal{I}^{(k)}|} \sum_{i \in \mathcal{I}^{(k)}} \widehat{\varphi}_a^{(k)}(\mathbf{O}_i) - \theta_a \right\} \quad (\text{C.7})$$

$$= \left\{ \frac{1}{K} \sum_{k=1}^K \frac{1}{|\mathcal{I}^{(k)}|} \sum_{i \in \mathcal{I}^{(k)}} \widehat{\text{EIF}}^{(k)}(\mathbf{O}_i, \theta_a) \right\} \quad (\text{C.8})$$

$$= \frac{1}{n} \sum_{i=1}^n \text{EIF}(\mathbf{O}_i, \theta_a) + \left\{ \frac{1}{K} \sum_{k=1}^K \frac{1}{|\mathcal{I}^{(k)}|} \sum_{i \in \mathcal{I}^{(k)}} \widehat{\text{EIF}}^{(k)}(\mathbf{O}_i) - \frac{1}{n} \sum_{i=1}^n \text{EIF}(\mathbf{O}_i) \right\} \quad (\text{C.9})$$

$$= \frac{1}{n} \sum_{i=1}^n \text{EIF}(\mathbf{O}_i, \theta_a) + \left\{ \frac{1}{K} \sum_{k=1}^K \frac{1}{|\mathcal{I}^{(k)}|} \sum_{i \in \mathcal{I}^{(k)}} \left[\widehat{\text{EIF}}^{(k)}(\mathbf{O}_i, \theta_a) - \text{EIF}(\mathbf{O}_i, \theta_a) \right] \right\}.$$

We define

$$R_k = \frac{1}{|\mathcal{I}^{(k)}|} \sum_{i \in \mathcal{I}^{(k)}} \left\{ \widehat{\text{EIF}}^{(k)}(\mathbf{O}_i, \theta_a) - \text{EIF}(\mathbf{O}_i, \theta_a) \right\}, \text{ for } k = 1, \dots, K.$$

C.4.1 Part (i)

Since K is independent of data, to show that $\widehat{\theta}_{\text{EIF},a}$ is consistent, it suffices to show

$$R_1 = o_p(1).$$

From Lemma C.1,

$$\begin{aligned} \mathbb{E}(R_1) &\leq O(1) \cdot \left\{ \|\widehat{w}^{(k)}(\mathbf{V}_i) - w^{(k)}(\mathbf{V}_i)\| \cdot \|\widehat{\rho}_a^{(k)}(\mathbf{V}_i) - \rho_a^{(k)}(\mathbf{V}_i)\| + \|\widehat{\rho}_a^{(k)}(\mathbf{V}_i) - \rho_a^{(k)}(\mathbf{V}_i)\|^2 \right\} \\ &\quad + O(1) \cdot \|\widehat{\pi}^{(k)}(\mathbf{X}_i) - \pi^{(k)}(\mathbf{X}_i)\| \cdot \|\widehat{\mu}_a^{(k)}(\mathbf{X}_i) - \mu_a^{(k)}(\mathbf{X}_i)\| \\ &\leq o_p(1), \end{aligned}$$

where the second inequality follows from the conditions that $\|\widehat{\rho}_a^{(k)}(\mathbf{V}_i) - \rho_a^{(k)}(\mathbf{V}_i)\| = o_p(1)$

and (4.3). Next, we show $R_1 - \mathbb{E}(R_1) = o_p(1)$. Conditioning on $\mathcal{I}_k^c = \mathcal{I} \setminus \mathcal{I}_k$, we calculate

the mean and variance for $R_1 - \mathbb{E}(R_1)$:

$$\begin{aligned} \mathbb{E}\{R_1 - \mathbb{E}(R_1) \mid \mathcal{I}_k^c\} &= \mathbb{E} \left[\widehat{\text{EIF}}^{(k)}(\mathbf{O}_i, \theta_a) - \mathbb{E}\{\widehat{\phi}_{\text{EIF},a}^{(k)}(\mathbf{O}_i, \theta_a)\} \mid \mathcal{I}_k^c \right] - \mathbb{E} [\text{EIF}(\mathbf{O}_i, \theta_a) - \mathbb{E}\{\text{EIF}(\mathbf{O}_i, \theta_a)\}] \\ &= 0, \end{aligned}$$

$$\text{Var}(R_1 - \mathbb{E}(R_1) \mid \mathcal{I}_k^c) = \text{Var}(R_1 \mid \mathcal{I}_k^c) \leq K \|\widehat{\text{EIF}}^{(k)}(\mathbf{O}_i, \theta_a) - \text{EIF}(\mathbf{O}_i, \theta_a)\|^2/n.$$

Then for any $\varepsilon > 0$, by Chebyshev's inequality,

$$\begin{aligned} \mathbb{P}\left(\frac{R_1 - \mathbb{E}(R_1)}{\|\widehat{\text{EIF}}^{(k)}(\mathbf{O}_i, \theta_a) - \text{EIF}(\mathbf{O}_i, \theta_a)\|/\sqrt{n}} \geq \varepsilon\right) &= \mathbb{E}\left\{\mathbb{P}\left(\frac{R_1 - \mathbb{E}(R_1)}{K\|\widehat{\text{EIF}}^{(k)}(\mathbf{O}_i, \theta_a) - \text{EIF}(\mathbf{O}_i, \theta_a)\|/\sqrt{n}} \geq \varepsilon \mid \mathcal{I}_k^c\right)\right\} \\ &\leq 1/\varepsilon^2. \end{aligned}$$

Therefore,

$$R_1 - \mathbb{E}(R_1) = KO_p(\|\widehat{\text{EIF}}^{(k)}(\mathbf{O}_i, \theta_a) - \text{EIF}(\mathbf{O}_i, \theta_a)\|/\sqrt{n}) \leq O_p(1/\sqrt{n}) = o_p(1).$$

C.4.2 Part (ii)

The decomposition at the beginning of the proof suggests

$$\sqrt{n}(\widehat{\theta}_{\text{EIF},a} - \theta_a) = \frac{1}{\sqrt{n}} \sum_{i=1}^n \text{EIF}(\mathbf{O}_i, \theta_a) + \sqrt{n} \left\{ \frac{1}{K} \sum_{k=1}^K \frac{1}{|\mathcal{I}^{(k)}|} \sum_{i \in \mathcal{I}^{(k)}} \left[\widehat{\text{EIF}}^{(k)}(\mathbf{O}_i, \theta_a) - \text{EIF}(\mathbf{O}_i, \theta_a) \right] \right\}$$

Since K is independent of the data, it suffices to show

$$R_1 = o_p(n^{-1/2}).$$

From Lemma C.1 and the rate conditions (4.4a), (4.4b) and (4.4c) in Theorem 4.3, we have

$$\mathbb{E}(R_1) = o_p(n^{-1/2}).$$

In what follows we show $R_1 - \mathbb{E}(R_1) = o_p(n^{-1/2})$. Conditioning on $\mathcal{I}_k^c = \mathcal{I} \setminus \mathcal{I}_k$, we calculate

the mean and variance for $R_1 - \mathbb{E}(R_1)$:

$$\begin{aligned} \mathbb{E}\{R_1 - \mathbb{E}(R_1) \mid \mathcal{I}_k^c\} &= \mathbb{E}\left[\widehat{\text{EIF}}^{(k)}(\mathbf{O}_i, \theta_a) - \mathbb{E}\{\widehat{\phi}_{\text{EIF},a}^{(k)}(\mathbf{O}_i, \theta_a)\} \mid \mathcal{I}_k^c\right] - \mathbb{E}[\text{EIF}(\mathbf{O}_i, \theta_a) - \mathbb{E}\{\text{EIF}(\mathbf{O}_i, \theta_a)\}] \\ &= 0, \end{aligned}$$

$$\text{Var}(R_1 - \mathbb{E}(R_1) \mid \mathcal{I}_k^c) = \text{Var}(R_1 \mid \mathcal{I}_k^c) \leq K \|\widehat{\text{EIF}}^{(k)}(\mathbf{O}_i, \theta_a) - \text{EIF}(\mathbf{O}_i, \theta_a)\|^2/n.$$

Then for any $\varepsilon > 0$, by Chebyshev's inequality,

$$\begin{aligned} \mathbb{P} \left(\frac{R_1 - \mathbb{E}(R_1)}{\|\widehat{\text{EIF}}^{(k)}(\mathbf{O}_i, \theta_a) - \text{EIF}(\mathbf{O}_i, \theta_a)\|/\sqrt{n}} \geq \varepsilon \right) &= \mathbb{E} \left\{ \mathbb{P} \left(\frac{R_1 - \mathbb{E}(R_1)}{K\|\widehat{\text{EIF}}^{(k)}(\mathbf{O}_i, \theta_a) - \text{EIF}(\mathbf{O}_i, \theta_a)\|/\sqrt{n}} \geq \varepsilon \mid \mathcal{I}_k^c \right) \right\} \\ &\leq 1/\varepsilon^2. \end{aligned}$$

Since all nuisance parameters are consistently estimated by assumption (i.e., $\|\widehat{\rho}_a^{(k)}(\mathbf{V}_i) - \rho_a^{(k)}(\mathbf{V}_i)\| = o_p(1)$, $\|\widehat{\mu}_a^{(k)}(\mathbf{X}_i) - \mu_a^{(k)}(\mathbf{X}_i)\| = o_p(1)$, $\|\widehat{w}^{(k)}(\mathbf{V}_i) - w^{(k)}(\mathbf{V}_i)\| = o_p(1)$, $\|\widehat{\pi}^{(k)}(\mathbf{X}_i) - \pi^{(k)}(\mathbf{X}_i)\| = o_p(1)$), Lemma C.1 suggests that $\|\widehat{\text{EIF}}^{(k)}(\mathbf{O}_i, \theta_a) - \text{EIF}(\mathbf{O}_i, \theta_a)\| = o_p(1)$. Therefore,

$$R_1 - \mathbb{E}(R_1) = K O_p(\|\widehat{\text{EIF}}^{(k)}(\mathbf{O}_i, \theta_a) - \text{EIF}(\mathbf{O}_i, \theta_a)\|/\sqrt{n}) = o_p(1/\sqrt{n}).$$

C.4.3 Part (iii)

In order to show

$$\widehat{\sigma}_{\text{EIF},a}^2(\gamma_a) - \sigma_{\text{EIF},a}^2(\gamma_a) = \frac{1}{K} \sum_{k=1}^K \frac{1}{|\mathcal{I}^{(k)}|} \sum_{i \in \mathcal{I}^{(k)}} \widehat{\text{EIF}}^2(\mathbf{O}_i, \widehat{\theta}_{\text{EIF},a}(\gamma_a)) - \mathbb{E}\{\text{EIF}^2(\mathbf{O}_i, \theta_a(\gamma_a))\} = o_p(1),$$

it's sufficient to show

$$R_{k,1} - R_{k,2} = \frac{1}{|\mathcal{I}^{(k)}|} \sum_{i \in \mathcal{I}^{(k)}} \widehat{\text{EIF}}^2(\mathbf{O}_i, \widehat{\theta}_{\text{EIF},a}(\gamma_a)) - \mathbb{E}\{\text{EIF}^2(\mathbf{O}_i, \theta_a(\gamma_a))\} = o_p(1), \quad (\text{C.10})$$

where

$$\begin{aligned} R_{k,1} &= \frac{1}{|\mathcal{I}^{(k)}|} \sum_{i \in \mathcal{I}^{(k)}} \left\{ \widehat{\text{EIF}}^2(\mathbf{O}_i, \widehat{\theta}_{\text{EIF},a}(\gamma_a)) - \text{EIF}^2(\mathbf{O}_i, \theta_a(\gamma_a)) \right\}, \\ R_{k,2} &= \frac{1}{|\mathcal{I}^{(k)}|} \sum_{i \in \mathcal{I}^{(k)}} \left[\text{EIF}^2(\mathbf{O}_i, \theta_a(\gamma_a)) - \mathbb{E}\{\text{EIF}^2(\mathbf{O}_i, \theta(\gamma_a))\} \right]. \end{aligned}$$

(C.10) can be concluded since $R_{k,2} = O_p(n^{-1/2})$ by $\mathbb{E}\{\text{EIF}^4(\mathbf{O}_i, \theta(\gamma_a))\} < \infty$, and $R_{k,1} = O_p(n^{-1/2})$ by the following argument. Note that

$$|R_{k,1}| \leq \frac{1}{|\mathcal{I}^{(k)}|} \sum_{i \in \mathcal{I}^{(k)}} \left| \widehat{\text{EIF}}^2(\mathbf{O}_i, \widehat{\theta}_{\text{EIF},a}(\gamma_a)) - \text{EIF}^2(\mathbf{O}_i, \theta_a(\gamma_a)) \right|$$

$$\begin{aligned}
&= \frac{1}{|\mathcal{I}^{(k)}|} \sum_{i \in \mathcal{I}^{(k)}} \left| \widehat{\text{EIF}}(\mathbf{O}_i, \hat{\theta}_{\text{EIF},a}(\gamma_a)) - \text{EIF}(\mathbf{O}_i, \theta_a(\gamma_a)) \right| \cdot \left| \widehat{\text{EIF}}(\mathbf{O}_i, \hat{\theta}_{\text{EIF},a}(\gamma_a)) + \text{EIF}(\mathbf{O}_i, \theta_a(\gamma_a)) \right| \\
&\leq \sqrt{\frac{1}{|\mathcal{I}^{(k)}|} \sum_{i \in \mathcal{I}^{(k)}} \left| \widehat{\text{EIF}}(\mathbf{O}_i, \hat{\theta}_{\text{EIF},a}(\gamma_a)) - \text{EIF}(\mathbf{O}_i, \theta_a(\gamma_a)) \right|^2} \sqrt{\frac{1}{|\mathcal{I}^{(k)}|} \sum_{i \in \mathcal{I}^{(k)}} \left| \widehat{\text{EIF}}(\mathbf{O}_i, \hat{\theta}_{\text{EIF},a}(\gamma_a)) + \text{EIF}(\mathbf{O}_i, \theta_a(\gamma_a)) \right|^2} \\
&\leq \sqrt{\frac{1}{|\mathcal{I}^{(k)}|} \sum_{i \in \mathcal{I}^{(k)}} \left| \widehat{\text{EIF}}(\mathbf{O}_i, \hat{\theta}_{\text{EIF},a}(\gamma_a)) - \text{EIF}(\mathbf{O}_i, \theta_a(\gamma_a)) \right|^2} \left(\sqrt{\frac{1}{|\mathcal{I}^{(k)}|} \sum_{i \in \mathcal{I}^{(k)}} \left| \widehat{\text{EIF}}(\mathbf{O}_i, \hat{\theta}_{\text{EIF},a}(\gamma_a)) - \text{EIF}(\mathbf{O}_i, \theta_a(\gamma_a)) \right|^2} \right. \\
&\quad \left. + \sqrt{\frac{4}{|\mathcal{I}^{(k)}|} \sum_{i \in \mathcal{I}^{(k)}} \phi_{\text{EIF},a}^2(\mathbf{O}_i, \theta_a(\gamma_a))} \right),
\end{aligned}$$

we have

$$R_{k,1}^2 \lesssim R_n \left\{ \frac{4}{|\mathcal{I}^{(k)}|} \sum_{i \in \mathcal{I}^{(k)}} \text{EIF}^2(\mathbf{O}_i, \theta_a(\gamma_a)) + R_n \right\}$$

where $R_n = \frac{1}{|\mathcal{I}^{(k)}|} \sum_{i \in \mathcal{I}^{(k)}} \left| \widehat{\text{EIF}}(\mathbf{O}_i, \hat{\theta}_{\text{EIF},a}(\gamma_a)) - \text{EIF}(\mathbf{O}_i, \theta_a(\gamma_a)) \right|^2$. Since $\frac{1}{|\mathcal{I}^{(k)}|} \sum_{i \in \mathcal{I}^{(k)}} \text{EIF}^2(\mathbf{O}_i, \theta_a(\gamma_a)) = O_p(1)$, it's sufficient to show $R_n = O_p(n^{-1/2})$, which holds by the proof of Theorem 4.3.

D Details and Examples of the Calibration Procedure

This section provides details and illustrations for the calibration procedure introduced in Section 5. We start with some remarks about the implementation of our calibration procedure. First, it's important to have the ratio of the sample sizes between the proxy source and target data be equal to that of the original source and the target data. This can be accomplished by downsampling one of the two proxy data. Relatedly, to make the comparisons fairer, it's useful to rescale the standard error estimate in the transported CI from the calibration procedure by multiplying it with $\sqrt{|\mathcal{I}_{s_2}|/n_t}$ in order to mimic the length of the CI for the original TATE. Algorithm 2 provides a step-by-step procedure for calibrating the sensitivity parameters. Figure D.1 exemplifies the calibration regions for estimating the ad effect in Philadelphia in 2024.

We illustrate the overall analysis pipeline for estimating the ad effect in Philadelphia in 2024. First, estimate the TATE across (γ_0, γ_1) 's using approaches introduced in Section

Algorithm 2 Calibrating Sensitivity Parameters

Require: Source data and confidence level $1 - \alpha$

- 1: **Step 1 (Partition source data):** Partition the source data into two parts and denote their corresponding indices as \mathcal{I}_{s_1} and \mathcal{I}_{s_2} where $\mathcal{I}_{s_1} \cup \mathcal{I}_{s_2} = \mathcal{I}_s$ and $\mathcal{I}_{s_1} \cap \mathcal{I}_{s_2} = \emptyset$.
- 2: **Step 2 (Construct CI via the standard approach):** With data in \mathcal{I}_{s_2} , estimate the ATE and its $(1 - \alpha)$ confidence interval, denoted as $\widehat{\text{CI}}_{s_2}(1 - \alpha)$.
- 3: **Step 3 (Construct CI via our transfer learning approach) :**
- 4: **if** $|\mathcal{I}_{s_1}|/|\mathcal{I}_{s_2}| \neq n_s/n_t$ **then**
- 5: Randomly sample from \mathcal{I}_{s_2} a subsample of size $\mathcal{I}_t \cdot (n_t/n_s)$, which without loss of generality assumed to be an integer. Denote the resulting set of indices as \mathcal{I}_{s_2} .
- 6: **end if**
- 7: With $\{(\mathbf{X}_i, A_i, Y_i, S_i = 1) : i \in \mathcal{I}_{s_1}\} \cup \{(\mathbf{V}_i, S_i = 0) : i \in \mathcal{I}_{s_2}\}$, estimate the ATE on \mathcal{S}_2 and its standard error with any $(\gamma_0, \gamma_1) \in \mathcal{C}_{\text{all}}$, denoted as $\widehat{\theta}_{s_1 \rightarrow s_2}(\gamma_0, \gamma_1)$ and $\widehat{\text{SE}}_{s_1 \rightarrow s_2}$. Denote the re-scaled confidence interval as

$$\widehat{\text{CI}}_{s_1 \rightarrow s_2}(\gamma_0, \gamma_1; 1 - \alpha) = \left[\widehat{\theta}_{s_1 \rightarrow s_2}(\gamma_0, \gamma_1) \mp z_{1-\alpha/2} \cdot \widehat{\text{SE}}_{s_1 \rightarrow s_2}(\gamma_0, \gamma_1) \cdot \sqrt{|\mathcal{I}_{s_2}|/n_t} \right]. \quad (\text{D.1})$$

- 8: **Step 4 (Find the plausible range) :** Find the plausible range of sensitivity parameters when transporting from \mathcal{S}_1 to \mathcal{S}_2 :

$$\mathcal{C}_1 = \left\{ (\gamma_0, \gamma_1) \in \mathcal{C}_{\text{all}} : \widehat{\text{CI}}_{s_2} \cap \widehat{\text{CI}}_{s_1 \rightarrow s_2}(\gamma_0, \gamma_1) \neq \emptyset \right\}. \quad (\text{D.2})$$

- 9: **Step 5 (Calibration in the other direction)** Exchange \mathcal{S}_1 and \mathcal{S}_2 and repeat Steps 1-4, resulting in the plausible range \mathcal{C}_2 .

Ensure: Intersect two plausible regions to construct the final region: $\mathcal{C} = \mathcal{C}_1 \cap \mathcal{C}_2$.

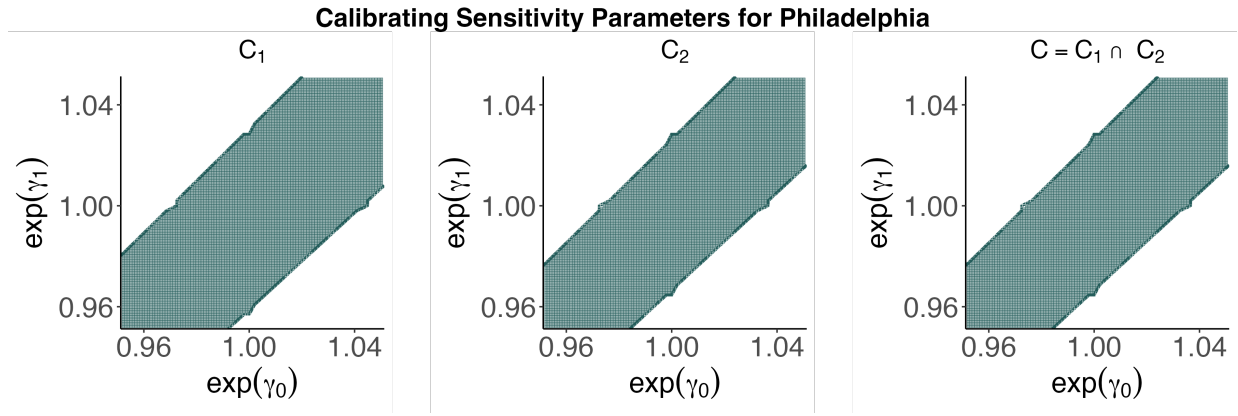


Figure D.1: The calibration procedure for the analysis in Philadelphia in 2024. Panels from left to right plots C_1 , C_2 and $C = C_1 \cap C_2$ in shadowed areas along $\exp(\gamma_1)$ in the y-axis and $\exp(\gamma_0)$ in the x-axis.

4. Specifically, for each (γ_0, γ_1) , one will have a $(1 - \alpha)$ CI for the TATE. From the left panel of Figure D.2, the ad effect could be insignificant, significant and positive, or significant and negative for Philadelphia voters in 2024 under different choices of (γ_0, γ_1) 's. Second, calibrate the sensitivity parameters using Algorithm 2 (i.e., the calibration procedure introduced in Section 5); see middle panel of Figure D.2. Finally, interpreting the ad effect estimates obtained from the first step within the calibrated region obtained from the second step. From the right panel of Figure D.2, this calibration procedure rules out the possibility of having significant and negative effect in Philadelphia in 2024. Therefore, we say Philadelphia is sensitive for a positive effect only. Figure D.3 provides another example on the analysis pipeline for Fulton.

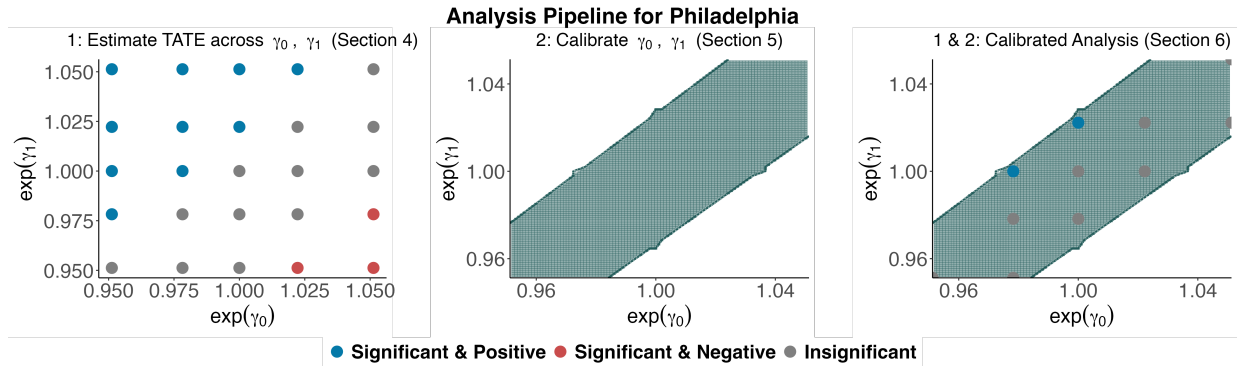


Figure D.2: Analysis pipeline for estimating the ad effect in Philadelphia in 2024. First, estimate the TATE across sensitivity parameters using approaches in Section 4. Note that we only included a few choices of (γ_0, γ_1) 's for illustration purposes. Second, calibrate the range of sensitivity parameters using the procedure in Section 5. Finally, overlay the two planes and interpret the TATE within the valid region. Final results are interpreted in Section 6.

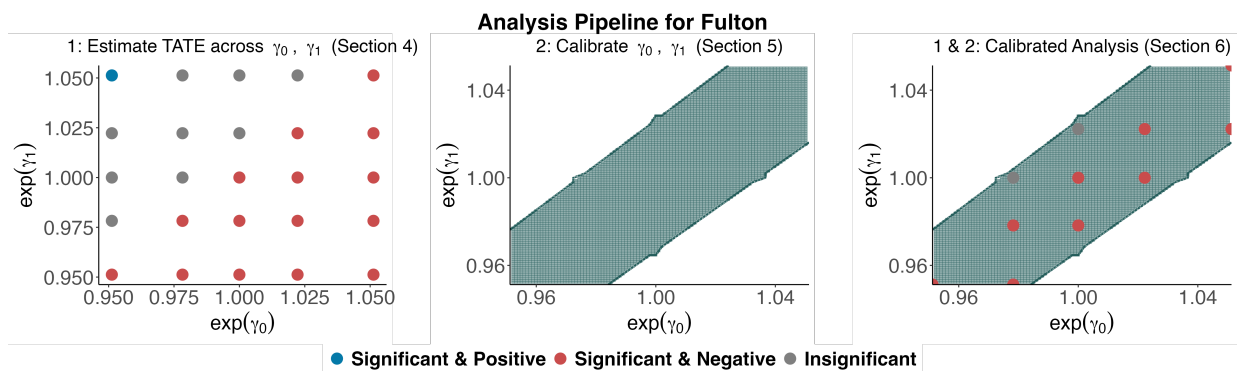


Figure D.3: Analysis pipeline for estimating the ad effect in Fulton in 2024. The figure layout is identical to Figure D.2.

E Supplementary Materials for the Ad Effect in Pennsylvania

E.1 Additional Data Description

Our analysis consists of two datasets, the source data derived from the 2020 RCT data from Aggarwal et al. (2023) and the target data derived from the 2024 PA voter database. Prior to analysis, we recoded the shared covariates \mathbf{V}_i from these two datasets for them to match. A description is provided as follows.

The age was coded as four groups (18-24, 25-24, 35-39, and 40+) in the 2020 RCT data and as date of birth in the 2020 PA voter database. For the target data, we calculated their age by the year of 2024 and excluded voters above 55 years' old to match the range of age in Aggarwal et al. (2023), and then constructed a variable of age groups according to the source data. The resulting age group variable for analysis is a discrete variable with four levels.

For each voter, their party information from the 2020 RCT data was coded as one of the four levels: Democratic, Republican, Unknown and Other, whereas in the 2024 PA voter database was one of fifty choices including Democratic and Republican. For analysis, we constructed a party variable with three levels: Democratic, Republican, and Other/Unknown, whereas voters that didn't belong to the first two levels would have their party level being "Other/Unknown". We note that the party information from the 2020 RCT data was inaccurate with 72% being unknown and we refer readers to Aggarwal et al. (2023) for details.

The gender was coded in two levels (female and other) in the 2020 RCT data and three levels (female, male, unknown) in the 2024 voter database. Our gender variable for analysis

has two levels: female and non-female where the non-female level includes voters whose gender weren't coded as female.

The voting history information from the 2020 RCT was coded as ten binary variables. Each variable indicated whether a voter has voted in a specific year for every other year between 2000 and 2018 (i.e., voted in 2000, voted in 2002, voted in 2004, voted in 2006, voted in 2008, voted in 2010, voted in 2012, voted in 2014, voted in 2016, voted in 2018). The voting history information from the PA voter database differed across counties and the availability is provided in Figure E.1. Later, to check robustness of the estimation results with respect to the coding of voting history, we also repeated the analysis with two alternative ways of coding the voting history. The total three coding types are summarized below. Unless specified, the voting history was coded as in (1), i.e., following Aggarwal et al. (2023).

- (1) Voting history is coded as in Aggarwal et al. (2023), i.e., as ten binary variables indicating voting participation every two year from 2000 to 2018.
- (2) Voting history is coded as ten binary variables indicating voting participation 2/4/6/.../20 years ago.
- (3) Voting history is coded as two binary variables indicating voting participation in past presidential mid-term elections.

In addition to the common covariates, the 2020 RCT data also contains the race information, which is a categorical variable with four levels: White, Black, Latinx, and Other. Finally after pre-processing, the source covariates \mathbf{X}_i include age group, gender, party, race, and ten binary variables indicating voting participation from 2000 to 2018, among which the common covariates \mathbf{V}_i include age group, gender, party, and part of the voting history.

The availability of covariates across counties in PA is provided in Figure E.1. Figure E.1 also provides the sample size n_t across counties in the x-axis. Table E.1 summarizes the covariates (which are all discrete) and their levels.

Covariate	Levels	Available from target?
Age group	18-24, 25-34, 35-39, 40+	Yes
Gender	Female, non-female	Yes
Party	Democratic, Republican, Other/Unknown	Yes
Race	White, Black, Latinx, other	No
Voted in 2000	0, 1	No
Voted in 2002	0, 1	No
Voted in 2004	0, 1	Available in some counties
Voted in 2006	0, 1	Available in some counties
Voted in 2008	0, 1	Available in some counties
Voted in 2010	0, 1	Yes
Voted in 2012	0, 1	Yes
Voted in 2014	0, 1	Yes
Voted in 2016	0, 1	Yes
Voted in 2018	0, 1	Yes

Table E.1: Descriptions on covariates in pooled data.

E.2 Values of County-Level Ad Effect with the OR Estimator

We provide a comprehensive result (i.e., the specific numbers of confidence intervals) for the results presented in Section 6.2. Specifically, Table E.2 lists the ad effect estimated by the OR estimator under transportability for each county in Pennsylvania. It also lists the

Covariate Availability across Counties in Pennsylvania

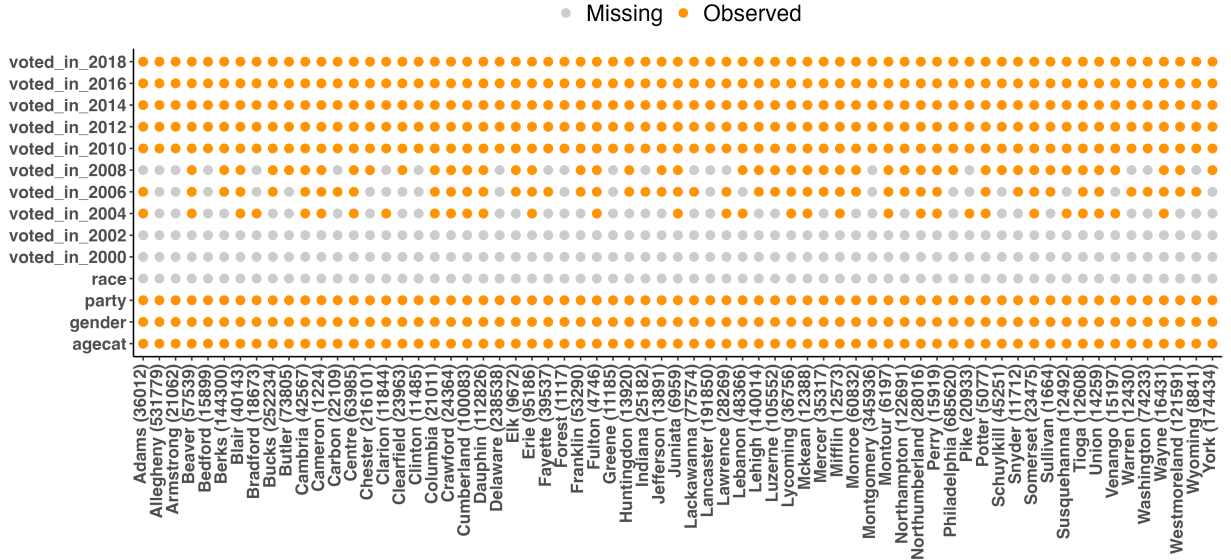


Figure E.1: Target data availability across Pennsylvania counties in 2024. The y-axis lists the source covariate \mathbf{X} and the points indicate the availability of these covariates in the target covariate \mathbf{V} across counties. The x-axis is county with the number of voters (i.e., n_t) in parentheses.

effect direction for the sensitivity analysis after calibration and the smallest $\exp(|\gamma_1 - \gamma_0|)$ that makes the ATE significant.

Table E.2: County-level ad effect with the OR estimator in Pennsylvania, the smallest $\exp(|\gamma_1 - \gamma_0|)$ that makes the effect significant, and the effect direction. The voting history is coded in the original way as in Aggarwal et al. (2023), i.e., as binary variables of whether one has voted each year from 2000 to 2018.

County	$\hat{\theta}_{\text{OR}}$ (95% CI) $\times 100$	Min $\exp\{ \gamma_1 - \gamma_0 \}$	Effect direction
Adams	-0.41 (-1.05, 0.22)	1.012072	Negative Only
Allegheny	0.06 (-0.55, 0.67)		Neither Direction
Armstrong	-0.6 (-1.3, 0.1)	1.006018	Negative Only
Beaver	-0.26 (-0.86, 0.34)	1.020201	Negative Only

Continued on next page

Table E.2: County-level ad effect with the OR estimator in Pennsylvania, the smallest $\exp(|\gamma_1 - \gamma_0|)$ that makes the effect significant, and the effect direction. The voting history is coded in the original way as in Aggarwal et al. (2023), i.e., as binary variables of whether one has voted each year from 2000 to 2018. (Continued)

Bedford	-0.77 (-1.55, 0)	1.000000	Negative Only
Berks	-0.18 (-0.76, 0.4)	1.022244	Negative Only
Blair	-0.52 (-1.19, 0.15)	1.010050	Negative Only
Bradford	-0.57 (-1.26, 0.12)	1.006018	Negative Only
Bucks	-0.13 (-0.71, 0.46)	1.028396	Negative Only
Butler	-0.42 (-1.06, 0.22)	1.014098	Negative Only
Cambria	-0.4 (-1.05, 0.24)	1.014098	Negative Only
Cameron	-0.54 (-1.24, 0.16)	1.010050	Negative Only
Carbon	-0.34 (-0.97, 0.28)	1.016129	Negative Only
Centre	-0.06 (-0.62, 0.51)	1.028396	Negative Only
Chester	-0.05 (-0.62, 0.52)	1.032518	Negative Only
Clarion	-0.57 (-1.28, 0.13)		Neither Direction
Clearfield	-0.55 (-1.24, 0.14)	1.010050	Negative Only
Clinton	-0.45 (-1.1, 0.21)	1.012072	Negative Only
Columbia	-0.32 (-0.93, 0.3)	1.016129	Negative Only
Crawford	-0.45 (-1.13, 0.22)	1.014098	Negative Only
Cumberland	-0.17 (-0.77, 0.43)	1.024290	Negative Only
Dauphin	0.04 (-0.56, 0.63)	1.034585	Negative Only
Delaware	0.02 (-0.59, 0.64)		Neither Direction
Elk	-0.51 (-1.19, 0.16)	1.010050	Negative Only
Erie	-0.19 (-0.78, 0.39)	1.024290	Negative Only

Continued on next page

Table E.2: County-level ad effect with the OR estimator in Pennsylvania, the smallest $\exp(|\gamma_1 - \gamma_0|)$ that makes the effect significant, and the effect direction. The voting history is coded in the original way as in Aggarwal et al. (2023), i.e., as binary variables of whether one has voted each year from 2000 to 2018. (Continued)

Fayette	-0.39 (-1.04, 0.26)	1.014098	Negative Only
Forest	-0.61 (-1.34, 0.12)	1.008032	Negative Only
Franklin	-0.52 (-1.18, 0.15)		Neither Direction
Fulton	-0.84 (-1.64, -0.04)	1.000000	Negative Only
Greene	-0.49 (-1.15, 0.18)	1.012072	Negative Only
Huntingdon	-0.56 (-1.26, 0.15)	1.010050	Negative Only
Indiana	-0.39 (-1.04, 0.26)	1.016129	Negative Only
Jefferson	-0.63 (-1.36, 0.1)	1.006018	Negative Only
Juniata	-0.7 (-1.46, 0.05)	1.004008	Negative Only
Lackawanna	-0.09 (-0.71, 0.53)		Neither Direction
Lancaster	-0.3 (-0.9, 0.29)	1.018163	Negative Only
Lawrence	-0.39 (-1.02, 0.25)	1.014098	Negative Only
Lebanon	-0.35 (-0.98, 0.27)	1.016129	Negative Only
Lehigh	-0.02 (-0.59, 0.56)	1.030455	Negative Only
Luzerne	-0.19 (-0.79, 0.42)	1.024290	Negative Only
Lycoming	-0.45 (-1.09, 0.2)	1.012072	Negative Only
Mckean	-0.54 (-1.22, 0.15)	1.008032	Negative Only
Mercer	-0.41 (-1.03, 0.21)	1.012072	Negative Only
Mifflin	-0.6 (-1.33, 0.12)		Neither Direction
Monroe	0.06 (-0.53, 0.65)		Neither Direction
Montgomery	0.03 (-0.58, 0.64)		Neither Direction

Continued on next page

Table E.2: County-level ad effect with the OR estimator in Pennsylvania, the smallest $\exp(|\gamma_1 - \gamma_0|)$ that makes the effect significant, and the effect direction. The voting history is coded in the original way as in Aggarwal et al. (2023), i.e., as binary variables of whether one has voted each year from 2000 to 2018. (Continued)

Montour	-0.25 (-0.87, 0.37)	1.020201	Negative Only
Northampton	-0.01 (-0.58, 0.56)	1.030455	Negative Only
Northumberland	-0.39 (-1.04, 0.26)		Neither Direction
Perry	-0.5 (-1.22, 0.22)	1.012072	Negative Only
Philadelphia	0.38 (-0.35, 1.11)	1.020201	Positive Only
Pike	-0.21 (-0.82, 0.39)	1.020201	Negative Only
Potter	-0.67 (-1.43, 0.09)	1.006018	Negative Only
Schuylkill	-0.43 (-1.08, 0.21)	1.012072	Negative Only
Snyder	-0.58 (-1.27, 0.12)	1.008032	Negative Only
Somerset	-0.64 (-1.35, 0.07)	1.004008	Negative Only
Sullivan	-0.53 (-1.26, 0.2)	1.012072	Negative Only
Susquehanna	-0.37 (-1.08, 0.33)	1.020201	Negative Only
Tioga	-0.55 (-1.25, 0.15)	1.008032	Negative Only
Union	-0.28 (-0.86, 0.31)	1.018163	Negative Only
Venango	-0.51 (-1.19, 0.16)		Neither Direction
Warren	-0.45 (-1.13, 0.22)		Neither Direction
Washington	-0.35 (-0.99, 0.28)	1.016129	Negative Only
Wayne	-0.41 (-1.08, 0.25)	1.014098	Negative Only
Westmoreland	-0.37 (-1, 0.27)	1.016129	Negative Only
Wyoming	-0.5 (-1.18, 0.17)	1.010050	Negative Only
York	-0.33 (-0.93, 0.28)		Neither Direction

E.3 Robustness Checks on County Level Ad Effects

In this section, we provide the estimated county level ad effects from both estimators across three ways of coding the voting history mentioned in Section E.1. Figures E.2 and E.3 show the estimation across these three ways of coding voting history for the OR estimator and the EIF-based estimator, respectively. From each figure, across panels, we find the estimation results are robust to the coding methods, especially for the OR estimator. Comparing Figures E.2 and E.3, we find that the EIF-based estimator generally has wider confidence intervals than the OR estimator for small counties and narrower ones for large counties (county sizes have been listed in Figure E.1).

E.4 Details on Data Pre-Processing for Subgroup Analysis

This section details the construction of variables regarding urbanicity and education attainment in the subgroup analysis presented in Section 6.3.

E.4.1 Percentage of Bachelor’s Degree Or Higher in ZIP Codes

To construct a variable as a proxy for a voter’s education attainment, we leverage the ZIP code information from the PA voter database. In specific, for every ZIP code in the PA voter database, we calculate the percentage of receiving a Bachelor’s degree or higher from the 2022 American Community Survey (ACS), which is a comprehensive census that represents the U.S. population. To preserve privacy, we excluded ZIP codes with fewer than 20 voters from the PA voter database or from the ACS data. This step removed 146 ZIP codes and 2149 voters. As a result, for each voter, we have the percentage of Bachelor’s degree or higher in their ZIP-code area. And for analysis, we divided the percentages into five groups by every 20 percent.

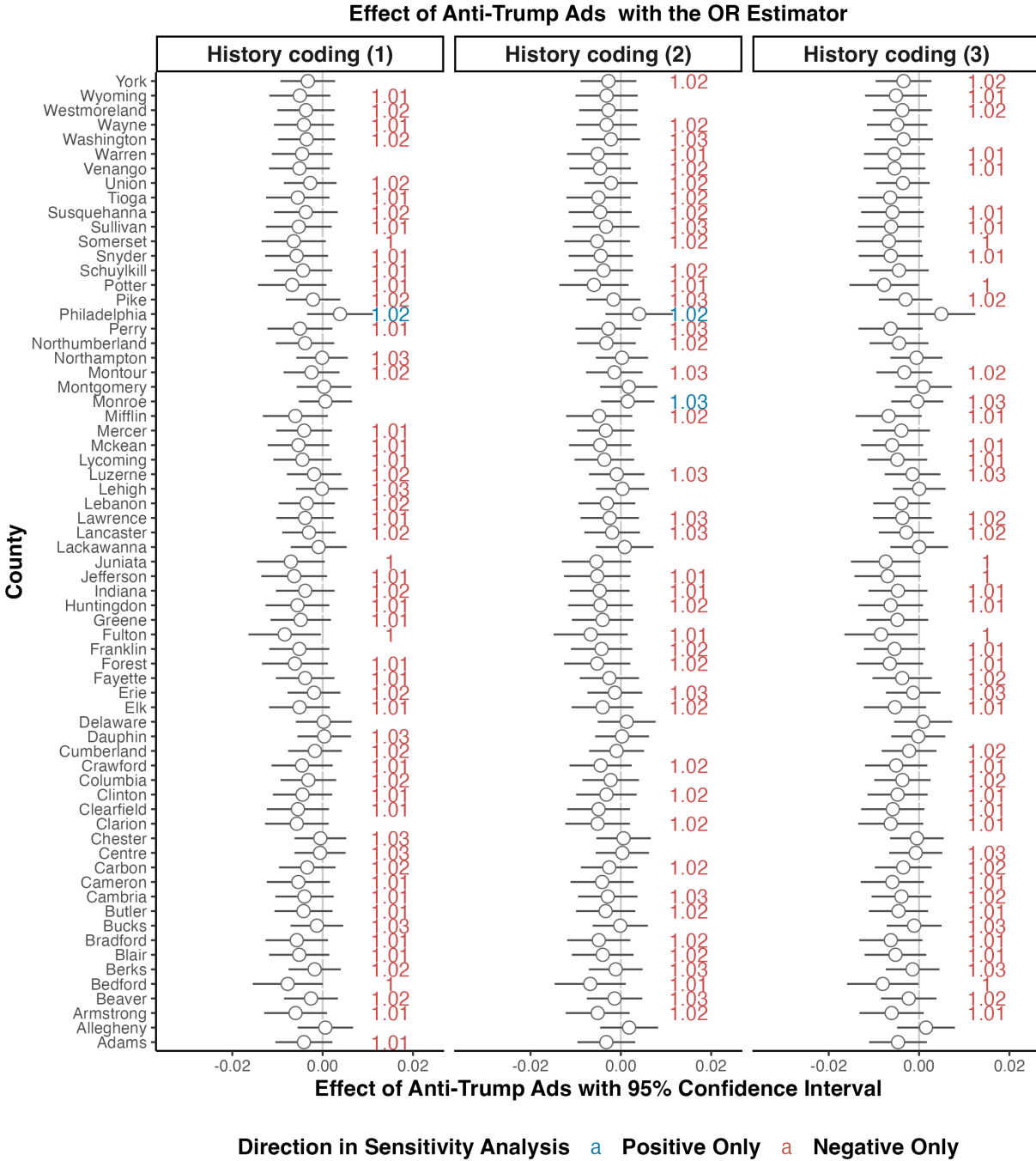


Figure E.2: Robustness checks of the OR estimator with respect to the voting history coding types. In each panel, the bar represents the ad effect under the transportability assumption. The number is the smallest $\exp(|\gamma_1 - \gamma_0|)$ that makes the ad effect significant, colored by the direction of the corresponding ad effect.

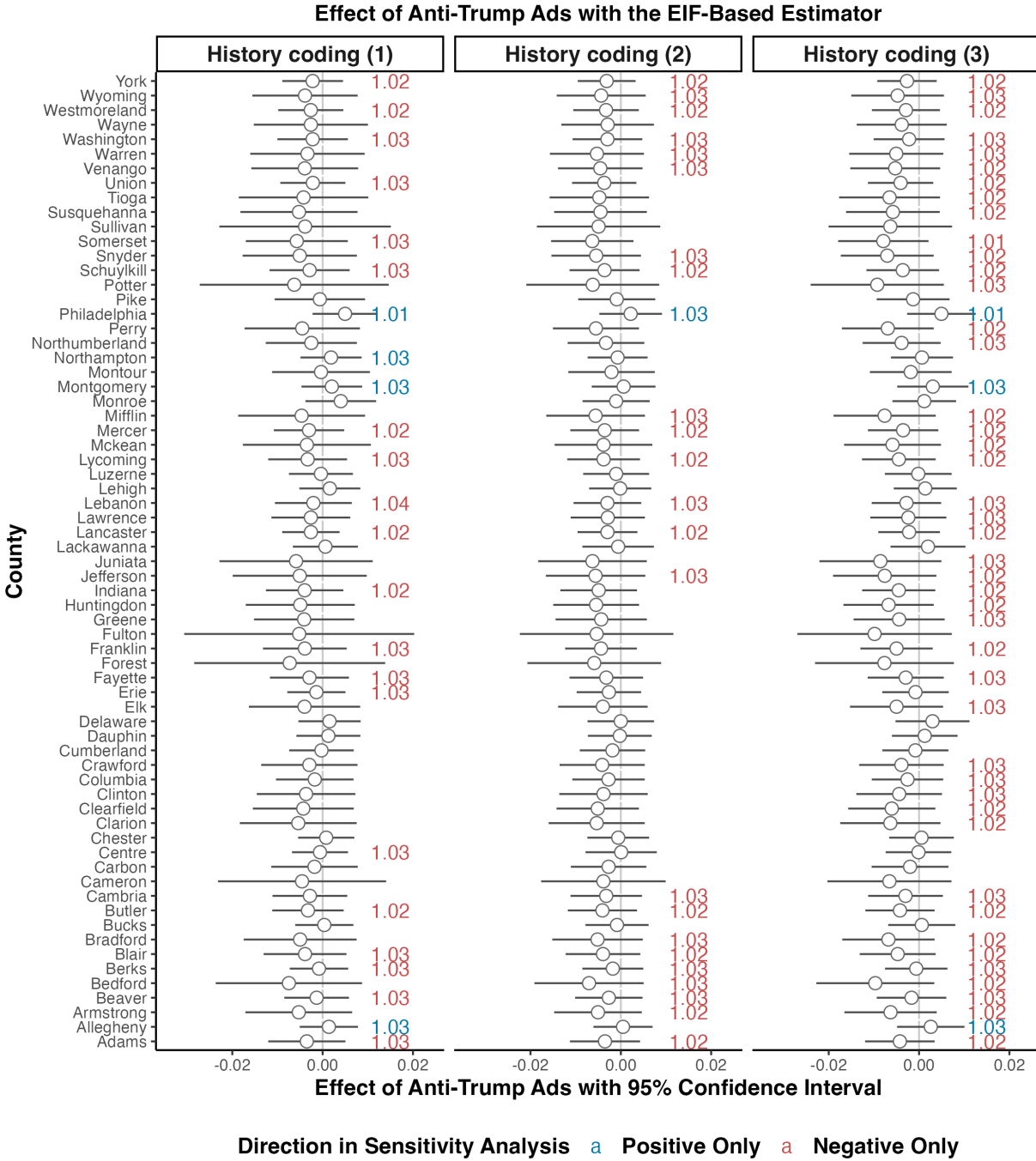


Figure E.3: Estimation results of the EIF-based estimator across the voting history coding types. Panels are organized and scaled in the same way as in Figure E.2.

E.4.2 Urbanicity in Census Tracts

For urbanicity, we mapped a voter’s address with the 2020 U.S. census which classifies a census tract as urban or rural (i.e., not urban) based on characteristics including population, housing, and land area among others. We refer readers to the U.S. Census Bureau’s urban-rural classification for the criterion of classifying a census tract as urban or rural. Among all 4,880,729 voters, the addresses of 176,866 (0.04%) cannot be matched with a census tract. Their urbanicity was imputed by the proportion of urban voters with the same ZIP code (if the proportion is less than 50%, we imputed the urbanicity to be rural and vice versa), except for 1,147 whose urbanicity cannot be imputed because their ZIP codes are either missing or do not match with ZIP codes of other voters. These voters take 0.02% of the original voters and have been excluded from the analysis in Section 6.3.

E.5 Robustness Checks on Subgroup Analysis in Section 6.3

In this section, we provide the estimated ad effects in subgroups from both estimators across three ways of coding the voting history. Figure E.4 presents the estimation results of both estimators by the interaction between gender, urbanicity, and education attainment in 2022. Under the transportability assumption, point estimates and 95% confidence intervals by the EIF-based estimator is close to those by the OR estimator presented in the main text. The calibrated results by the EIF-based estimator also mostly coincide with the OR estimator.



Figure E.4: Ad effect estimates in subgroups defined by the interaction between gender, urbanicity, and percentage of Bachelor’s degree within the same ZIP-code area using both OR estimator and the EIF-based estimator. The results of the OR estimator are exactly those in Figure 6.3.

F Replication of Section 6 When Excluding Three States from the Source

In this section, we repeat the analysis in Section 6 when excluding voters from Pennsylvania (PA), Michigan (MI), and Wisconsin (WI) from the source data. The source data now consists of $n_s = 662225$ voters from North Carolina (NC) and Arizona (AZ) in the 2020 experiment by Aggarwal et al. (2023). Table F.1 summarizes the voter demographics and turnout in (PA, MI, WI) and (NC, AZ).

Table F.1: Voter demographics for (PA, MI, WI) and (NC, AZ) in the RCT data from Aggarwal et al. (2023).

States	(PA, MI, WI)	(NC, AZ)
Size	1337057	662225
Gender = Other (%)	638840 (47.8)	382401 (57.7)
Age groups (%)		
18-24	288783 (21.6)	224352 (33.9)
25-34	430123 (32.2)	208818 (31.5)
35-39	161576 (12.1)	65365 (9.9)
40+	456575 (34.1)	163690 (24.7)
Party (%)		
Democrat	108810 (8.1)	74135 (11.2)
Other	1195792 (89.4)	548670 (82.9)
Republican	32455 (2.4)	39420 (6.0)
Voted in 2020 = Yes (%)	761181 (56.9)	329639 (49.8)

Sections F.1 and F.2 provide results for a county-by-county analysis and a subgroup analysis, respectively.

F.1 Ad Effects by Counties

We start with the result with the OR estimator and the original way of coding the voting history in Aggarwal et al. (2023). When $\gamma_0 = \gamma_1 = 0$, i.e., under transportability, the ad effect is insignificant in all counties of PA. When $\gamma_1\gamma_0 \neq 0$, after calibration, the ad effect is sensitive for a negative effect in 52 counties and insensitive in the other 15 counties. Figure F.1 plots the calibrated county-by-county analysis on the map of PA.

Figures F.2 and F.3 show the analysis result across three types of coding the voting history for the OR estimator and the EIF-based estimator, respectively.

F.2 Subgroup Analysis

We estimate the ad effect in 20 subgroups of gender, urbanicity, and education attainment for voters within the same ZIP-code area. Results are shown in Figure F.4. When $\gamma_1 = \gamma_0 = 0$, i.e., under transportability, the effects are in general higher for non-female voters than female voters, and higher for urban voters than rural voters. When $\gamma_1\gamma_0 \neq 0$, after calibration, none of the subgroups are sensitive for a significant ad effect.

G Simulations

In this section, we validate asymptotic properties of our proposed estimators on simulated datasets generated according to the 2020 RCT data.

In order to generate data that mimics the 2020 RCT data, we let the source covariate \mathbf{X}_i be gender, race, and age groups and set its distribution $\mathbf{X}_i | S_i = 1$ to be the empirical

Sensitivity of Ad Effect for the 2024 U.S. Presidential Election When (PA, WI, MI) Excluded from the Source Data

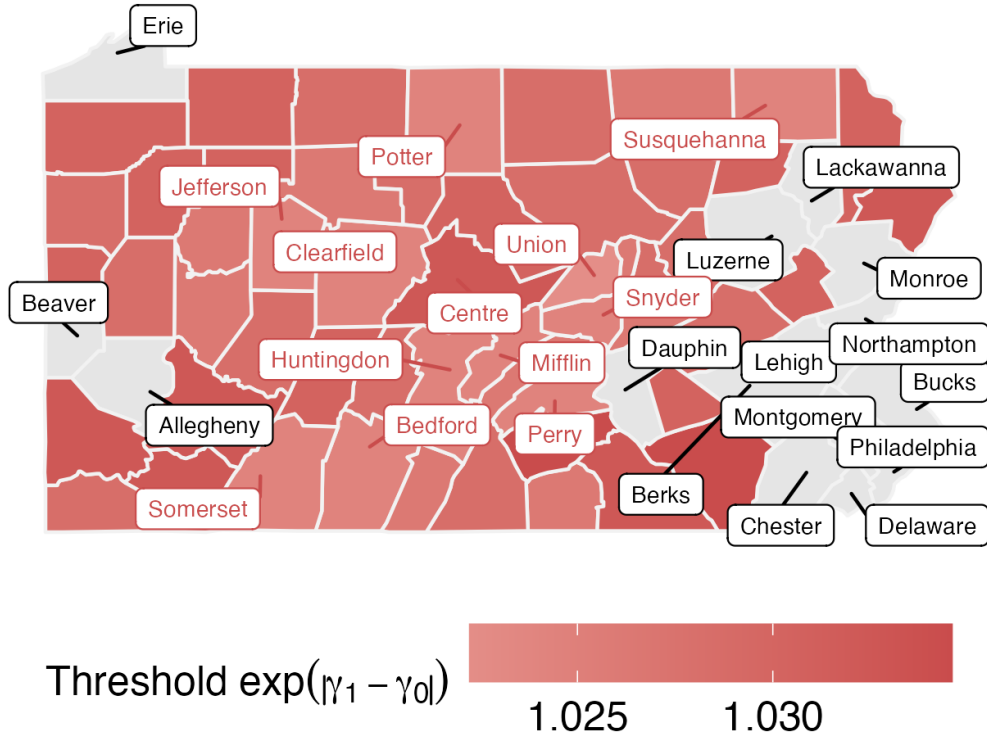


Figure F.1: Sensitivity analysis of the ad effect in every county of PA when the source data only consists of voters in NC and AZ. The color gradient represents the smallest $\exp(|\gamma_1 - \gamma_0|)$ that makes the ad effect significant and negative after calibration. Counties that are insensitive to a significant effect are in gray.

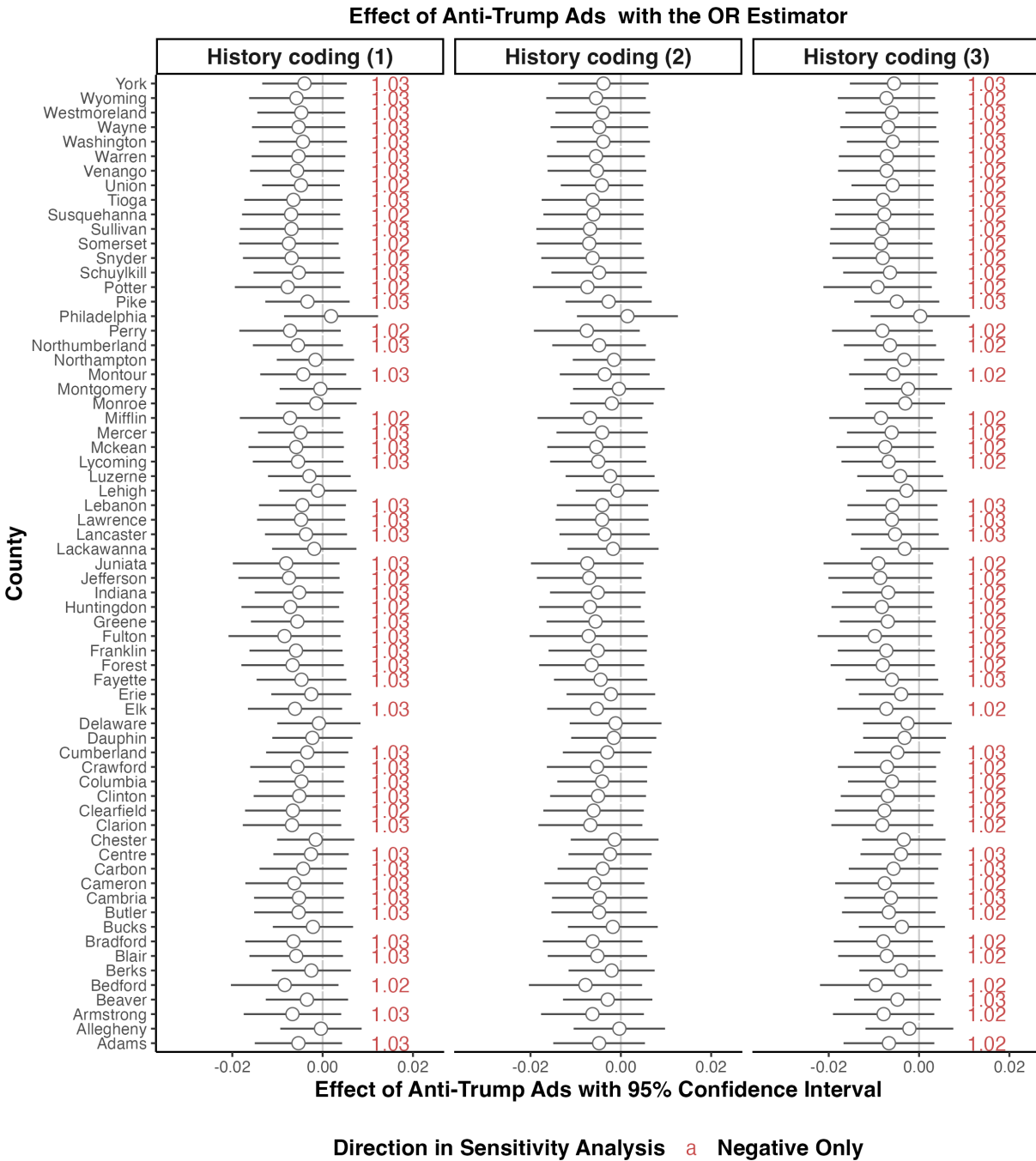


Figure F.2: County-by-county analysis with the OR estimator when the source data consists of NC and AZ across three ways of coding the voting history coding. In each panel, the bar represents the ad effect under the transportability assumption. The number is the smallest $\exp(|\gamma_1 - \gamma_0|)$ that makes the ad effect significant, colored by the direction of the corresponding ad effect.

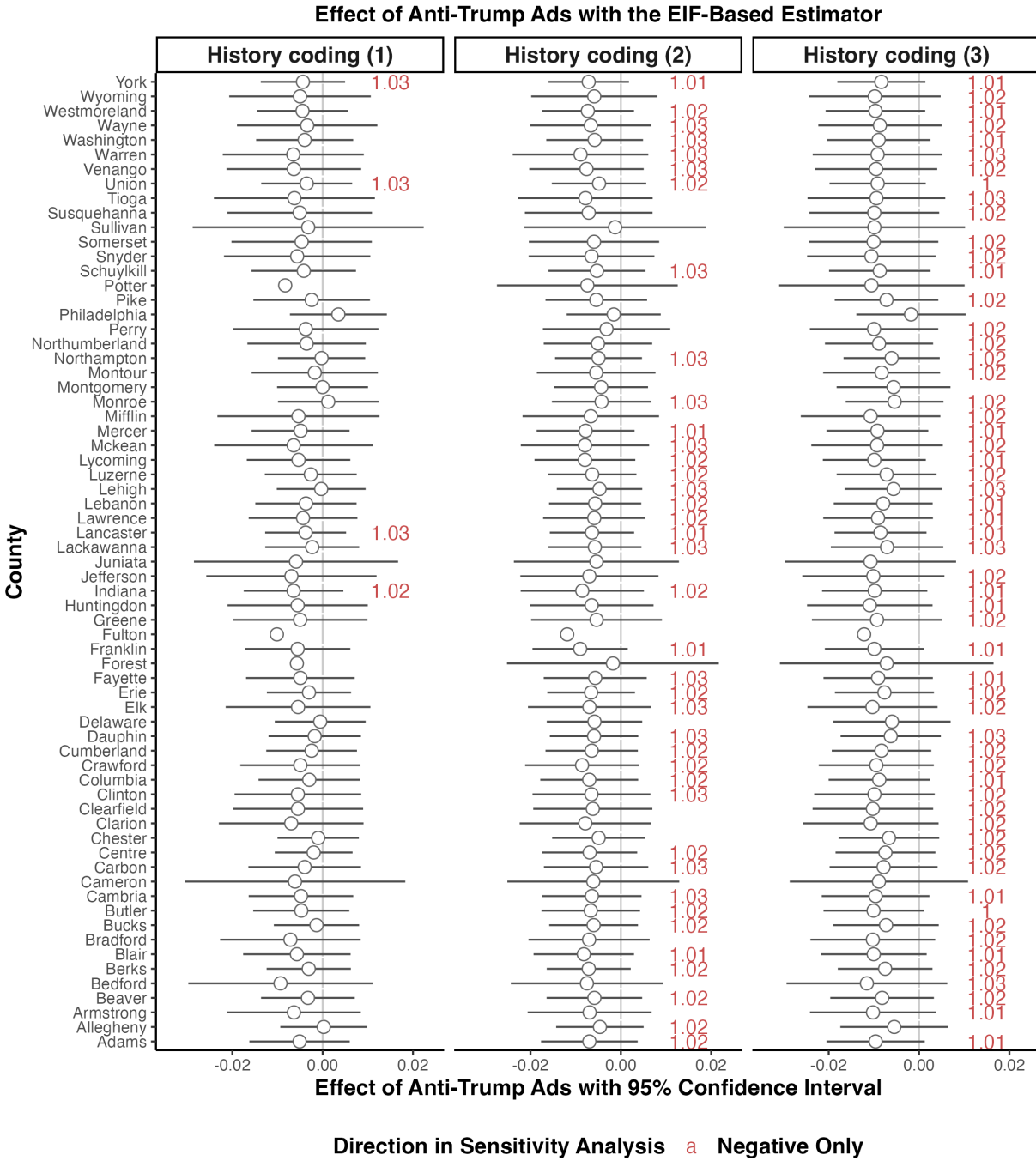


Figure F.3: County-by-county analysis with the EIF estimator when the source data consists of NC and AZ across three ways of coding the voting history coding. In each panel, the bar represents the ad effect under the transportability assumption. The number is the smallest $\exp(|\gamma_1 - \gamma_0|)$ that makes the ad effect significant, colored by the direction of the corresponding ad effect.

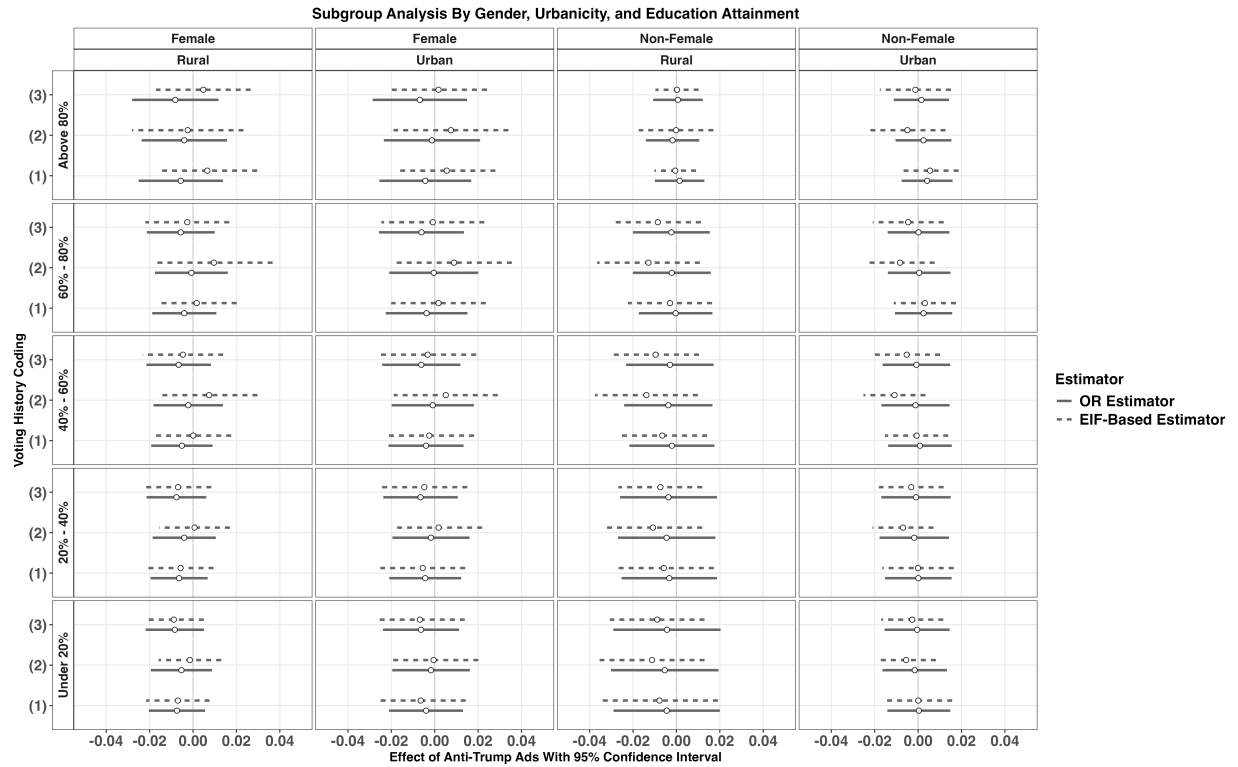


Figure F.4: Heterogeneous treatment effects by the interaction between gender, urbanicity, and education subgroups while including only the NC and AZ voters in the source data. The solid lines and dashed lines represent 95% CIs under transportability for the OR estimator and the EIF estimator, respectively. The gray squares represent that all subgroups are insensitive for a significant effect.

distribution of these covariates in the 2020 RCT data. Given $\mathbf{x} \in \mathcal{X}$, the treatment is randomized within 18 strata mimicking the design in Aggarwal et al. (2023). The $\mu_1(\mathbf{x})$ and $\mu_0(\mathbf{x})$ are generated in two scenarios. In Scenario (A), they differ by 0.005 or -0.005 whereas the overall average effect is close to zero, mimicking the real data where the overall ad effect is negligible despite small, heterogeneous effects in subgroups. In Scenario (B), the difference between $\mu_1(\mathbf{x})$ and $\mu_0(\mathbf{x})$ is larger in magnitude and more heterogeneous. The covariate distribution on the target population, $p_{\mathbf{x}|S=0}$ is generated such that $p_{\mathbf{x}|S=0}(\mathbf{x})/p_{\mathbf{x}|S=1}(\mathbf{x})$ is between 0.9 and 1.1. Table G.1 presents the values of this generation. The target covariate \mathbf{V}_i is set to be the gender variable alone. The sensitivity parameter γ_0 is set to zero and γ_1 varies. The source sample size n_t and target sample size n_t are set equal.

After generating datasets, the propensity score $\pi(\mathbf{x})$ is estimated with the average proportion of treated units within each. The outcome regression functions $\mu_a(\mathbf{x})$ and $\rho_a(\mathbf{v})$ are estimated by reweighing samples with $S_i = 1$ and $A_i = a$ as in (4.2). The density ratio $w(\mathbf{v})$ is estimated with (C.1). For the OR estimator, the inference is based on 1000 bootstrap iterations. For the EIF-based estimator, the inference is based on the cross-fitting procedure with $K = 2$ splits. The confidence level is set to $1 - \alpha = 0.95$. Simulation results are based on 1000 replicates.

From results in Table G.2, both estimators are consistent and their empirical standard deviation (SD) decays with \sqrt{n} . The estimated SEs are close to the empirical SDs and the coverage rate nears the nominal level 0.95. These results validate bootstrap CI consistency in Theorem 4.1 as well as the asymptotic Normality of the EIF-based cross-fitting estimator in Theorem 4.2.

Table G.1: Data generation in simulated datasets.

Gender	Race	Age Group	$p_{\mathbf{x} S=1}(\mathbf{x})$	$p_{\mathbf{x} S=0}(\mathbf{x})$	$\pi(\mathbf{x})$	Scenario (A)		Scenario (B)	
						$\mu_0(\mathbf{x})$	$\mu_1(\mathbf{x})$	$\mu_0(\mathbf{x})$	$\mu_1(\mathbf{x})$
Female	Black	18-24	0.0061	0.0055	0.6	0.4	0.35	0.2	0.6
Female	Black	25-34	0.0077	0.0071	0.7	0.4	0.35	0.2	0.6
Female	Black	Other	0.0157	0.0150	0.8	0.5	0.45	0.7	0.2
Female	Latinx	18-24	0.0073	0.0066	0.6	0.5	0.45	0.7	0.2
Female	Latinx	25-34	0.0089	0.0083	0.8	0.4	0.35	0.3	0.3
Female	Latinx	Other	0.0147	0.0139	0.9	0.5	0.45	0.7	0.2
Female	Other	18-24	0.1001	0.1042	0.6	0.6	0.55	0.3	0.5
Female	Other	25-34	0.1271	0.1353	0.8	0.5	0.45	0.6	0.2
Female	Other	Other	0.2016	0.2218	0.9	0.6	0.55	0.3	0.5
Other	Black	18-24	0.0197	0.0193	0.6	0.3	0.35	0.2	0.6
Other	Black	25-34	0.0280	0.0285	0.8	0.2	0.25	0.2	0.6
Other	Black	Other	0.0397	0.0409	0.8	0.3	0.35	0.2	0.6
Other	Latinx	18-24	0.0174	0.0169	0.6	0.3	0.35	0.25	0.55
Other	Latinx	25-34	0.0201	0.0200	0.8	0.3	0.35	0.25	0.55
Other	Latinx	Other	0.0211	0.0212	0.9	0.4	0.45	0.25	0.55
Other	Other	18-24	0.1061	0.1118	0.7	0.5	0.55	7	0.2
Other	Other	25-34	0.1277	0.1375	0.8	0.4	0.45	0.25	0.55
Other	Other	Other	0.1310	0.1425	0.9	0.5	0.55	0.7	0.2

Table G.2: Simulation results. Bias, RMSE, empirical standard deviation (Emp.SD) and estimated standard error (Est.SE) have been multiplied with 1000.

$\gamma_1 = 0$		Scenario (A)					Scenario (B)				
Estimator	$n_s (= n_t)$	Bias	RMSE	Emp.SD	Est.SE	Rate	Bias	RMSE	Emp.SD	Est.SE	Rate
OR	10^5	-0.135	4.317	4.317	4.275	0.943	0.076	4.169	4.171	4.123	0.952
OR	2×10^5	-0.126	3.047	3.046	3.018	0.953	0.030	2.951	2.952	2.913	0.939
EIF	10^5	0.004	4.307	4.309	4.283	0.953	-0.082	3.943	3.944	4.135	0.955
EIF	2×10^5	-0.008	3.029	3.030	3.024	0.953	-0.549	2.996	2.947	2.920	0.945
$\gamma_1 = 0.05$		Scenario (A)					Scenario (B)				
OR	10^5	-0.136	4.318	4.318	4.276	0.945	0.076	4.178	4.180	4.130	0.953
OR	2×10^5	-0.126	3.047	3.046	3.019	0.954	0.029	2.957	2.958	2.920	0.940
EIF	10^5	0.225	4.356	4.357	4.283	0.947	-0.265	4.152	4.145	4.142	0.948
EIF	2×10^5	0.095	3.028	3.028	3.024	0.943	-0.483	2.984	2.946	2.925	0.941